ABSTRACT

SNYDER, TESSA JOAN. From Productivity to Diversity: Effects of Canopy Gap Size and Spatial Gradients on Ground-layer Vegetation in Southern Appalachian Mixed-Oak Forests (Under the direction of Dr. Jodi Forrester).

Temperate mixed-oak forests in the Southern Appalachians face altered understory dynamics due to historical mesophication and shifting disturbance regimes. To evaluate how the initial entry of an expanding-gap silviculture influences ground-layer structure and function, we integrated biomass and diversity assessments from the Southern Appalachian Femelschlag Experiment (SAFE). In 2019, we created small (0.1–0.4 ha) and large (0.7–1.3 ha) canopy gaps, retaining uncut controls. We measured the pre- (2014) and post-treatment (2021-2022) cover of vascular plant species richness, evenness, and composition in permanent 1 m^2 subplots across gap centers, edges, and adjacent forest matrix and estimated the aboveground biomass of seven plant lifeform groups (trees, shrubs, subshrubs, forbs, graminoids, ferns, vines) using destructive sampling and allometric models. Mixed-effects models revealed that ground-layer productivity was driven primarily by proximity to gap centers rather than gap size: biomass peaked at centers and declined toward the matrix, with *Rubus* spp. and graminoids exhibiting the largest increases and tree and vine responses varying by aspect and microhabitat. Despite major changes to canopy structure, soil moisture did not vary significantly by treatment or spatial gradients during the measurement period. Species richness rose from 32.8 ± 1.1 (2014) to over 40 ± 1.2 species per subplot (2021–2022), and Shannon and Simpson's diversity indices increased and remained elevated, with the highest diversity in gap centers and matrix zones. Multivariate analyses (Non-metric Multidimensional Scaling and Multi-Response Permutation Procedure) documented rapid compositional differentiation among zones—especially in large gap centers—and a fourfold increase in indicator species, signaling emerging habitat specialization. Despite greater resource

availability, non-native species establishment was limited and transient. Our findings demonstrate that expanding-gap silviculture can simultaneously enhance ground-layer biomass and biodiversity, creating fine-scale environmental heterogeneity that counters mesophication and fosters specialized understory assemblages. Emulating natural disturbance gradients, this approach offers a promising framework for balancing oak and hickory regeneration, carbon cycling, and long-term ecosystem resilience in managed temperate forests.

From Productivity to Diversity: Effects of Canopy Gap Size and Spatial Gradients on Ground-layer Vegetation in Southern Appalachian Mixed-Oak Forests

by
Tessa Joan Snyder

A thesis submitted to the Graduate Faculty of
North Carolina State University
in partial fulfillment of the
requirements for the degree of
Master of Science

Forestry and Environmental Resources

Raleigh, North Carolina
2025

APPROVED BY:

Dr. Jodi Forrester Committee Chair	Dr. Tara Keyser
Dr. Jeffrey Doser	Dr. Robert Scheller

DEDICATION

I dedicate this work to the memory of my mother

Mary Fay Carrithers (1959 - 2023)

BIOGRAPHY

Tessa Snyder grew up in Chapel Hill, North Carolina, where she developed a passion for nature by exploring local woods and spending extra time in her elementary school's science lab. In high school, she took an advanced placement environmental science course, solidifying her desire to major in environmental studies. She earned her Bachelor of Science in Environmental Studies, concentrating in Ecology and Field Biology, from the University of North Carolina at Asheville. After graduation, the COVID-19 pandemic altered her plans, leading her to work as a Purification Specialist in a High-Pressure Liquid Chromatography lab for a biotechnology company in Research Triangle Park. Within a year, she advanced to a team leader position, where she worked for two years while seeking a return to her ecological roots. She found this opportunity at North Carolina State University, where she is pursuing a Master of Science in Forestry. Her thesis research encompasses statistics, plant community ecology, silviculture, coding, and botany. She aims to leverage this expertise in a future ecology-related role.

ACKNOWLEDGMENTS

I thank Dr. Jodi Forrester for her unwavering support, expert guidance, and enduring patience throughout my graduate studies and this research project. Her belief in my potential made this work possible. I also thank Dr. Jeffrey Doser for serving on my graduate committee and for his invaluable assistance with statistical analyses. My sincere appreciation goes to Drs. Robert Scheller and Tara Keyser for their thoughtful insights and readiness to discuss experimental design. I extend my gratitude to Morgan Arteman for her extensive knowledge of graduate program logistics, mentorship as I returned to academia, and her steadfast encouragement.

I wish to thank the researchers, technicians, and volunteers at Bent Creek Experimental Forest who established and maintained the Southern Appalachian Femelschlag Experiment and collected the three years of field data underpinning my analyses. In particular, I am grateful to Brandy Benz, Philip Whiting, and Antigone Burke for their help with vegetation and biomass surveys, and to Jacqui Adams, Ruth Cumberland, Elin Swank, and Tracy Roof for their invaluable contributions during the 2014, 2021, and 2022 sampling seasons. I also appreciate the faculty, staff, and students of the Forestry Department for fostering such a collaborative research environment.

I owe profound thanks to my teachers who first kindled my passion for the natural world: Ms. Manning, my first-grade environmentalist and nature-loving teacher at Frank Porter Graham Elementary School, and Stefan Klakovich, my AP Environmental Science instructor at Carrboro High School, for fostering environmental stewardship at an early age.

Finally, I extend heartfelt thanks to my friends and family: to my partner, William Ragland, for his constant encouragement; to my roommate and best friend, Beck Jones, for

comic relief and unwavering support; and to my loving family—Brittany, Jack, and Sandy Snyder; my aunt, Sandy Carrithers; and my uncle, Alexander Bergo—for always pushing me to persevere. I am especially grateful to my father, Chris Snyder, for instilling in me an appreciation for North Carolina's native flora and its importance for landscape and wildlife. I also thank my lab mates—Morgan Arteman, Thomas Hatling, Bini Dahal, Kevin McCarthy, and Reid Pitts—for their camaraderie, thoughtful feedback on presentations, and willingness to lend a hand whenever challenges arose.

TABLE OF CONTENTS

LIST OF TABLES

LIST OF FIGURES

CHAPTER 1 : INTRODUCTION

Background

Temperate forests represent globally significant reservoirs of biodiversity and provide critical ecosystem services, including carbon storage, atmospheric regulation, and wildlife habitat provision. Within this broader context, Southern Appalachian forests emerge as some of the most species-rich temperate ecosystems in eastern North America, distinguished by their exceptional understory vascular plant diversity that underpins essential ecosystem processes. These forests exemplify the complex, multi-layered structure characteristic of temperate ecosystems, where ground-layer vegetation serves as the principal reservoir of vascular plant diversity despite contributing less than 1% of total aboveground biomass (Muller 2003; Gilliam 2007; Spicer et al. 2020).

The importance of understory communities extends beyond their modest biomass contribution. Ground-layer vegetation, encompassing herbaceous species, woody seedlings, and low shrubs, harbors up to 80% of total vascular plant species richness compared to just 7% for trees (Spicer et al. 2020; Gilliam 2007). This remarkable diversity reflects the "downshifted" vertical distribution of biodiversity characteristic of temperate forests, where most species achieve maturity within the first two meters above ground (Spicer et al. 2020). The ecological significance of this stratum is magnified by its disproportionate contribution to ecosystem functioning. Despite minimal biomass representation ground-layer vegetation accounts for 1-22% of annual carbon flux to soil through rapid litter production, exhibits nutrient concentrations 1.5 to 5 times higher than overstory foliage, contributes 10-40% of total forest evapotranspiration (Landuyt et al. 2019), and determines the future overstory composition.

Recent decades have witnessed profound changes in the structure and composition of Southern Appalachian forests, primarily driven by altered disturbance regimes and their cascading ecological effects. Historically, these forests were maintained as relatively open, oak-dominated systems through frequent low- to moderate-intensity fires, often initiated by Native Americans (Nowacki and Abrams 2008). The widespread exclusion of fire throughout the twentieth century has precipitated a fundamental shift in forest dynamics, which in turn initiated a process known as mesophication—a positive feedback cycle whereby shade-tolerant, fire-sensitive species progressively create conditions favoring their own persistence while suppressing fire-adapted oaks (Nowacki and Abrams 2008; Alexander et al. 2021). This transformation manifests as increasingly dense, closed-canopy conditions dominated by mesophytic species such as maples, beech, and cherries, fundamentally alter light regimes and understory conditions (Abrams and Nowacki 1992; Nowacki and Abrams 2008; Alexander et al. 2021).

Central to these ecological changes is the "oak regeneration bottleneck," a phenomenon whereby oak seedlings persist in understory layers but fail to advance into sapling and midstory size classes due to intense competition from mesophytic species and the absence of fire-mediated release mechanisms (Nowacki and Abrams 1992; Alexander et al. 2021). This demographic constraint threatens the long-term persistence of oak-dominated ecosystems and their associated biodiversity, as mature oaks lack adequate recruitment to sustain their dominance over successional timescales. The consequences extend beyond single-species concerns, as oak decline fundamentally alters forest structure, microclimate conditions, and the complex ecological relationships that support diverse understory plant communities (Alexander et al. 2021; Rodewald 2003).

In response to the structural simplification and regeneration challenges driven by mesophication, managers have increasingly turned to disturbance-based approaches—including timber harvesting and prescribed fire—to restore ecological complexity and promote oak recruitment. However, the effects of such interventions on ground-layer plant diversity are complex and context-dependent. A growing body of studies indicates that conventional timber harvesting often does not reduce ground-layer species richness, although outcomes vary with harvest method and stand development stage (Roberts & Gilliam, 2003; Moola & Vasseur, 2008; Duguid & Ashton, 2013). For instance, a global meta-analysis of 96 temperate-forest studies reported no overall change in understory richness (+4.9% SMD = 0.02; 95% CI –0.24 to 0.29;), with only uneven-aged (selection) treatments enhancing richness (+30%; SMD = 0.97; 95% CI 0.45–1.49; n = 20). Even-aged clearcut, shelterwood and thinning regimes showed no effect, while very late-successional (> 50 yr) clearcut stands had suffered a 28% decline in richness (SMD = –1.54; 95% CI –2.85 to –0.24; n = 16; Duguid & Ashton 2013).

The Southern Appalachian Femelschlag Experiment (SAFE) was developed in response to these challenges, aiming to test whether an expanding-gap silvicultural approach can overcome the oak regeneration bottleneck while sustaining ground-layer diversity under a realistic, disturbance-based management regime. By explicitly creating and then progressively enlarging canopy openings, the SAFE, established within the Pisgah Ranger District of the Pisgah National Forest (35°28′N, 82°40′W), directly addresses this oak regeneration bottleneck by providing the disturbance-mediated release mechanisms historically supplied by fire. In its initial entry, the SAFE functions analogously to a conventional group-selection system, creating discrete canopy gaps that mirror many uneven-aged forestry approaches. Unlike static selection cuts, the SAFE's gaps are intentionally designed to enlarge over successive entries—emulating

the natural expansion of canopy openings through intermediate-scale disturbances and fire regimes. As these gaps expand beyond their initial 0.1–1.3 ha footprints, we anticipate that edge-released oak and hickory advance from the adjacent intact canopy, accelerating recruitment at the gap margins and gradually shifting microsite light and soil conditions deeper into the matrix. This dynamic, multi-entry framework thus not only tests immediate responses in biomass and diversity but also offers a mechanistic window into how progressive gap enlargement may sustain oak-hickory regeneration and reshape understory community assembly over the full 100-year Femelschlag rotation.

The SAFE provides a unique research platform for examining how gap-based silviculture influences understory vegetation dynamics across multiple scales of ecological organization. Established across 60 ha divided into nine relatively homogeneous forest units, the SAFE employs a rigorous experimental design featuring three treatment categories for the initial harvests: large gaps (0.7-1.3 ha), small gaps (0.1-0.4 ha), and uncut controls, each randomly assigned to three replicate units (Figure 1.1). The experimental framework incorporates two gap sizes reflecting different scales of natural disturbance: smaller gaps approximating the upper limit of openings created by minor natural disturbances in old-growth forests (Runkle 1982), and larger gaps simulating intermediate-scale events such as hurricanes and ice storms (McNab et al. 2004; Mou and Warrillow 2000). This dual-treatment approach creates diverse light environments intended to enhance conditions for oak and hickory establishment while simultaneously affecting understory plant communities and broader ecosystem processes.

The mixed-oak forests of the Blue Ridge Physiographic Province in North Carolina's southern Appalachian Mountains, where this study was conducted, represent some of the most botanically diverse temperate forest systems in North America, with 175 unique species

identified in this study across the experimental framework. This remarkable species richness highlights the multi-layered complexity of understory plant communities. Forbs are the dominant component, comprising 93 species (53% of total richness), followed by 27 tree species, 17 shrub species, 15 ferns, 13 vines, 8 graminoids, and 2 subshrubs. This distribution pattern, in which herbaceous species constitute the majority of plant diversity, reflects the characteristic "downshifted" vertical distribution of biodiversity in temperate forests and provides critical context for the ecological processes examined in both thesis chapters (Spicer et al. 2020).

My thesis investigates the multifaceted responses of understory vegetation to gap-based silviculture through two complementary research chapters. Both research components utilize complex sampling designs that capture the full gradient of disturbance effects from gap centers through edge environments to undisturbed forest conditions (Figure 1.2). Ground-layer subplots positioned along cardinal-direction transects at 7.5-meter intervals provide comprehensive spatial coverage of treatment effects, while systematic aggregation into ecologically meaningful treatment zones enables robust statistical analysis of broad spatial patterns. The temporal framework spans the critical early post-disturbance period (2021-2022) when understory responses are most pronounced, complemented by pre-treatment baseline data (2014) for gap treatments only, which enables assessment of treatment-induced changes relative to natural variability.

The first chapter quantifies understory productivity dynamics by analyzing biomass accumulation across six lifeform groups—trees, shrubs, subshrubs, forbs, graminoids, and ferns—during the second- and third-years post-disturbance. Using a combination of 68 destructive harvests and lifeform-specific allometric equations applied to 504 permanent subplots, we established non-destructive biomass monitoring across the experimental landscape.

Concurrent microclimate data—including photosynthetic photon flux density (PPFD), canopy openness, and soil moisture—provided ecological context for observed biomass patterns (Table 1.1). This integrated approach allowed us to (1) quantify how biomass accumulation and productivity differ among lifeform groups in response to gap creation, (2) analyze the competitive interactions between *Rubus* spp. L. and other co-occurring lifeforms, and (3) relate spatial patterns of productivity to microclimate and canopy structure, particularly light availability, soil moisture, and canopy openness, across gap centers and forest matrices. Together, these objectives advance the understanding of how disturbance-mediated changes in resource availability shape carbon allocation and ecosystem function in managed Southern Appalachian forests.

The second chapter centers on the effects of gap-based silviculture on understory plant species composition and diversity, leveraging a comprehensive growing season dataset that integrates spring and summer surveys into a single, nonredundant record of ground-layer plant occurrences and cover. This research addresses three primary objectives within the SAFE experimental framework. First, it quantifies how canopy gap treatments (large and small) and their spatial zones (centers, edges, forest matrix subplots, and uncut controls) shape growing season species richness and diversity across the disturbance gradient and evaluates how these patterns have shifted from pre-treatment (2014) to within two to three years post-treatment (2021–2022). Second, it characterizes the structuring of the total growing season species pool among treatment zones, thereby identifying which zones support the most diverse and compositionally distinct plant assemblages. Third, it identifies taxa whose specificity to particular treatment zones makes them reliable biological markers of microhabitat conditions during the growing season. Together, these objectives provide a robust assessment of how

expanding-gap silviculture alters spatial and temporal patterns of understory diversity and composition and clarify the mechanisms by which disturbance intensity and spatial context shape community assembly in a Southern Appalachian mixed-oak forest.

The integration of species composition and biomass productivity analyses provides a comprehensive understanding of how gap-based silviculture influences understory vegetation dynamics in Southern Appalachian forests. By quantifying both aboveground biomass accumulation and describing the occurrence of understory species, this dual approach addresses the conservation imperative to maintain diverse plant communities and the practical need to understand productivity trade-offs associated with different management intensities. Examining responses across multiple lifeforms, spatial gradients (gap centers, edges, and forest matrix), and temporal scales (pre-treatment baseline vs. post-treatment surveys) advances mechanistic understanding of carbon dynamics in managed forests while providing actionable guidance for balancing silvicultural objectives with ecosystem conservation goals.

By demonstrating that harvest method, stand age, and structural legacies together shape understory diversity and spatial patterning, these findings inform sustainable management strategies for Southern Appalachian mixed-oak forests, particularly efforts to reconcile oak regeneration goals with the need to conserve understory plant communities under changing disturbance regimes. As climate change, invasive species, and altered fire regimes increasingly pressure these forests, mechanistic insights into how canopy manipulation and light regimes interact to support understory biodiversity will be essential for maintaining ecosystem resilience and function. This thesis leverages those insights to advance both theoretical understanding and practical application of gap-based silviculture in temperate forest management.

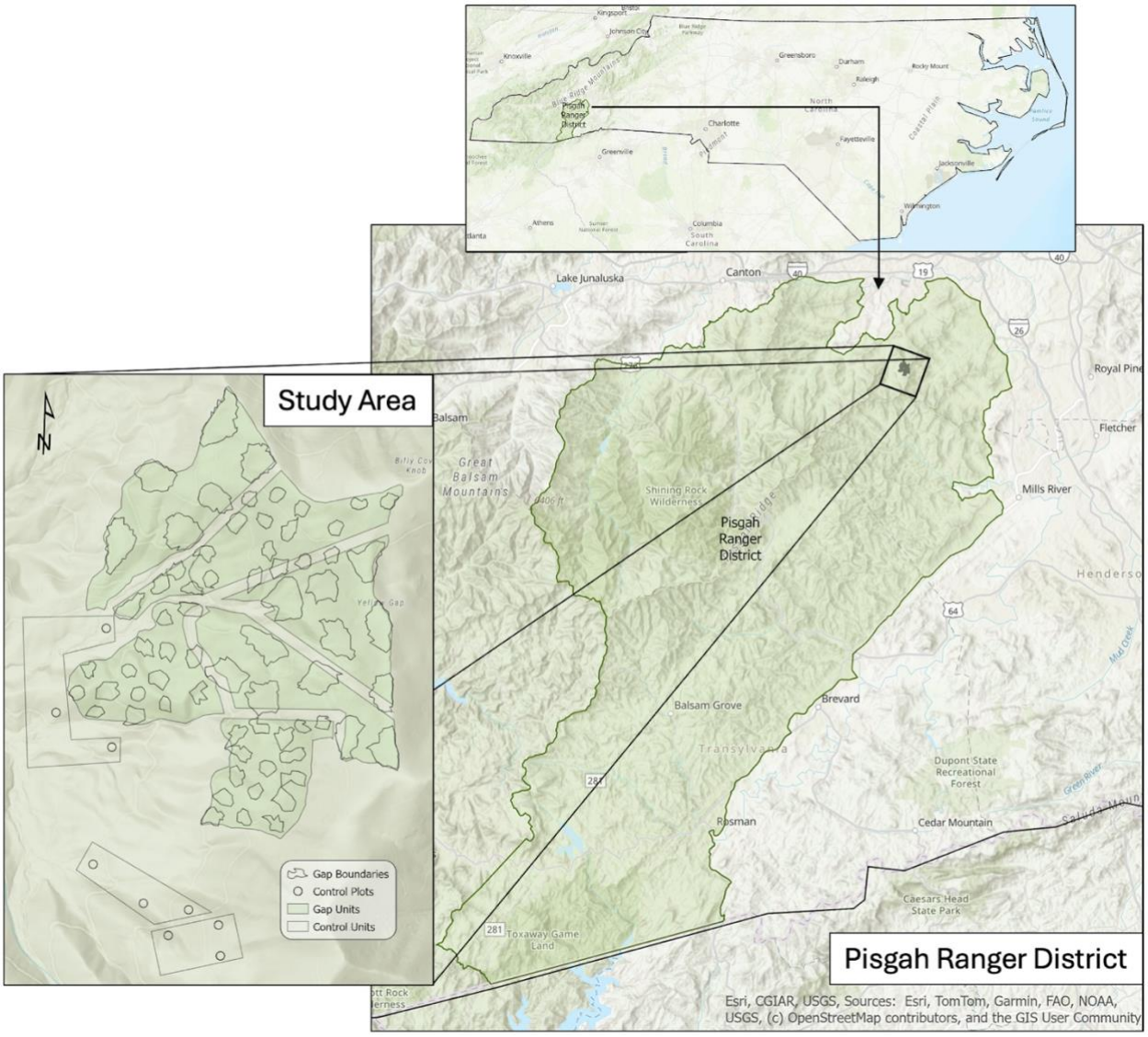

Figure 1.1 Location of the study area within the Pisgah Ranger District, Pisgah National Forest, North Carolina, USA. The main panel shows the boundary of the Pisgah Ranger District (green outline) and the position of the study area (black box). The upper-right inset locates the Pisgah Ranger District in North Carolina. The lower-left inset provides a detailed map of the study area, illustrating gap unit boundaries (light green), control unit boundaries (dark grey outline), and individual gap boundaries (black outlines).

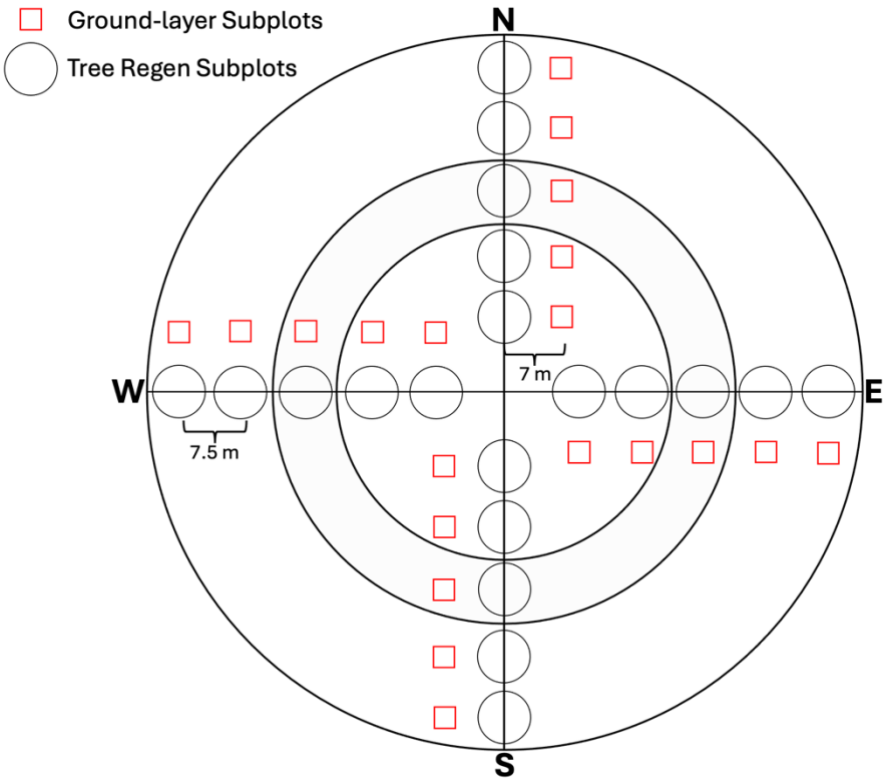

Figure 1.2 Subplot sampling layout within a small canopy gap. Black circles represent regeneration subplots (0.002 ha) and red squares represent ground-layer subplots (1 m²), arranged along cardinal-direction transects at 7.5 m intervals. Transects extend from the gap center, through the gap edge, and into the surrounding forest matrix. Ground-layer subplots are offset by 7 m from regeneration subplots to minimize sampling interference and trampling effects.

Table 1.1 Data collection schedule for vegetation and environmental measurements. Check marks indicate the years when each measurement was conducted.

Year	2014	2021	2022	2024
Measurement				
Spring Herbs		✓	✓	
Summer Herbs	✓	✓	✓	
Summer Biomass		✓		
Spring Biomass				✓
PPFD		✓		
Soil Moisture		✓		
Canopy Openness		✓		

REFERENCES

Abrams, M. D., & Nowacki, G. J. (1992). Historical Variation in Fire, Oak Recruitment, and Post-Logging Accelerated Succession in Central Pennsylvania. Bulletin of the Torrey Botanical Club, 119(1), 19–28. https://doi.org/10.2307/2996916

Abrams, M. D., Orwig, D. A., & Demeo, T. E. (1995). Dendroecological Analysis of Successional Dynamics for a Presettlement-Origin White-Pine-Mixed-Oak Forest in the Southern Appalachians, USA. Journal of Ecology, 83(1), 123–133. https://doi.org/10.2307/2261156

Alexander HD, Siegert C, Brewer JS, Kreye J, Lashley MA, McDaniel JK, Paulson AK, Renninger HJ, Varner JM. 2021. Mesophication of oak landscapes: evidence, knowledge gaps, and future research. BioScience. 71(5):531–542. https://doi.org/10.1093/biosci/biaa169

Duguid, M. C., & Ashton, M. S. (2013). A meta-analysis of the effect of forest management for timber on understory plant species diversity in temperate forests. Forest Ecology and Management, 303, 81–90. https://doi.org/10.1016/j.foreco.2013.04.009

Gilliam, F. S. (2007). The ecological significance of the herbaceous layer in temperate forest ecosystems. BioScience, 57(10), 845–858. https://doi.org/10.1641/B571007

Landuyt D, De Lombaerde E, Perring MP, et al. (2019) The functional role of temperate forest understory vegetation in a changing world. Glob Change Biol. 2019; 25: 3625–3641. https://doi-org.prox.lib.ncsu.edu/10.1111/gcb.14756

McNab, W., Greenberg, C. H., & Berg, E. C. (2004). Landscape distribution and characteristics of large hurricane-related canopy gaps in a southern Appalachian watershed. Forest Ecology and Management, 196(2-3), 435-447. https://doi.org/10.1016/j.foreco.2004.04.004

Moola, F.M., Vasseur, L., 2008. The maintenance of understory residual flora with even-aged forest management: A review of temperate forests in northeastern North America. Environmental Reviews 16, 141. https://doi-org.prox.lib.ncsu.edu/10.1139/A08-005

Mou, P., & Warrillow, M. P. (2000). Ice Storm Damage to a Mixed Hardwood Forest and Its Impacts on Forest Regeneration in the Ridge and Valley Region of Southwestern Virginia. The Journal of the Torrey Botanical Society, 127(1), 66–82. https://doi.org/10.2307/3088748

Muller, R.N. (2003). Nutrient relations of the herbaceous layer in deciduous forest ecosystems. In: Gilliam, F.S. and Roberts, M.R. (eds) The herbaceous layer in forests of eastern North America, pp. 15–37. Oxford University Press, New York.

Nowacki, G. J., & Abrams, M. D. (1992). Community, edaphic, and historical analysis of mixed oak forests of the Ridge and Valley Province in central Pennsylvania. Canadian Journal of Forest Research. 22(6): 790-800. https://doi-org.prox.lib.ncsu.edu/10.1139/x92-108

Nowacki, G. J., & Abrams, M. D. (2008). The Demise of Fire and "Mesophication" of Forests in the Eastern United States. BioScience, 58(2), 123-138. https://doi.org/10.1641/B580207

Roberts, Mark R, and Frank S Gilliam, 'Response of the Herbaceous Layer to Disturbance in Eastern Forests', in Frank S Gilliam, and Mark R Roberts (eds), *The Herbaceous Layer in Forests of Eastern North America* (New York, NY, 2003; online edn, Oxford Academic, 31 Oct. 2023), https://doi.org/10.1093/oso/9780195140880.003.0013, accessed 10 Nov. 2025.

Rodewald, A.D. 2003. Decline of oak forests and implications for forest wildlife conservation. Natural Areas Journal. 23: 368-371.

Runkle, J.R. (1982), Patterns of Disturbance in Some Old-Growth Mesic Forests of Eastern North America. Ecology, 63: 1533-1546. https://doi.org/10.2307/1938878

Spicer, Michelle & Mellor, Hannah, & Carson, Walter. (2020). Seeing beyond the trees: a comparison of tropical and temperate plant growth forms and their vertical distribution. Ecology. 101. https://doi.org/10.1002/ecy.2974

stevemorgan1. 2024. Pisgah Ranger District [Pisgah_Ranger_District]. ArcGIS Online. Item ID: eb0b87ad2de64713a140e4228c98198c. Available at: https://services.arcgis.com/zTM0LZtJeE1HzO09/arcgis/rest/services/Pisgah_Ranger_District/FeatureServer [Accessed 4 July 2025].

CHAPTER 2 : EARLY SUCCESSIONAL DYNAMICS IN SOUTHERN APPALACHIAN MIXED-OAK FORESTS: THE ROLE OF SPATIAL HETEROGENEITY AND PLANT LIFEFORM RESPONSES

Abstract

Understanding how spatial heterogeneity and plant lifeform groups responses shape early successional dynamics is critical for sustainable management of temperate mixed-oak forests. We examined ground-layer abundance patterns following canopy gap creation in the Southern Appalachian Femelschlag Experiment (SAFE), a large-scale field experiment designed to emulate natural disturbance regimes and promote oak and hickory regeneration. We quantified aboveground biomass across plant lifeforms (trees, shrubs, subshrubs, forbs, graminoids, ferns, and vines) in 0.1–0.4 ha and 0.7–1.3 ha gaps as well as controls, using a combination of destructive sampling and allometric modeling. Mixed-effects models assessed the effects of gap size, spatial position, and microenvironmental gradients on biomass accumulation over the first three years post-treatment. Results revealed that proximity to gap centers, rather than gap size, was the primary driver of ground-layer productivity, with the highest biomass observed at gap centers and a marked decline toward the forest matrix. *Rubus* spp. and graminoids exhibited pronounced increases in gap centers, while tree and vine biomass responses varied with aspect and microhabitat. Contrary to expectations, soil moisture did not change significantly following disturbance, and gap size had minimal effect on total biomass during the study period. These findings highlight the importance of fine-scale spatial variation and plant lifeform dynamics in shaping early forest recovery, with implications for balancing regeneration goals, carbon cycling, and long-term ecosystem resilience in managed temperate forests.

Introduction

Temperate forest ecosystems are globally important reservoirs of biodiversity and provide essential ecosystem services. While the structural dominance of trees has long shaped perceptions of forest function, research increasingly highlights the pivotal role of the herbaceous layer in sustaining forest health, productivity, and resilience. Despite accounting for less than 1% of aboveground biomass, this layer contributes disproportionately to net primary productivity, nutrient cycling, and overall biodiversity, often harboring up to 80% of total vascular plant diversity compared to just 7% for trees (Muller 2003; Gilliam 2007; Spicer et al. 2020).

Expanding this perspective to the entire ground layer—including herbaceous species, woody seedlings, and low shrubs—reveals that this stratum plays an important but context-dependent role in temperate forest ecosystem functioning. The ground layer directly contributes to processes such as carbon assimilation, nutrient uptake, and evapotranspiration, with its relative significance varying by forest type, stand age, and environmental conditions (Landuyt et al. 2019). While typically a smaller component than the overstory, the ground layer supports disproportionately high rates of biomass turnover and is characterized by elevated foliar nutrient concentrations—often 1.5 to 5 times greater than those in the canopy. These attributes can enable the ground layer to contribute as much as 1–22% of annual carbon fluxes to the soil, especially during early successional stages or in open-canopied stands (Landuyt et al. 2019). These patterns reflect the high nutrient assimilation efficiency of herbaceous species, in particular, whose fine roots are concentrated in nutrient-rich surface soils, facilitating effective uptake of essential elements such as nitrogen, phosphorus, magnesium, and potassium (Bakker et al. 2006; Jobbágy and Jackson 2001).

The critical importance of the ground-layer is matched by its vulnerability. Many ground-layer species—particularly herbaceous plants—are inherently susceptible to environmental changes, leading to an elevated risk of extinction (Levin and Wilson 1976). This vulnerability highlights the importance of forest management strategies incorporating considerations for the entire ground-layer, including herbaceous species and low woody plants. Integrated, adaptive management approaches—including targeted disturbance regimes, invasive species control, and monitoring of ground-layer composition—are essential for sustaining biodiversity and ecosystem processes in temperate forests. Additionally, the ground-layer supports critical ecological functions such as providing habitat and floral resources for insect pollinator communities and modulating tree regeneration. Studies have shown that reducing tree basal area, which leads to increased ground-layer cover, enhances the abundance and richness of pollinator species in the short term by increasing floral resource availability and habitat heterogeneity (Campbell et al. 2007; Romey et al. 2007). However, these benefits are often transient, such as shifts in ground-layer composition and the proliferation of competitive taxa like *Rubus* spp. L., can impede the regeneration of target tree species and alter successional trajectories if not actively managed (Tappeiner et al. 1991).

The consequences of overlooking ground-layer dynamics are exemplified by the emergence of recalcitrant understory layers—dense, persistent herbaceous or woody vegetation strata that can profoundly alter forest regeneration trajectories by suppressing tree establishment and growth. Interactions between canopy disturbance and altered understory conditions often give rise to these layers. Anthropogenic activities such as logging, fire suppression, and chronic overbrowsing by herbivores frequently exacerbate their development (Royo and Carson 2006).

For example, in Pacific Northwest forests, post-logging disturbances can lead to the proliferation of salmonberry (*Rubus spectabilis* Pursh) thickets, with densities reaching up to 300% higher than those in undisturbed stands. These dense thickets create persistent physical barriers that impede conifer regeneration for decades (Tappeiner et al. 1991). Similarly, in the northeastern United States, chronic overbrowsing and canopy opening has facilitated the expansion of hay-scented fern (*Dennstaedtia punctilobula* (Michx.) T. Moore), which has increased from historically rare occurrences of less than 3% cover (Lutz 1930) to dominance across more than 30% of forest floors, thereby displacing hardwood seedlings (De La Cretaz and Kelty 2002). In boreal forests, the grass *Calamagrostis canadensis* (Michx.) P. Beauv. can delay white spruce (*Picea glauca* (Moench) Voss) stand development by 20 to 30 years, primarily through light competition that prolongs successional transitions (Lieffers et al. 1993). These cases collectively illustrate how management decisions, such as logging intensity and control of herbivore populations, directly shape understory dynamics and, if not carefully monitored, may inadvertently trigger long-term successional arrest by facilitating the establishment and persistence of recalcitrant layers.

These challenges do not exist in isolation. Changes in historical disturbance regimes, primarily due to fire suppression, have led to a dramatic decline in the persistence of numerous oak species from the overstory and midstory into the sapling and seedling layers of forests across the Eastern United States since the 1930s (Nowacki and Abrams 2008). This shift has resulted in more homogenized forest structures than past landscapes and has influenced the process of mesophication in Eastern hardwood forests. Mesophication, the gradual increase in the abundance of shade-tolerant and moisture-loving species, varies along stand and environmental gradients, with its intensity depending on specific functional traits. For example, mesophication

is more advanced in areas with acidic soils, which exhibit a higher prevalence of shade- and drought-tolerant traits (Woodbridge et al. 2020). These changes in forest composition, including differences in light quantity and quality and shifts in soil moisture, could lead to shifts in species composition, thereby altering the overall forest diversity, including the understory layer.

A large-scale field experiment was established in a Southern Appalachian mixed oak forest to test the outcome of an expanding gap silvicultural approach designed to mimic the small-scale to moderate disturbances historically characteristic of this region. The experiment includes two gap-based treatments to regenerate oak and hickory species through a 100-year Femelschlag management plan. The small-gap treatment targets a gap size of 0.1 ha, at the upper limit of gap sizes typically formed by small-scale natural disturbances in old-growth forests (Runkle 1982). The large-gap treatment simulates intermediate-scale disturbance events, such as those caused by hurricanes or ice storms, with a target gap size of 0.4 ha (McNab et al. 2004; Mou and Warrillow 2000). This size reflects the upper limit of gaps formed by significant disturbance events documented in the Southern Appalachians, such as those resulting from Hurricane Opal (McNab et al. 2004). Both treatments are designed to diversify the light environment, promoting oak and hickory regeneration while influencing the herbaceous layer and overall forest dynamics.

This study investigates how canopy gaps—emulating natural disturbance regimes—affect understory productivity in Southern Appalachian forests, with implications for carbon assimilation and ecosystem function. While the ground-layer contributes disproportionately to nutrient cycling and carbon turnover relative to its biomass, the role of individual lifeforms in driving net primary productivity across spatial and microhabitat gradients in gap-driven systems is not yet fully characterized, despite recent advances in quantifying total ground-layer

productivity. Using data from the Southern Appalachian Femelschlag Experiment (SAFE), we assess temporal and spatial biomass dynamics across lifeform groups (trees, shrubs, subshrubs, forbs, graminoids, ferns) during the second- and third-years post-gap creation. By comparing small gaps, large gaps, and controls, we evaluate how gap size and microhabitat (center, edge, forest matrix) mediate productivity along cardinal light gradients. Lifeform-specific responses are critical to resolve, as ruderal taxa like *Rubus* spp., an important subshrub species, may dominate post-disturbance carbon assimilation but suppress slower-growing woody regeneration, creating tradeoffs between short-term productivity and long-term carbon sequestration.

We examined interactions between *Rubus* spp. and other co-occurring lifeforms to better understand competitive dynamics in the ground layer. To contextualize observed biomass patterns, we also considered associated microclimate and canopy structure variables—specifically, light availability, soil moisture, and canopy openness. While these environmental variables were not included as predictors in the biomass models, they provide important ecological context for interpreting the drivers of variation in understory productivity. Spatial productivity gradients within gaps refine our understanding of microhabitat-driven carbon allocation, particularly at transitions between gap centers and forest matrices. This work furthers ecological models of carbon dynamics in managed forests by integrating lifeform-specific responses with environmental factors such as light and moisture that are altered by disturbance. The findings offer a framework to balance silvicultural objectives, such as promoting regeneration, conserving the ground-layer's functional capacity to sustain carbon assimilation, nutrient cycling, and ecosystem resilience.

Materials and Methods

STUDY SITE

The 60-hectare study site, known as the Southern Appalachian Femelschlag Experiment (SAFE; 35°28′N, 82°40′W), is in the Blue Ridge Physiographic Province of the southern Appalachian Mountains, North Carolina, USA (Fig. 1.1). It is part of the Pisgah Ranger District within Pisgah National Forest, characterized by mountainous terrain with steep slopes averaging approximately 75° (range 66–81°). The experimental gaps within the site have aspects averaging 266° for large gaps (just east of due west) and 247° for small gaps (southwest), resulting in most gaps facing west or southwest. Elevations range from 847 m to 1117 m (Grover 2020). Site productivity varies with topographic position, with lower, moister slopes supporting greater productivity than drier ridges. The site index (SI; base age 50) for mixed oaks ranges from 17 m to 29 m along the topographic gradient, and the subset of plots used in this study includes plots with SI ≥ 21.3 m. The underlying geology is primarily felsic to mafic high-grade metamorphic biotite and granitic gneisses (Hadley and Nelson 1971). Soils are predominantly Inceptisols and Ultisols, ranging from shallow to deep, well-drained, and moderately to extremely acidic, with textures from coarse-loamy to clayey (Allison and Hale 1997).

The study area has milder winters and longer, warmer summers. The average minimum and maximum air temperatures for 1993–2023 were 5.82°C and 19.13°C, respectively. The mean annual precipitation is 1,084.85 mm (1993–2023). Mean annual air temperature reported from a nearby weather station (Candler 1 W) was 13.3°C, 12.9°C, 12.6°C, and 14.1°C and yearly precipitation was 1574 mm, 1221 mm, 1226 mm, and 771 mm across the years 2020, 2021, 2022, and 2023, respectively (North Carolina State Climate Office, NC State University 2024; Fig. 2.2).

The stand is a mature, second-growth upland hardwood mixed-oak forest that naturally regenerated around the 1920s, following federal acquisition and prior Indigenous management. Historical land use practices included high-grading, land clearing, and domestic livestock grazing. The area has also experienced significant disturbances, including ice storms, droughts, disease (e.g., chestnut blight), and hurricanes, affecting stand growth over short and long periods (Grover et al. 2023). The main overstory species include various oaks (*Quercus alba L.*, *Q. rubra* L., *Q. montana* Willd., *Q. coccinea* Münchh., and *Q. velutina* Lam.), and hickories (*Carya cordiformis* (Wangenh.) K. Koch, *C. glabra* (Mill.) Sweet, *C. ovalis* (Wangenh.) Sarg. and *C. tomentosa* (Lam.) Nutt.), and tulip poplar (*Liriodendron tulipifera* L.). The midstory comprises shade-tolerant species such as sourwood (*Oxydendrum arboreum* (L.) DC.), flowering dogwood (*Cornus florida* L.), black gum (*Nyssa sylvatica* Marshall), and red maple (*Acer rubrum* L.). The oldest trees, particularly *Quercus alba*, have an average age of 151 years, ranging from 91 to 215 (Grover et al. 2023). The forest structure is typical of mixed hardwood stands in the region, with an average basal area of 37 $m^2\ ha^{-1}$ and a density of 1086 stems ha^{-1}. In Buncombe County, white-tailed deer density was estimated at 11-20 deer per square mile as of 2020 (North Carolina Wildlife Resources Commission 2020).

Pre-treatment vegetation inventories followed the methods described by Grover et al. (2023). Initial harvests were conducted in fall - winter of 2019 with the intention of regenerating oak and hickory. Merchantable trees were hand-felled and removed via skidders and forwarders while unmerchantable material was cut post-harvest and retained on site. A midstory removal treatment was conducted (summer 2019) throughout the entire stand with all stems <20 cm dbh of non-mast producing species were injected with herbicide. This treatment retained *Quercus*, *Carya*, *Ilex* L., and *Cornus* species, resulting in an average basal area removed of 1.45 $m^2\ ha^{-1}$.

STUDY DESIGN

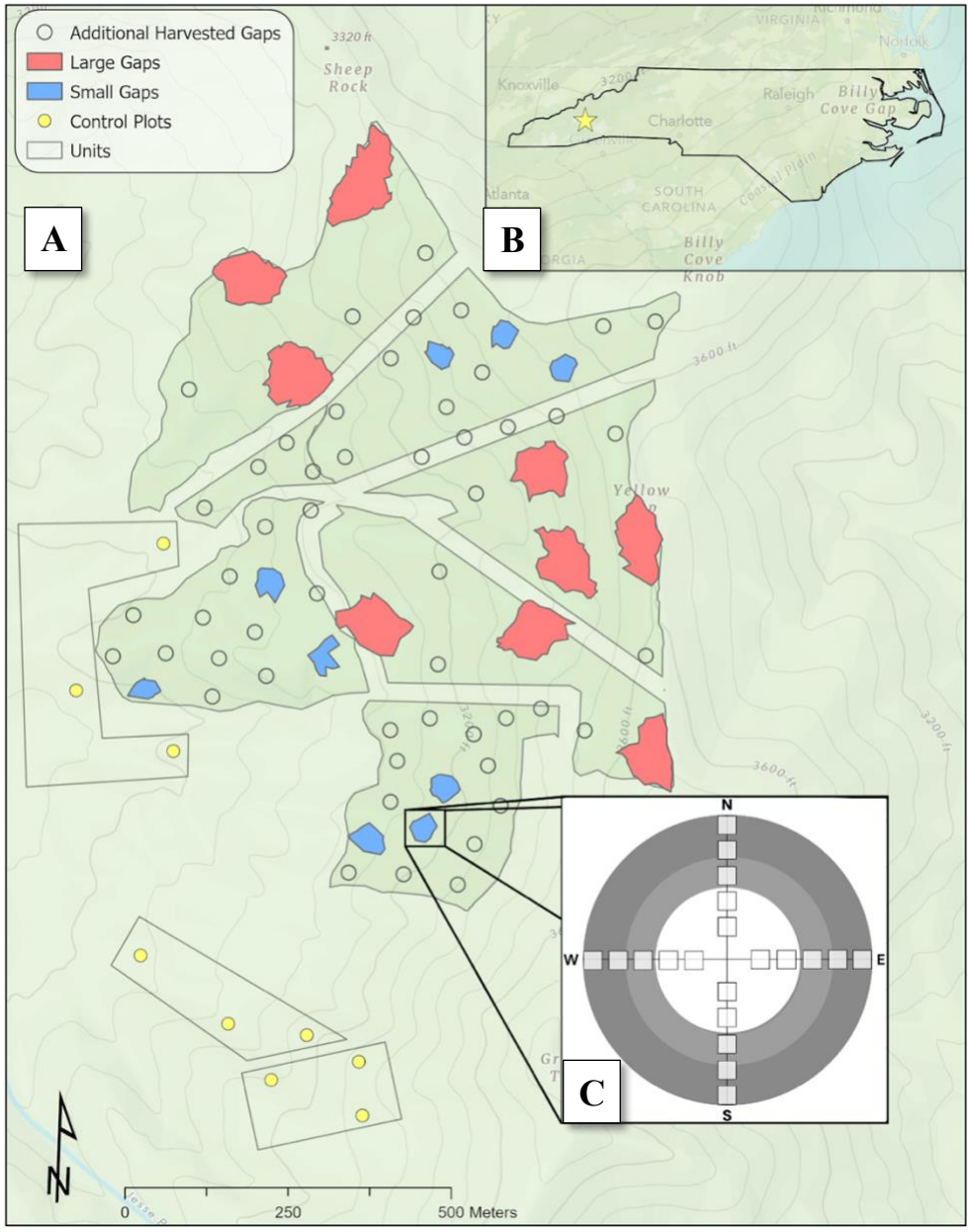

Figure 2.1 (A) Topographic map of the Southern Appalachian Femelschlag Experiment (SAFE) study area, showing nine experimental units (six experimental and three control) and the spatial arrangement of sampled large gaps, small gaps, and control plots . Hollow circles indicate additional gap locations that were not measured in this study. (B) Inset map showing the location of the study site in western North Carolina. (C) Schematic of subplot layout within a small gap. The larger circular area represents a single "plot," corresponding to a specific gap or control location. Transects are oriented along cardinal directions , and the principal ecological zones sampled include gap interior (white), gap edge (grey), and forest matrix (dark grey). The small individual squares within the schematic represent "subplots" placed at defined intervals along each transect. Each subplot is a discrete sampling unit where measurements were collected. Neither the schematic nor the inset map is to scale.

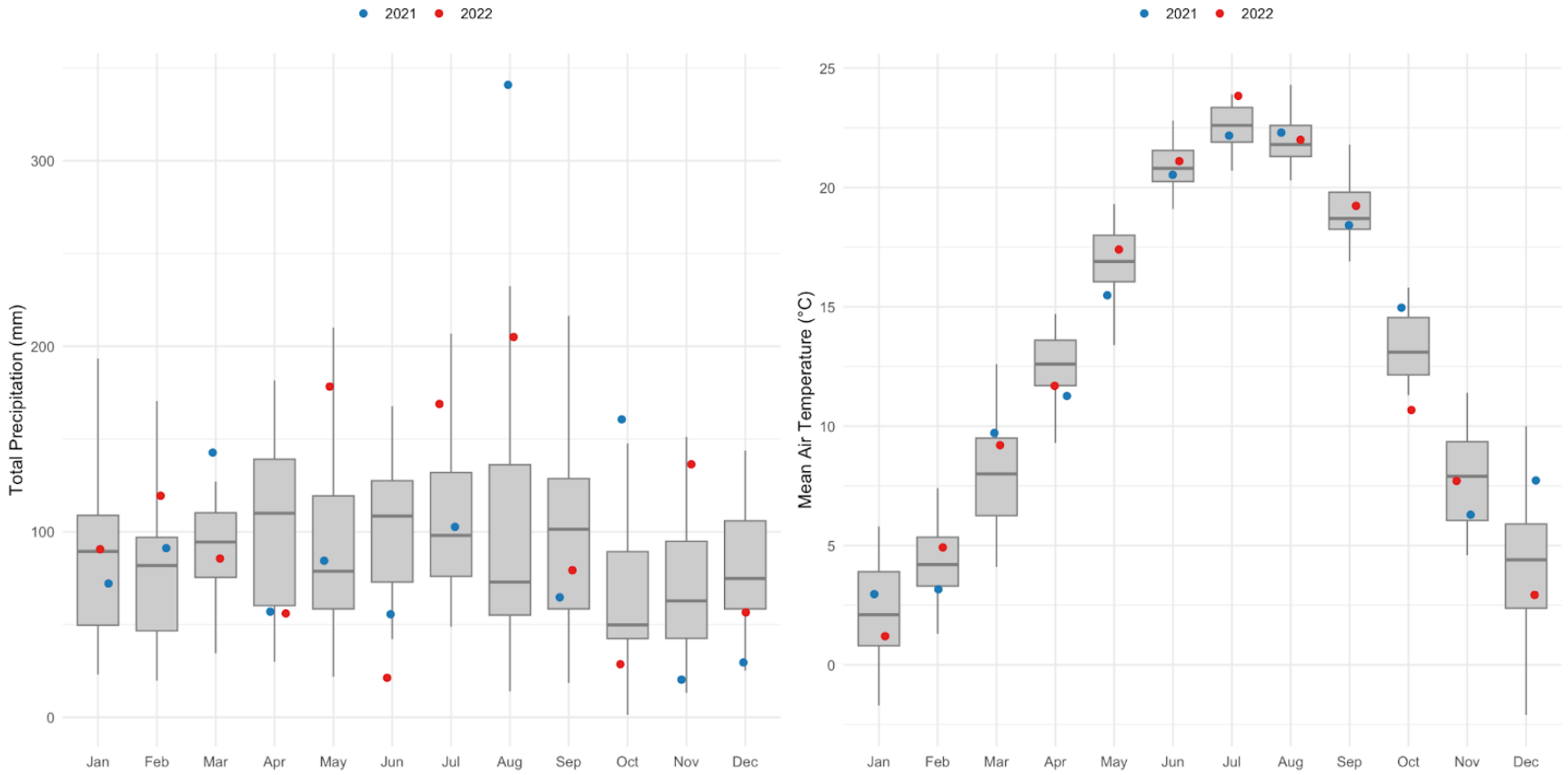

Figure 2.2 Monthly comparison of 2021–2022 study-period climate against 27-year baseline (1993–2020) at Candler 1 W Station, NC. Gray boxplots show the distribution of (a) total monthly precipitation (mm) and (b) mean monthly air temperature (°C) over the 27-year baseline; overlaid points indicate individual months in 2021 (blue) and 2022 (red), data from North Carolina State Climate Office, NC State University 2024.

The Southern Appalachian Femelschlag Experiment (SAFE) was implemented across nine forest units in Pisgah National Forest, North Carolina, with each experimental unit randomly assigned to one of three treatments: large canopy gaps (0.7–1.3 ha), small canopy gaps (0.1–0.4 ha), or unharvested controls, ensuring three units per treatment type (see Fig. 2.1A). In this study, a plot refers to one discrete sampling location—either a large gap, small gap, or uncut control area—within a treatment unit. Plot centers were positioned using a grid system spaced 60–80 meters apart based on stand size and gap configuration.

Within each plot, subplots were systematically arranged along four cardinal-direction transects radiating from the plot center, allowing comprehensive coverage of ecological gradients from gap center through the edge and into the surrounding forest matrix (see Fig. 2.1C). Transects accommodated two main types of permanent subplots: regeneration subplots—circular plots of 0.002 ha for surveying seedlings and saplings less than 1.5 cm DBH—and ground-layer subplots, each 1 m^2 in size, spaced at regular 7.5-meter intervals from the plot center outward. To minimize trampling disturbance, ground-layer subplots were offset by 7 meters from regeneration subplots along each transect (Fig. 1.2).

The number and spacing of subplots varied by treatment to match the physical dimensions and spatial context of large gaps, small gaps, and controls. Large gap plots each consisted of 24 ground-layer subplots—six spaced at 7.5-meter intervals along each transect—extending from the center of the gap up to 22.5 meters into the matrix, offering the greatest sampled distance from the gap edge. Small gap plots contained 20 subplots per plot (five per transect), ranging from gap center to a maximum distance of 15 meters into the matrix from gap edge. Control plots included 12 subplots (three per transect), positioned at 0 meters (plot center), 7.5 meters, and 15 meters from the designated center along each cardinal direction. This spatial

arrangement provided consistent and ecologically meaningful sampling coverage, enabling fine-scale investigation of vegetation and microclimate responses across varying gap sizes and control conditions within the SAFE study area. In this study, all analyses and results focus exclusively on the ground-layer subplots (n = 504), hereby referred to simply as 'subplots.'

DATA COLLECTION

Annual plant cover measurements

Ground-layer vegetation was surveyed annually in all permanent subplots prior to harvest (2014) and during each of the first three summers following harvest (2020–2022). In each subplot, the percent cover of all vascular herbaceous and woody plants less than 1 m tall was visually estimated at the species level. Species were identified using the USDA PLANTS database (USDA, NRCS 2025). Cover estimates were recorded in seven ordinal classes (<1%, 1–<5%, 5–<25%, 25–<50%, 50–<75%, 75–<95%, and 95–100%), and the midpoint of each class was used for analysis.

Plant biomass measurements

In summer 2021, 63 destructive subplots (1 m^2 each) were established across all treatments to collect representative ground-layer biomass samples. For each treatment—large gap, small gap, and control—subplots were distributed among experimental units, with randomly selected plots per treatment and three destructive subplots per selected plot placed along the northeast transect. For gap plots, destructive subplots were installed at approximately 5 m, 10 m, and gap edge; in controls, subplots were installed at 5 m, 10 m, and 15 m from the plot center. To ensure broader representation of vegetation types and lifeforms, fifteen additional "targeted" destructive subplots were established as needed, yielding a total of 78 destructive subplots. In

each destructive subplot, total vegetation cover and cover by lifeform (herb, tree, shrub, graminoid, vine, fern/fern ally, and subshrub–*Rubus* spp.) were visually estimated, then all live aboveground plant material (<1 m tall) was clipped to mineral soil, sorted by lifeform, oven-dried at 50°C to constant weight, and weighed to the nearest 0.01 g.

Microclimate and canopy structure

Soil moisture was measured in 2021 at systematically spaced regeneration subplots coinciding with cardinal transects across gradients from gap center to forest matrix. Sampling locations corresponded to defined spatial positions (e.g., for small gaps: +15 m forest matrix, +7.5 m transition, 0 m edge, –7.5 m mid-center, –15 m center), while in controls, measurements were taken at 0, 7.5, and 15 m from center. Moisture data were collected during three periods (May, June, and October), with two readings per subplot per event, averaged, and transformed into z-scores for analysis; these were subsequently averaged to provide integrated moisture values for each subplot.

Canopy structure was assessed using hemispherical photography at ground-layer subplot locations in summer 2021. Spherical images (Ricoh Theta 360) were taken at multiple heights (1.6–4.75 m), with primary analysis using 1.6 m images to represent understory conditions. Following Wang (2017), panoramic images were converted to hemispherical photos, and canopy openness, direct light, diffuse light, and daily photosynthetic photon flux density (PPFD) were quantified using WinsCanopy software (Regent Instruments, Canada).

DATA ANALYSIS

Development of Biomass Estimation Equations

Allometric relationships between ground-layer biomass (g/m^2) and percent cover were developed to enable non-destructive, repeatable quantification of vegetation responses over time. For each lifeform, biomass measured in destructive clip-quads was regressed against percent cover using five model forms: linear, log-biomass, log-cover, log-log (power), and quadratic. The best-fitting model was selected for each lifeform based on the highest R^2, resulting in a mix of power and linear regressions (see Table 2.1). Power equations were used for ferns, *Rubus* spp., shrubs, vines, and trees; linear equations best fit graminoids and forbs.

To estimate annual subplot biomass, percent cover values for each lifeform (with zero values assigned zero biomass) were input into the corresponding regression equation. For analyses of total aboveground biomass, estimated biomass values for all modeled lifeforms were summed within each subplot, an approach that better accommodates vertical overlap and compositional heterogeneity in the herb layer than direct regression on total cover. Model assumptions were checked by visually inspecting residual and fitted value distributions, and by confirming no systematic directional bias. Model fits were deemed satisfactory for all lifeforms, with only minor deviations from normality for graminoids that did not materially affect biomass estimation.

Table 2.1 Regression equations for estimating biomass (g/m²) from percent cover (x) by lifeform. Models are either power or linear regressions, as indicated. Sample size (*n*), coefficient of determination (R^2), and standard error of estimate (SE) are shown for each model.

Lifeform	*n*	Regression Equation	R^2	SE
Ferns	23	$y = 0.188x^{1.466}$	0.761	1.35
Forbs	59	$y = 1.872x + 2.833$	0.699	27.04
Graminoids	36	$y = 2.200x + 0.592$	0.895	16.24
Rubus spp.	37	$y = 3.090x^{0.740}$	0.462	1.21
Shrubs	15	$y = 1.360x^{1.152}$	0.880	0.62
Trees	65	$y = 0.628x^{1.451}$	0.623	1.32
Vines	51	$y = 0.820x^{1.433}$	0.611	1.27

Data Transformation and Outlier Treatment

To meet model assumptions, a shift constant was added to response variables that required square-root transformation, ensuring all analyzed values were positive. The shift constant was set as the minimum observed value plus 0.1. Thus, transformations were performed as

$$y_{transformed} = \sqrt{y_{original} + c}$$

for datasets with zeros or negatives, or as

$$y_{transformed} = \sqrt{y_{original}}$$

for strictly positive datasets (e.g., PPFD). For percentage data bounded between 0 and 100 (e.g., canopy openness), values were first converted to proportions by dividing by 100. The logit transformation was then applied as,

$$y_{transformed} = log\left(\frac{p}{1-p}\right)$$

where is the proportion value. No shift was required as all values fell within the open interval (0, 1). All hypothesis testing (ANOVAs and pairwise comparisons) was conducted on the transformed scale. Estimated means and differences from the transformed models were not reported. All ecological outliers were retained in analyses after verification against field notes and raw datasets to confirm their plausibility and rule out data entry errors. Although some outlier points influenced residual plots, they were preserved to represent the full observed spectrum of biomass variation.

Subplot Position Standardization and Exclusion Criteria

To ensure balanced inference across a three-way interaction of Treatment × Direction × Distance, one mid-center subplot (–7.5 m) was excluded from large gap plots, bringing their transect subplot counts into alignment with small gaps. Controls retained their original three subplots per transect. Each subplot was assigned a position label reflecting its spatial context relative to the gap edge: Gap Center (GC; –22.5 m in large gaps, –15 m in small gaps), Mid-Center (MC; –15 m in large gaps, –7.5 m in small gaps), Gap Edge (E; 0 m), Transition (T; +7.5 m, adjacent to the gap), and Forest Matrix (F; +15 m, deeper in the forest). These labels (GC, MC, E, T, F) are used consistently across all results and figures.

To avoid zero-inflation and ensure interpretability, only lifeforms present in at least one-third of subplots post-treatment were modeled; forbs, graminoids, *Rubus* spp., trees, and vines were included, while shrubs and ferns—present in fewer than 33% of subplots—were excluded from statistical analysis but included in descriptive summaries. Analyses based on 2020 data (limited to two transects due to COVID-19) were omitted after confirming year-to-year consistency among included years.

Analytical Model Structure and Rationale

Biomass responses for each lifeform and for total biomass were analyzed using a mixed-effects repeated-measures framework tailored to the experimental design and data availability. Three model groups were used (see Table 2.2). Model Group 1 (MG1) compared pre- and post-treatment (2014 vs. 2021/2022) biomass change in large and small gap plots only, with pre-treatment (2014) subplot-level biomass included as a covariate to control for any initial differences in vegetation structure or site productivity among subplots. Fixed effects in MG1 included Year, Treatment, Direction, Distance, and all possible two- and three-way interactions among Treatment, Direction, and Distance; interactions between Year and other effects were not included.

Because controls only had three subplots per transect, gap vs. control models were split: Model Group 2 (MG2) tested whether the rate of biomass change from 2021 to 2022 in gap center, mid-center, and edge subplots differed from control positions (0, +7.5 m, +15 m, respectively); Model Group 3 (MG3) tested whether transition and forest matrix subplots (+7.5 m, +15 m) differed from the same positions in controls, focusing on more distal effects beyond gap edges. Both models included Treatment, Direction, Distance, and all their interactions as fixed effects. No covariates were included, as pre-treatment control data were unavailable for these locations. In all models, random effects reflected the hierarchical sampling design (unit, plot nested within unit, direction nested within plot nested within unit) to account for spatial clustering and repeated measures.

Model Fitting, Diagnostics, and Selection

Model assumptions were first evaluated using residual diagnostic plots, and response variables were transformed where needed to satisfy normality or homoscedasticity requirements.

For all selection and simplification steps involving fixed effects—such as backward stepwise removal of non-significant interactions—models were fit using maximum likelihood estimation to ensure valid likelihood comparisons as fixed model structure changed. Once the minimal adequate model—including only main effects and retained significant interactions—was identified, the final model was refit using restricted maximum likelihood.

All analyses were conducted in R (v4.3.2; R Core Team 2023) with the lme4 (Bates et al. 2015), lmerTest (Kuznetsova et al. 2017), and emmeans (Lenth 2025) packages. Where random effects had zero variance, they were excluded to avoid model singularity, and all main effects were retained given their ecological importance. All Analysis of Variance tables were estimated using Satterthwaite's method for denominator degrees of freedom (as implemented in lmerTest), and Kenward-Roger degrees of freedom adjustment was applied for post hoc pairwise comparisons (as returned by emmeans). P-values for post hoc comparisons were adjusted using Tukey's method to control Type I error.

Table 2.2 Summary of mixed-effects model groups (MG1–MG3) used to analyze ground-layer biomass change in the Southern Appalachian Femelschlag Experiment. Each model group represents a distinct comparison framework, with fixed effects, random effects, and covariates structured to address specific ecological questions about gap size, spatial position, and treatment effects on biomass change.

Model Group	Comparison Type and Years	Treatments Included	Subplots Included	Fixed Effects	Random Effects	Covariates
MG1	pre- vs. post-treatment (2014 vs. 2021/2022)	small gaps, large gaps	GC, MC, E, T, F	gap size, direction, subplot position, year	unit, plot nested in unit, direction nested in plot nested in unit	pre-treatment biomass
MG2	post-treatment (2022–2021)	small gaps, large gaps, controls	GC, MC, E,	treatment, direction, subplot position	unit, plot nested in unit, direction nested in plot nested in unit	none
MG3	post-treatment (2022–2021)	small gaps, large gaps, controls	T, F	treatment, direction, subplot position	unit, plot nested in unit, direction nested in plot nested in unit	none

GC = Gap Center; MC = Mid-Center; E = Edge; T = Transition; F = Forest.
"Direction" refers to cardinal orientation of transects (N, S, E, W).
"Unit" refers to experimental unit

Results

TEMPORAL PATTERNS IN BIOMASS CHANGE

Canopy gap creation in the Southern Appalachian Femelschlag Experiment produced substantial changes in ground-layer biomass composition and productivity. The magnitude and direction of these responses varied markedly among lifeforms, with clear evidence of both colonization by new species and growth of established vegetation.

Pre- and post-treatment biomass comparisons revealed the scale of vegetation responses to gap creation (Table 2.3a; Fig. 2.3). *Rubus* spp. exhibited by far the most dramatic gains, with mean gap center biomass rising from 0.83 ± 0.47 g/m² in 2014 to 13.92 ± 2.85 g/m² in 2021—a roughly 17-fold increase. Trees showed strong and sustained increases at most positions, notably at gap centers where biomass more than doubled from 40.70 ± 6.67 g/m² in 2014 to 87.15 ± 11.91 g/m² by 2021 and remained high in 2022 (79.14 ± 12.16 g/m²). Graminoids steadily increased at gap centers from 2.74 ± 0.72 to 7.70 ± 1.95 g/m² by 2021, and vines posted substantial gains with gap center means rising from 30.77 ± 7.34 g/m² to 43.22 ± 11.16 g/m² in 2021 and 46.33 ± 8.90 g/m² in 2022. In contrast, shrubs were the only lifeform to show consistent declines after treatment, with gap center biomass decreasing from 4.13 ± 1.90 g/m² pre-treatment to 1.24 ± 0.67 g/m² in 2021 and remaining low in 2022 (1.41 ± 0.69 g/m²; Table 2.3a).

Scatterplots comparing pre-treatment (2014) and post-treatment (2021, 2022) biomass (Fig. 2.3) revealed three distinct response patterns. First, extensive new establishment was evident as dense clusters of points along the y-axis at $x = 0$, particularly prominent for graminoids, forbs, and *Rubus* spp., indicating widespread colonization following gap creation. Second, points above the 1:1 line demonstrated biomass increases, with *Rubus* spp. and trees showing the largest absolute gains. Third, some plots showed biomass declines (points below the

1:1 line), notably shrubs, reflecting the heterogeneous nature of early successional responses. These patterns were consistent between 2021 and 2022, indicating that the initial post-disturbance responses were maintained through the study period.

TREATMENT EFFECT MODEL RESULTS (MG1)

Woody Response

Trees

Trees exhibited a significant three-way interaction for Treatment × Direction × Distance ($F_{12,573.2} = 1.92$, $p = 0.030$; Table 2.4a), as well as a significant main effect for Distance ($F_{4,572.7} = 4.70$, $p < 0.001$; Table 2.4b). In large gaps, east-facing transects showed significantly greater biomass change at the edge compared to south-facing transects (E vs. S at edge: $p = 0.006$). At the forest matrix position, east-facing transects also had significantly higher biomass change than west-facing transects (E vs. W at forest matrix: $p = 0.035$). In small gaps, no pairwise differences among directions at any position were significant (all $p > 0.15$).

No significant two-way interactions between direction and position or between gap size and direction were detected (all $p > 0.1$), nor were there significant main effects of Direction or Treatment alone. Pre-treatment biomass strongly predicted post-treatment responses ($F_{1,494.8} = 159.2$, $p < 0.001$), underscoring the critical importance of advance regeneration for post-disturbance recovery (Table 2.4b).

Vines

Vines exhibited a significant three-way interaction for Treatment × Direction × Distance ($F_{12,573.7} = 1.80$, $p = 0.045$), as well as a significant Direction × Distance interaction ($F_{12,573.3} = 2.00$, $p = 0.022$; Table 2.4a). At the transition zone, north-facing transects showed significantly

higher biomass change than south-facing transects in both large ($p = 0.022$) and small ($p = 0.034$) gaps. In small gaps, south-facing transects at the transition had significantly lower biomass change than at the forest matrix (F; $p = 0.0126$). In large gaps, there was a significant decline from the gap center to the transition in south-facing transects ($p = 0.0277$). Pre-treatment biomass was a highly significant predictor of vine responses ($F_{1,512.9} = 142.3$, $p < 0.001$; Table 2.4b).

***Rubus* spp.**

Rubus spp. biomass change was significantly affected by Year ($F_{1,592.2} = 4.03$, $p = 0.045$) and Distance ($F_{4,598.3} = 16.92$, $p < 0.001$), with no significant effects of Treatment or Direction. Biomass was higher in 2022 than 2021 ($p = 0.045$). Across the spatial gradient, *Rubus* spp. biomass change declined sharply from gap centers to more interior forest positions (Fig. 2.4). All pairwise contrasts between gap center and mid-center versus edge, transition, or forest matrix were highly significant ($p < 0.001$), indicating much greater *Rubus* biomass change near gap centers compared to the edge or matrix. Pre-treatment biomass was not a significant predictor of *Rubus* responses ($F_{1,590.25} = 2.00$, $p = 0.16$).

A marginally non-significant three-way interaction for Treatment × Direction × Distance ($F_{12,605.1} = 1.70$, $p = 0.064$) indicated that patterns of *Rubus* biomass change across the spatial gradient varied among specific treatment-by-direction combinations. Post hoc pairwise contrasts identified several significant differences.

For large-gap treatments in north transects, biomass at gap center was significantly greater than at edge, transition, and forest matrix locations (all $p < 0.05$), with the largest difference between gap center and forest matrix ($p = 0.0001$). Large gap west transects, biomass at the gap center was significantly higher than at forest matrix subplots ($p = 0.046$). Among

large-gap south transects, significant differences occurred between mid-center positions and transition subplots ($p = 0.039$).

For small-gap treatments in east transects, biomass near the gap center was significantly greater than at edge, transition, and forest matrix positions ($p < 0.05$); mid-center was also higher than transition and forest matrix subplots ($p < 0.05$). A similar pattern was observed along the north transect in small gaps, where mid-center positions exhibited greater biomass gains compared to edge ($p = 0.015$) and transition ($p = 0.014$) subplots. In south transects, the most pronounced differences in biomass were detected between gap center and transition ($p = 0.038$) as well as forest matrix ($p = 0.039$) subplots. Estimated marginal means consistently confirmed a clear declining trend in *Rubus* biomass from gap center toward the forest matrix in all significant combinations, emphasizing that biomass change was concentrated closest to canopy gaps with sharp reductions further into the forest.

Herbaceous Response

Graminoids

Graminoid biomass change was significantly influenced by Distance ($F_{4,584.3} = 2.42$, $p = 0.048$; Table 2.4b), a Direction × Distance interaction ($F_{12,584.3} = 2.65$, $p = 0.0018$), and a Treatment × Distance interaction ($F_{4,583.9} = 2.90$, $p = 0.021$; Table 2.4a), while pre-treatment biomass also predicted responses ($F_{1,527.4} = 4.62$, $p = 0.032$). There were no significant main effects of Year, Treatment, or Direction alone (all $p > 0.10$; Table 2.4b).

At mid-center subplots, south-facing plots had higher biomass gains than east-facing ($p = 0.0287$) and west-facing ($p = 0.0268$) plots. In north-facing transects, forest matrix subplots showed significantly less biomass gain than gap centers ($p = 0.0152$), mid-centers ($p = 0.0013$), edges ($p = 0.0342$), and transition subplots ($p = 0.0110$). Within south-facing transects, mid-

center subplots showed greater biomass gain than gap centers ($p = 0.0020$) and forest transition subplots ($p = 0.039$).

The Treatment × Distance interaction showed that in large gaps, mid-center positions had the highest biomass gains, with significant differences versus forest transition ($p = 0.023$) and forest matrix subplots ($p < 0.001$). No significant distance effects were found in small gaps (all $p > 0.40$).

Forbs

Forb biomass change showed no significant main effects of Year, Distance, Treatment, or Direction (all $p > 0.25$; Table 2.4b). The only significant predictor of post-treatment biomass change for forbs was pre-treatment biomass ($F_{1,597.5} = 15.35$, $p < 0.001$; Table 2.4b), indicating strong influence of initial conditions on subsequent responses.

Total Biomass Response

Total biomass change was significantly influenced by pre-treatment biomass ($F_{1,520.0} = 316.37$, $p < 0.001$), Year ($F_{1,569.0} = 4.84$, $p = 0.028$), Distance ($F_{4,575.5} = 7.08$, $p < 0.001$), and a significant three-way interaction for Treatment × Direction × Distance ($F_{12,576.0} = 1.86$, $p = 0.037$). On average, total biomass change was higher in 2022 than 2021 ($p = 0.028$; Table 2.3a).

In large gaps, at the edge position, east-facing subplots had significantly higher biomass change than both south-facing ($p = 0.022$) and west-facing subplots ($p = 0.018$). At the forest transition position, east-facing subplots in small gaps had greater biomass than south-facing subplots ($p = 0.005$). In large gaps and east-facing transects, edge positions saw significantly higher biomass than transition positions ($p = 0.0089$). Among south-facing transects in large gaps, forest matrix positions gained the least biomass, with significant differences compared to

gap center (p = 0.014) and mid-center (p = 0.001) positions. For small gaps along south-facing transects, mid-center positions gained more biomass than transition subplots (p = 0.030)

CONTROL MODEL RESULTS (MG2 and MG3)

Gap Zone Comparison (MG2)

The Treatment × Direction interaction significantly influenced trees ($F_{6,67.9} = 3.23$, p = 0.008), vines ($F_{6,71.7} = 3.57$, p = 0.004), and total summer biomass change ($F_{6,68.6} = 4.52$, p < 0.001). For trees, north-facing transects in large gaps showed higher biomass change than south-facing transects (difference = 62.26 g/m², p = 0.046), and south-facing transects showed lower biomass change than west-facing transects (difference = −65.07 g/m², p = 0.034). In small gaps, east-facing transects had greater biomass change than west-facing transects (difference = 71.87 g/m², p = 0.007).

For vines, east-facing transects in large gaps had significantly lower biomass change than both small gaps (p = 0.0002) and controls (p = 0.013). Within large gaps, east-facing transects had lower biomass change than north-facing (p = 0.0002) and west-facing (p = 0.002) transects, and marginally lower than south-facing (p = 0.074).

For total summer biomass, no significant differences among transect directions were detected within control plots (all p > 0.90; Table 2.3b). In large gap treatments, north-facing transects showed the largest biomass gains, with significantly higher gains than both east-facing (difference = 108.97 g/m², p = 0.0085) and south-facing transects (difference = 116.19 g/m², p = 0.0084), the latter of which exhibited a decrease in biomass from 2021 to 2022 in gap interior subplots. West-facing transects also experienced an annual increase (marginal mean 44.43 ± 30.8 g/m²), with gains significantly greater than in both east- (p = 0.037) and south-facing transects (p

= 0.033). In small gaps, east-facing transects exhibited the greatest biomass gains (80.55 ± 29.4 g/m²), particularly when compared to the south- ($p = 0.024$) and west-facing transects ($p = 0.014$).

Distance significantly affected only total summer biomass ($F_{2,197.6} = 5.95$, $p = 0.003$; Table 2.4b). Further, the Treatment × Distance interaction significantly influenced total summer biomass change ($F_{4,197.4} = 2.43$, $p = 0.049$). In large gaps, biomass change decreased from the gap center (-39.5 ± 27.9 g/m²) and mid-center (-19.8 ± 27.1 g/m²) but increased substantially at the gap edge (63.5 ± 26.2 g/m²). Significant contrasts were observed between gap center and edge ($p < 0.001$) and between mid-center and edge ($p = 0.004$). No significant spatial patterns were detected for small gaps or control treatments (all $p > 0.30$).

Treatment effects on *Rubus* spp. biomass change were marginally non-significant ($F_{2,102.1} = 2.84$, $p = 0.063$; Table 2.4b). Pairwise comparisons indicated that from 2021 to 2022, *Rubus* spp. biomass increased in the small gap treatment (mean difference = 4.45 ± 1.58 g/m²), with the increase in small gaps exceeding that of large gaps and controls. No significant differences were observed between the large gap and control treatments ($p = 0.991$), while the contrast between large and small gaps was also non-significant (mean difference = -4.79 ± 2.29 g/m², $p = 0.097$). These results indicate that *Rubus* spp. tended to increase most in small gaps between 2021 and 2022, although this treatment effect did not meet conventional significance thresholds. No significant Direction × Distance interactions were detected for any lifeform in MG2 (all $p > 0.20$; Table 2.4a).

Forest Matrix Comparison (MG3)

The Treatment × Distance interaction significantly influenced graminoid biomass change ($F_{2,104.5} = 4.30$, $p = 0.016$; Table 2.4a). At transition subplots, graminoid biomass change was

significantly higher in small gaps than large gaps (difference = 3.84, p = 0.021) and marginally higher than in controls (difference = 3.21, p = 0.058; Fig. 5). Within small gaps, biomass change at transition subplots exceeded that at forest matrix subplots (difference = 4.31, p = 0.002). No other lifeforms exhibited significant Treatment × Distance interactions in MG3. The Treatment × Direction interaction did not significantly affect biomass change for any lifeform (all p > 0.05; Table 2.4a). However, this interaction for vines approached significance ($F_{6,107.6}$ = 2.07, p = 0.063; Table 2.4a). From 2021 to 2022 in small gaps, vine biomass declined by 30.1 ± 11.1 g along the north-facing transect across the gap exterior subplots, whereas the east-facing transect showed a net gain of 14.6 ± 11.1 g (pairwise p = 0.027).

Additionally, no significant Direction × Distance or Treatment × Direction × Distance interactions for any lifeform were found (all p > 0.05; Table 2.4a). Although, for trees, the three-way interaction approached significance ($F_{6,186.0}$ = 2.02, p = 0.065; Table 2.4a). The sole significant pairwise comparison for trees in large gaps was along the north-facing transect, where biomass was lost at the transition subplot (−24.3 ± 20.5 g) and gained in the forest matrix (29.98 ± 18.1 g) (difference p = 0.044) from 2021 to 2022. No significant main effects of distance, direction, or treatment were detected for any lifeform (all p > 0.15; Table 2.4b).

ABIOTIC MODEL RESULTS

Light Quality

For the gap treatments, total PPFD in the understory varied significantly by Direction ($F_{3,50.7}$ = 4.59, p = 0.0064), with western aspects receiving significantly more light than eastern aspects (p = 0.004; Fig 2.6a). Distance from gap center also significantly affected understory light levels ($F_{4,272.7}$ = 11.41, p < 0.0001), along with the interaction between gap size and

distance ($F_{4,272.7} = 2.62$, $p = 0.036$; Table A2). In large gaps, there was a steeper gradient of light availability, with significantly higher PPFD at positions closer to the gap center than positions further into the forest matrix (Fig. 2.6b). Pairwise comparisons confirmed this pattern with significant differences between gap center and transitions ($p = 0.0009$), gap center and forest matrix ($p < 0.0001$), mid-center and edge ($p = 0.013$), mid-center and transition ($p = 0.0001$), and mid-center and forest matrix ($p < 0.0001$) within large gaps. In comparison, small gaps exhibited a more gradual decline in light levels across distances, with only the gap center and forest matrix comparisons approaching significance ($p = 0.073$; Fig. 2.6b).

In contrast to the gap treatments, control plots exhibited no significant differences in understory light levels by either Direction ($F_{3,24.3} = 0.33$, $p = 0.805$), Distance ($F_{2,63.8} = 1.39$, $p = 0.257$) or the interaction between Direction × Distance ($F_{6,63.8} = 1.22$, $p = 0.309$;Table A2).

Canopy Openness

Within experimental gaps, canopy openness varied significantly by gap size ($F_{3,15.28} = 15.7$, $p = 0.001$) and Distance ($F_{3,273.0} = 9.17$, $p < 0.0001$), and the interaction between Gap Size × Distance ($F_{4,273.0} = 5.57$, $p = 0.0003$; Table A2). For Direction, the main effect approached significance ($F_{3,50.21} = 2.25$, $p = 0.094$), with the highest values observed on southern transects, followed by eastern, western, and northern. Pairwise comparisons indicated that only the north-south contrast approached significance ($p = 0.0596$), with southern transects having greater openness than northern transects.

Analysis of the Gap Size × Distance interaction on the logit-transformed scale confirmed that, in large gaps, canopy openness was greatest at the mid-center, declining sharply at the edge and continuing to drop into the surrounding forest matrix. Small gaps exhibited less variation across the spatial gradient (Fig. 2.6c).

Pairwise post hoc Tukey tests supported these findings: for large gaps, canopy openness significantly differed between gap center and mid-center positions versus transition and forest matrix subplots (all $p < 0.001$), as well as between the edge and forest matrix ($p = 0.0003$). In small gaps, no pairwise contrasts reached significance ($p > 0.05$).

In contrast, control plots exhibited lower canopy openness overall and no significant directional effect ($F_{3,21.1} = 0.28$, $p = 0.84$; Table A2). Distance had a marginal effect in controls ($F_{2,61.2} = 2.60$, $p = 0.082$), but no significant pairwise contrasts were detected ($p > 0.05$ for all comparisons; Fig. 2.6c).

Soil Moisture

Unlike the pronounced spatial patterns observed in light availability, soil moisture did not vary significantly by gap size ($F_{1,4.01} = 0.55$, $p = 0.498$), direction ($F_{3,50.3} = 0.39$, $p = 0.763$), or distance from gap center ($F_{4,279.2} = 1.09$, $p = 0.361$) in the gap treatments two years following harvest. Similarly, control plots showed no significant soil moisture differences by direction ($F_{3,24} = 1.62$, $p = 0.211$) or distance ($F_{2,70} = 1.16$, $p = 0.321$; Table A2).

2014 vs 2022 Biomass Comparison

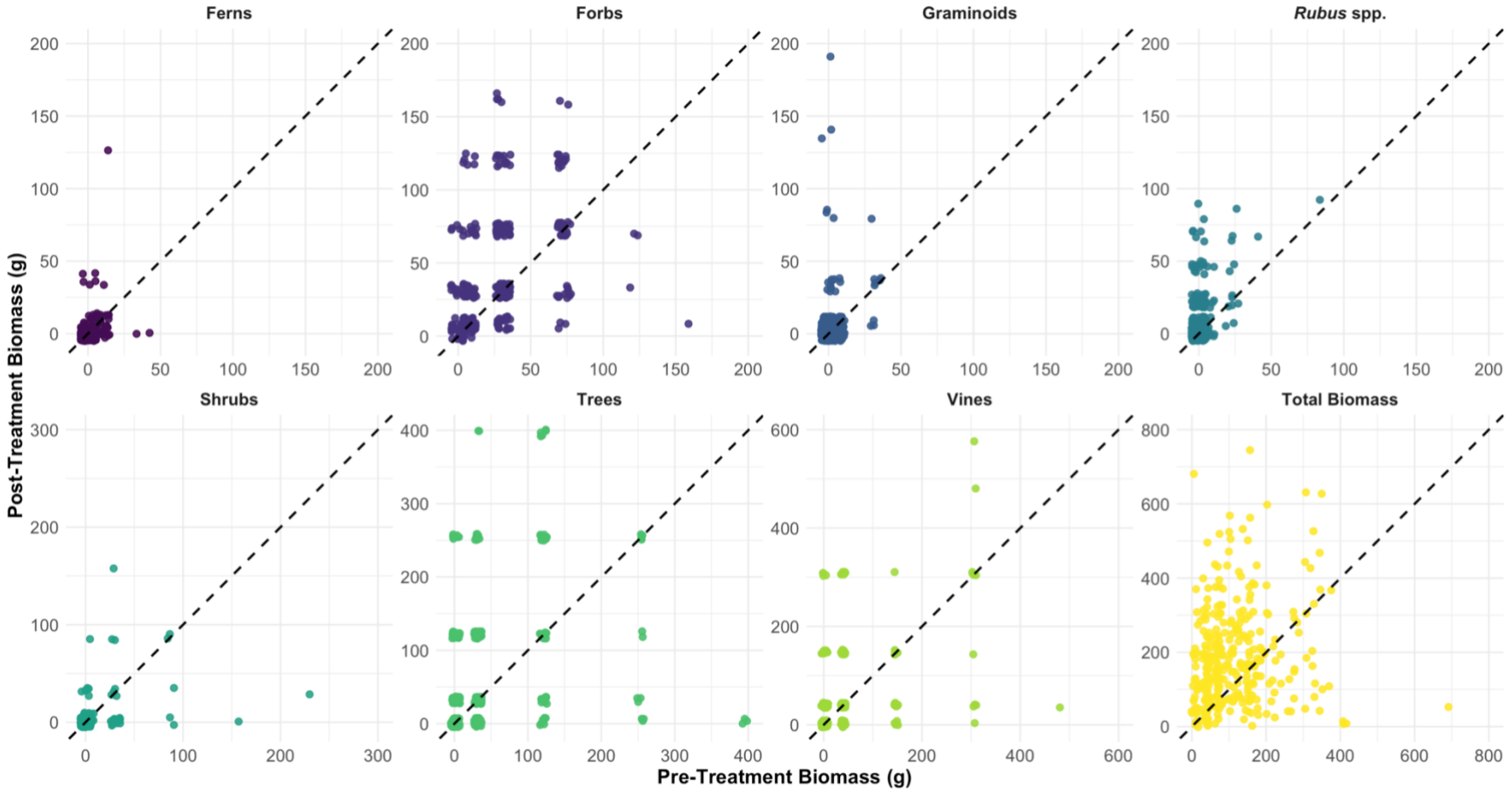

Figure 2.3. Pre- and post-treatment biomass for each lifeform and total biomass in 2014 and 2022, respectively. Each point represents a subplot. The dashed 1:1 line indicates no net change; points above the line increased in biomass post-treatment, points below decreased, and points along the y-axis at x = 0 represent newly established individual.

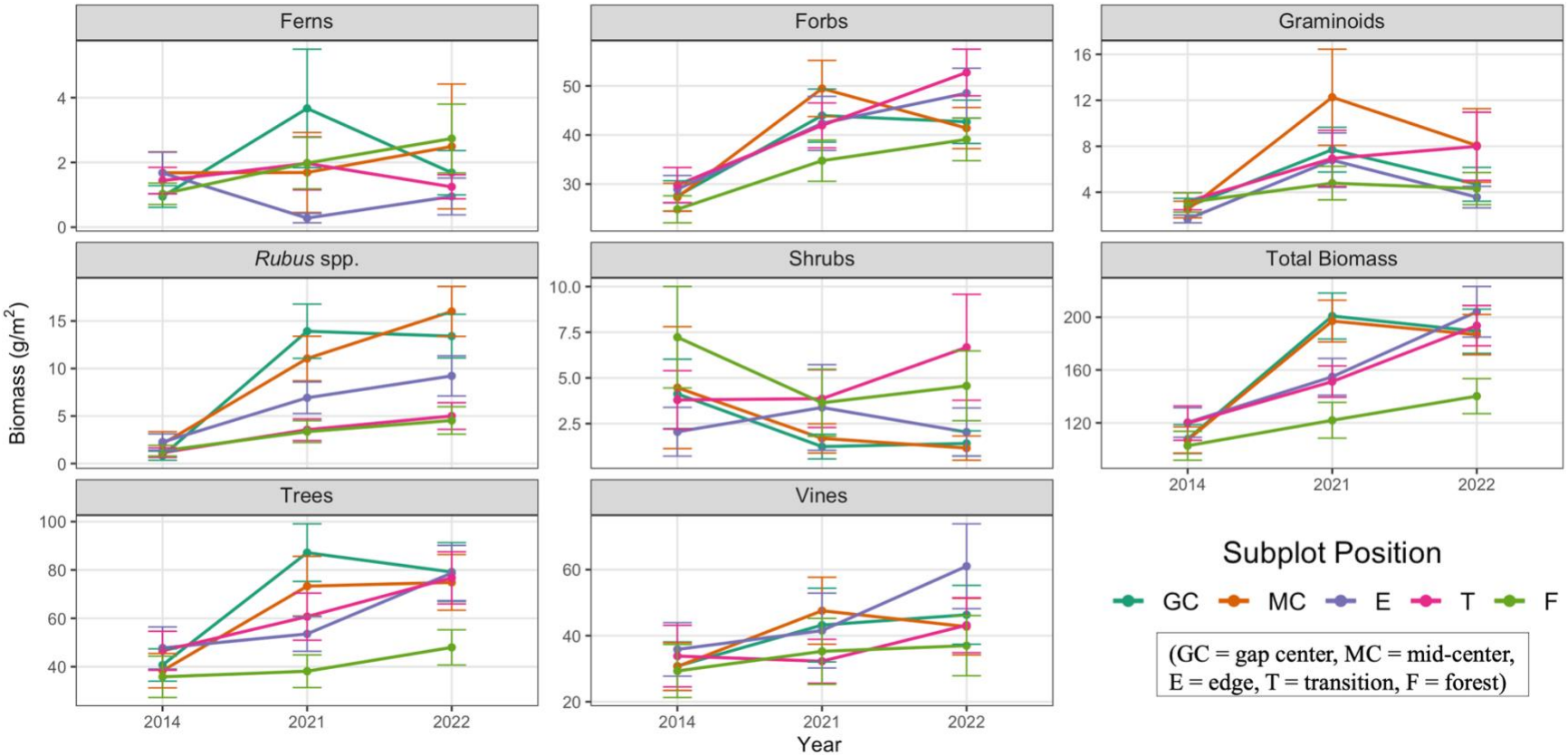

Figure 2.4. Mean (± SE) aboveground biomass (g/m²) of ground-layer vegetation by year (pre-treatment and 2–3 years post-harvest), subplot position and plant lifeform in the Southern Appalachian Femelschlag Experiment. Biomass was estimated in permanent 1 m² subplots, with means combined across gap sizes. Error bars indicate standard errors. Y-axis scales vary among panels to highlight patterns within each lifeform.

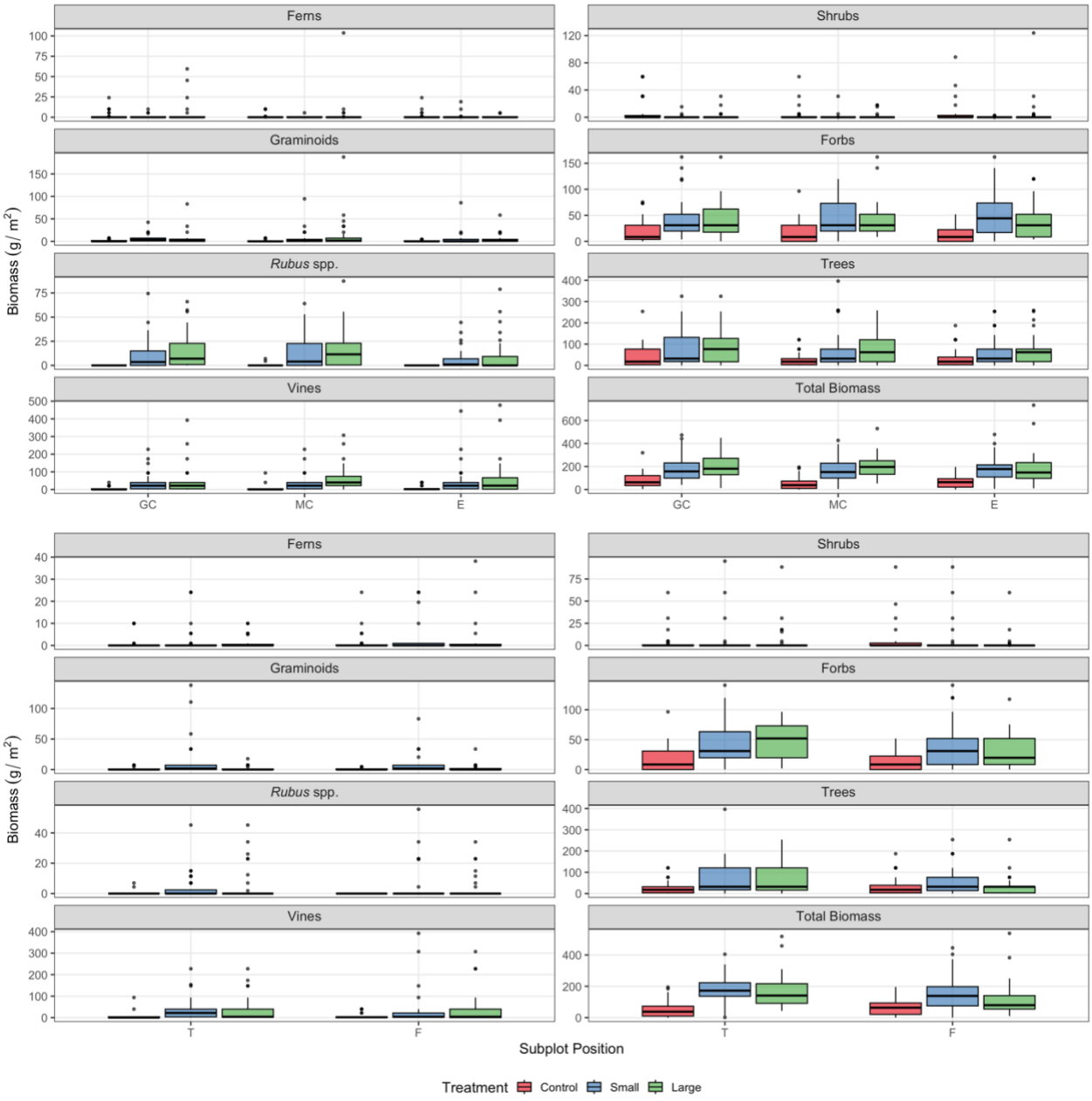

Figure 2.5. Distribution of ground-layer biomass (g m^{-2}) by subplot position, lifeform, and treatment in the Southern Appalachian Femelschlag Experiment. Top: Biomass by gap positions (GC = gap center, MC = mid-center, E = edge) for all treatments. Bottom: Biomass by matrix positions (T = transition, F = forest matrix), with gap treatments shown at T and F, and controls recorded for comparison (MC as T, E as F). Each panel shows boxplots for subplot-level means by lifeform and treatment (Control, Small, Large), with y-axis scales varying among panels. Biomass values are averaged across 2021 and 2022.

Table 2.3b. Mean ground-layer biomass (± standard error in g/m²) by lifeform and subplot position (GC = gap center, MC = mid-center, E = edge) for control plots in the 2nd and 3rd years post-harvest (2021, 2022). Δ (2022–2021) indicates the change in mean biomass between years. Values are subplot-level means for each lifeform and position.

Lifeform	Distance	Mean ± SE (2014)	Mean ± SE (2021)	Δ^1 (2021–2014)	Mean ± SE (2022)	Δ^2 (2022–2014)
Ferns	GC	0.95 ± 0.33	3.67 ± 1.83	2.72	1.68 ± 0.68	0.73
	MC	1.68 ± 0.65	1.69 ± 1.23	0.01	2.49 ± 1.93	0.81
	E	1.68 ± 0.64	0.28 ± 0.15	-1.40	0.95 ± 0.57	-0.73
	T	1.44 ± 0.41	1.97 ± 0.82	0.53	1.25 ± 0.37	-0.19
	F	1.03 ± 0.33	1.98 ± 0.80	0.95	2.74 ± 1.06	1.71
Forbs	GC	27.58 ± 3.08	43.95 ± 5.42	16.37	42.68 ± 4.41	15.10
	MC	27.29 ± 2.86	49.47 ± 5.73	22.18	41.40 ± 4.20	14.11
	E	28.94 ± 2.80	42.36 ± 5.51	13.43	48.52 ± 5.08	19.58
	T	29.80 ± 3.57	41.95 ± 4.58	12.15	52.74 ± 4.76	22.94
	F	24.84 ± 2.75	34.75 ± 4.19	9.91	39.09 ± 4.35	14.25
Graminoids	GC	2.74 ± 0.72	7.70 ± 1.95	4.96	4.69 ± 1.47	1.95
	MC	2.49 ± 0.73	12.27 ± 4.18	9.78	8.07 ± 3.20	5.58
	E	1.67 ± 0.33	6.79 ± 2.37	5.12	3.57 ± 0.94	1.90
	T	3.20 ± 0.74	6.94 ± 2.44	3.73	7.99 ± 2.96	4.79
	F	3.11 ± 0.84	4.79 ± 1.46	1.68	4.31 ± 1.40	1.20
Rubus spp.	GC	0.83 ± 0.47	13.92 ± 2.85	13.09	13.41 ± 2.30	12.58
	MC	2.07 ± 1.28	11.05 ± 2.35	8.98	16.01 ± 2.62	13.94
	E	2.26 ± 0.85	6.92 ± 1.66	4.66	9.22 ± 2.11	6.96
	T	1.15 ± 0.50	3.56 ± 1.14	2.41	5.00 ± 1.40	3.85
	F	1.33 ± 0.58	3.36 ± 1.14	2.03	4.53 ± 1.44	3.20
Shrubs	GC	4.13 ± 1.90	1.24 ± 0.67	-2.88	1.41 ± 0.69	-2.71
	MC	4.47 ± 3.34	1.69 ± 0.80	-2.78	1.16 ± 0.66	-3.31
	E	2.05 ± 1.33	3.38 ± 2.35	1.33	2.04 ± 1.32	-0.02
	T	3.80 ± 1.60	3.86 ± 1.58	0.07	6.68 ± 2.90	2.88
	F	7.23 ± 2.78	3.64 ± 1.83	-3.59	4.57 ± 1.91	-2.66
Trees	GC	40.70 ± 6.67	87.15 ± 11.91	46.45	79.14 ± 12.16	38.44
	MC	38.35 ± 7.10	73.30 ± 12.34	34.95	74.87 ± 11.52	36.52
	E	47.75 ± 8.71	53.56 ± 7.17	5.81	78.75 ± 11.42	31.01
	T	46.58 ± 8.05	60.70 ± 9.72	14.12	76.75 ± 10.78	30.17
	F	35.81 ± 8.54	38.13 ± 6.74	2.33	47.98 ± 7.28	12.17
Vines	GC	30.77 ± 7.34	43.22 ± 11.16	12.44	46.33 ± 8.90	15.55
	MC	30.67 ± 7.22	47.56 ± 10.14	16.89	42.74 ± 8.56	12.08
	E	35.86 ± 8.10	41.55 ± 11.34	5.69	61.03 ± 12.83	25.17
	T	33.83 ± 9.33	32.26 ± 6.65	-1.56	43.18 ± 8.33	9.35
	F	29.32 ± 8.04	35.26 ± 9.98	5.94	36.99 ± 9.10	7.66
Total	GC	107.70 ± 10.97	200.85 ± 17.41	93.15	189.34 ± 16.71	81.64
	MC	107.02 ± 9.89	197.03 ± 15.81	90.01	186.74 ± 15.23	79.72
	E	120.20 ± 11.16	154.85 ± 13.91	34.65	204.08 ± 19.12	83.88
	T	119.80 ± 12.99	151.24 ± 11.81	31.44	193.58 ± 15.24	73.78
	F	102.67 ± 10.93	121.92 ± 13.54	19.25	140.20 ± 13.26	37.53

Table 2.3b. Mean (± standard error) ground-layer biomass (g/m²) by lifeform and subplot position (GC = gap center, MC = mid-center, E = edge) for control plots in post-treatment years (2021, 2022). Δ (2022–2021) indicates the change in mean biomass between years. Values are subplot-level means for each lifeform and position.

Lifeform	Distance	Mean ± SE (2021)	Mean ± SE (2022)	Δ (2022–2021)
Ferns	GC	2.53 ± 1.17	1.21 ± 0.53	-1.31
	MC	0.91 ± 0.46	0.89 ± 0.46	-0.02
	E	0.74 ± 0.38	2.02 ± 1.13	1.29
Forbs	GC	17.18 ± 3.52	20.38 ± 4.51	3.20
	MC	15.07 ± 3.18	16.35 ± 4.01	1.27
	E	13.25 ± 3.17	14.19 ± 3.17	0.94
Graminoids	GC	1.73 ± 0.47	1.47 ± 0.41	-0.26
	MC	1.03 ± 0.38	0.93 ± 0.34	-0.11
	E	0.73 ± 0.29	0.78 ± 0.29	0.05
Rubus spp.	GC	0.00 ± 0.00	0.00 ± 0.00	0.00
	MC	0.39 ± 0.27	0.24 ± 0.20	-0.14
	E	0.00 ± 0.00	0.00 ± 0.00	0.00
Shrubs	GC	9.63 ± 3.69	7.89 ± 3.00	-1.74
	MC	4.25 ± 2.57	3.10 ± 1.43	-1.15
	E	4.42 ± 2.56	7.45 ± 3.53	3.03
Trees	GC	37.45 ± 9.86	50.31 ± 10.15	12.87
	MC	17.90 ± 4.81	30.21 ± 6.59	12.30
	E	29.30 ± 6.64	41.30 ± 9.62	12.00
Vines	GC	4.62 ± 1.81	4.62 ± 1.81	0.00
	MC	3.48 ± 1.52	6.69 ± 4.18	3.21
	E	6.58 ± 2.27	5.12 ± 1.79	-1.46
Total	GC	73.13 ± 11.85	85.89 ± 12.68	12.76
	MC	43.04 ± 8.58	58.41 ± 10.20	15.37
	E	55.02 ± 7.88	70.85 ± 10.47	15.84

Table 2.4a Results of mixed-effects models testing interaction effects on ground-layer biomass change for each lifeform and total biomass. Shown are numerator and denominator degrees of freedom (df), F-statistics, and p-values for each interaction term by model group (MG1: pre- vs. post-treatment in gaps; MG2: post-treatment comparison, controls and gaps, distances 1–3; MG3: post-treatment comparison, controls and gaps, distances 4–5). Significant results ($p < 0.05$) are bolded.

Interaction Term	Model	Forbs			Graminoids			*Rubus* spp.			Trees			Vines			Total		
		df	F	p	df	F	p	df	F	p	df	F	p	df	F	p	df	F	p
Treatment x Direction x Distance	MG1	12, 605.1	1.34	0.194	12, 607.0	1.17	0.304	12, 605.1	1.70	0.064	12, 573.2	**1.92**	**0.030**	12, 573.7	**1.80**	**0.045**	12, 576.0	**1.86**	**0.037**
	MG2	12, 280.5	1.45	0.143	12, 210.1	0.92	0.530	12, 208.4	0.77	0.680	12, 201.3	0.89	0.558	12, 209.7	0.56	0.875	12, 202.9	1.65	0.080
	MG3	6, 184.5	0.66	0.683	6, 107.6	0.450	0.844	6, 107.1	0.49	0.815	6, 186.0	2.02	0.065	6, 107.6	1.14	0.345	6, 212	0.31	0.933
Direction x Distance	MG1	12, 603.5	1.01	0.441	12, 584.3	**2.65**	**0.002**	12, 605.2	1.67	0.069	12, 572.7	1.13	0.330	12, 573.3	**2.00**	**0.022**	12, 575.5	1.67	0.071
	MG2	6, 280.3	1.35	0.234	6, 209.8	0.51	0.798	6, 208.5	1.02	0.411	6, 200.5	0.55	0.766	6, 209.2	0.35	0.908	6, 203.0	0.70	0.650
	MG3	3, 184.7	1.98	0.118	3, 107.5	1.20	0.312	3, 107.1	1.61	0.191	3, 186.1	0.52	0.671	3, 107.4	0.16	0.926	3, 212	0.25	0.865
Treatment x Direction	MG1	3, 51.5	1.40	0.252	3, 71.5	0.09	0.964	3, 50.0	0.92	0.437	3, 46.7	0.77	0.518	3, 46.6	0.08	0.971	3, 48.5	0.19	0.903
	MG2	6, 281.6	1.62	0.141	6, 109.9	1.01	0.422	6, 108.5	1.75	0.116	6, 67.9	**3.23**	**0.008**	6, 71.7	**3.57**	**0.004**	6, 68.6	**4.52**	**< .001**
	MG3	6, 185.3	1.73	0.117	6, 107.6	0.91	0.495	6, 97.5	1.14	0.347	6, 186.9	1.41	0.214	6, 107.6	2.07	0.063	6, 212	1.10	0.366
Treatment x Distance	MG1	4, 603.0	0.35	0.843	4, 583.9	**2.90**	**0.021**	4, 603.9	0.78	0.542	4, 572.30	0.41	0.799	4, 572.9	1.15	0.333	4, 575.1	1.31	0.267
	MG2	4, 280.3	0.82	0.511	4, 210.3	0.11	0.979	4, 208.7	0.840	0.501	4, 200.8	2.04	0.091	4, 209.6	1.14	0.337	4, 197.4	**2.43**	**0.049**
	MG3	2, 184.5	0.48	0.619	2, 104.5	**4.30**	**0.016**	2, 107.1	0.70	0.498	2, 171.0	0.09	0.908	2, 107.5	0.14	0.871	2, 212	0.27	0.763

Model Groups: MG1 = pre-treatment vs. post-treatment (gaps only; 2014 vs. 2021 and 2022). MG2 = post-treatment comparison (controls and gaps; 2022–2021; distances 1–3). MG3 = post-treatment comparison (controls and gaps; 2022–2021; distances 4 and 5).

Note: MG2 and MG3 models do not include a pre-treatment covariate or year effect, as pre-treatment data were unavailable for controls and the response variable is the difference in biomass between 2022 and 2021.

Table 2.4b Main effects from mixed-effects models of ground-layer biomass change by lifeform and total biomass. Shown are numerator and denominator degrees of freedom (df), F-statistics, and p-values for each main effect by model group (see Table 1.4a for definitions). Significant results ($p < 0.05$) are bolded.

Main Effect	Model	Forbs			Graminoids			*Rubus* spp.			Trees			Vines			Total Biomass		
		df	F	p	df	F	p	df	F	p	df	F	p	df	F	p	df	F	p
Treatment	MG1	1, 4.0	0.15	0.720	1, 15.8	0.14	0.713	1, 15.5	0.74	0.402	1, 3.9	0.17	0.703	1, 3.9	0.96	0.383	1, 15.8	0.16	0.698
	MG2	2, 24.2	1.14	0.336	2, 5.8	2.69	0.149	2, 102.1	2.84	0.063	2, 5.9	0.15	0.864	2, 22.3	0.86	0.437	2, 5.9	0.15	0.864
	MG3	2, 5.7	0.89	0.461	2, 101.6	0.77	0.466	2, 5.9	0.71	0.528	2, 6.0	0.03	0.967	2, 101.6	1.60	0.208	2, 5.9	1.08	0.399
Direction	MG1	3, 60.2	0.31	0.817	3, 50.7	0.48	0.695	3, 47.1	0.25	0.862	3, 46.6	1.86	0.150	3, 46.4	1.03	0.388	3, 48.3	2.53	0.068
	MG2	3, 276.2	0.79	0.502	3, 96.9	1.99	0.120	3, 101.8	1.57	0.201	3, 68.2	1.09	0.361	3, 72.0	1.45	0.237	3, 68.8	1.77	0.162
	MG3	3, 181.6	0.56	0.640	3, 101.5	1.19	0.317	3, 94.7	0.90	0.445	3, 182.6	0.53	0.664	3, 101.6	1.19	0.319	3, 95.4	1.04	0.380
Distance	MG1	4, 598.2	0.43	0.787	4, 584.3	**2.42**	**0.048**	4, 598.3	**16.92**	**< .001**	4, 572.7	**4.70**	**< .001**	4, 573.3	1.90	0.110	4, 575.5	**7.08**	**< .001**
	MG2	2, 275.1	2.42	0.090	2, 207.6	0.058	0.944	2, 205.8	1.52	0.220	2, 198.0	2.57	0.079	2, 206.3	1.41	0.246	2, 197.6	**5.95**	**0.003**
	MG3	1, 180.9	1.58	0.211	1, 104.5	1.70	0.196	1, 106.0	0.051	0.823	1, 181.9	0.17	0.685	1, 106.3	1.77	0.186	1, 105.7	0.79	0.376
Year	MG1	1, 592.4	1.17	0.281	1, 578.5	2.64	0.105	1, 592.2	**4.03**	**0.045**	1, 566.4	1.79	0.182	1, 566.9	1.73	0.189	1, 569.0	**4.84**	**0.028**
Pre Co	MG1	1, 597.5	**15.35**	**< .001**	1, 527.4	**4.62**	**0.032**	1, 590.3	2.00	0.158	1, 494.8	**159.12**	**< .001**	1, 512.9	**142.3**	**< .001**	1, 540.5	**316.37**	**< .001**

Note: MG2 and MG3 models do not include a pre-treatment covariate or year effect, as pre-treatment data were unavailable for controls and the response variable is the difference in biomass between 2022 and 2021.

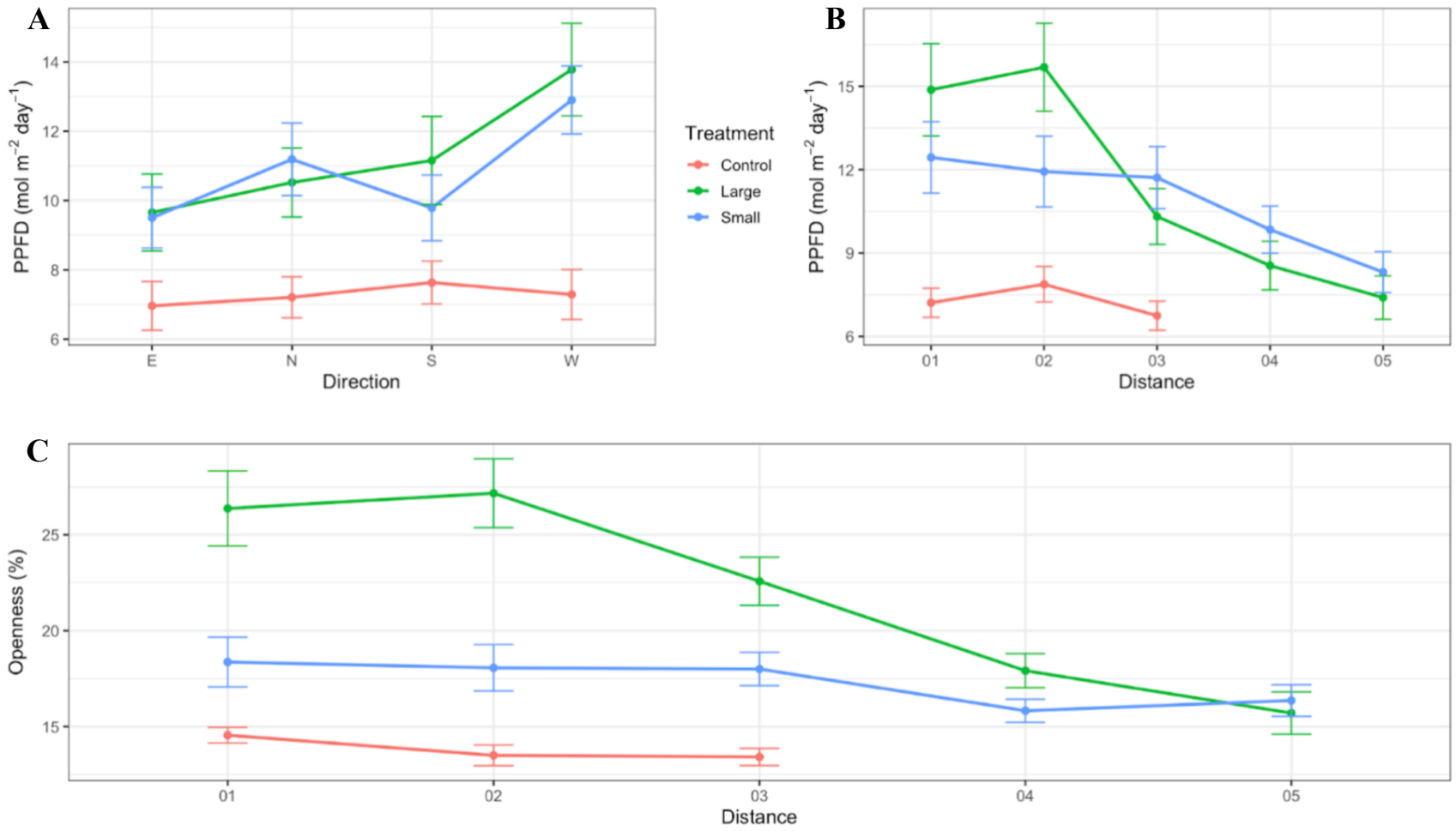

Figure 2.6. (A) Mean (± SE) photosynthetic photon flux density (PPFD; mol m^{-2} day^{-1}) in the understory by cardinal direction and (B) by distance from gap center, and (C) mean (± SE) canopy openness (%) by distance, for each silvicultural treatment in the Southern Appalachian Femelschlag Experiment two years post-harvest. Large gaps exhibited higher understory light and openness near gap centers, with both declining toward the forest matrix. Small gaps showed intermediate values, while controls remained low and uniform across all positions.

Discussion

OVERVIEW OF GROUND LAYER DYNAMICS

Spatial proximity to canopy gaps, rather than gap size or cardinal direction, was the primary determinant of ground-layer biomass dynamics during the first three years following canopy-gap creation in this Southern Appalachian mixed-oak forest. Total biomass and key plant lifeforms—including trees, *Rubus* spp., and graminoids—showed pronounced increases near gap centers, with a generally linear decline toward the forest matrix. Localized light availability declined by 40.7% from gap centers to the matrix and emerged as the primary abiotic filter structuring early successional dynamics.

The strongest biomass increases occurred in gap centers, where light availability and canopy openness peaked (18–27%). Tree regeneration exhibited aspect-dependent establishment, with east-facing transects in large gaps outperforming south-facing ones at edges and west-facing matrix positions—likely due to moderate morning light reducing photoinhibition stress compared to intense afternoon radiation on west-facing slopes. *Rubus* spp. thrived in north-facing gap centers, benefiting from high light while avoiding the desiccating conditions of south-facing aspects. At the same time, vines favored north-facing matrix positions, potentially exploiting moderated light and residual canopy cover for climbing support. These directional nuances highlight how microtopographic light gradients interact with lifeform-specific ecophysiological tolerances.

Pre-treatment biomass was a significant covariate for all lifeforms except *Rubus* spp., indicating that initial vegetation structure strongly mediated post-disturbance recovery for most groups. This pattern aligns with findings from catastrophic wind disturbance studies, where advance regeneration and pre-existing understory vegetation play critical roles in shaping early

successional trajectories, with the post-disturbance community largely reflecting pre-disturbance composition and structure (Castelli et al. 1999). In contrast, *Rubus* spp. proliferated in gaps regardless of its initial presence, likely due to its ruderal strategy and ability to exploit newly available light and space, possibly from a persistent seed bank (Donoso and Nyland 2006).

Biomass accumulation intensified from the second to third year post-harvest (2021 to 2022), reflecting both progressive colonization of new individuals and continued growth of established vegetation. Notably, large gaps exhibited declining biomass at centers but increased at edges by year three, suggesting early resource depletion (e.g., light competition or nutrient drawdown) in central zones, while edges provided optimal light-moisture balances. In contrast, small gaps sustained gradual biomass gains across all positions, likely due to less extreme microclimates.

Contrary to initial expectations, gap size alone (0.1–1.3 ha) had no significant effect on biomass responses for any lifeform or total ground-layer biomass. Even the smaller canopy openings in this study generated sufficient resource heterogeneity to stimulate understory productivity, indicating that disturbance scale within this range is less critical than microsite variation in driving early successional responses. Our results are broadly consistent with previous studies in the region. Trees have been shown to dominate aboveground net primary productivity (NPP) in the first two years following gap creation, with herbs also contributing substantially to early successional biomass (Phillips & Shure 1990). In our study, we observed steep spatial gradients in light availability, with values increasing from the edge of gaps toward the gap center. This pattern closely parallels gradients reported by Phillips & Shure (1990), who found that in large gaps (2.0 ha), solar radiation can be two to four times higher than in small gaps (0.016 ha), with light increasing markedly from the edge to the gap center. More rapid

biomass and NPP recovery have been documented in large compared to small gaps, with standing biomass reaching three to four times higher in large gaps by year two (Phillips & Shure 1990). In contrast, our results indicate that gap size alone was not a reliable predictor of biomass change; instead, spatial position and subplot orientation more strongly structured biomass responses, suggesting that microtopographic heterogeneity may override gap-size effects in the short term.

Unexpectedly, no significant differences were found in soil moisture between gap sizes, directions, or distances, implying that the acidic, well-drained soils or the surrounding forest matrix buffered short-term hydrological shifts in the site. This absence of a soil moisture response contrasts with findings from tropical systems, where gap creation often produces transient nutrient and moisture pulses (e.g., Denslow et al. 1998). The results suggest that steep slopes and well-drained ultisols in the Southern Appalachians mitigate hydrological changes, even in large gaps. Furthermore, rapid understory recovery—particularly from trees and graminoids—likely maintained evapotranspiration rates, offsetting potential moisture accumulation. These findings underscore the importance of site-specific factors such as soil texture, slope, and pre-treatment vegetation in mediating below-ground responses to canopy disturbance.

Long-term studies indicate that gap-size effects become more pronounced over time, with differences in biomass between the smallest and largest gaps widening from 2.5-fold at year two to 7.2-fold by year seventeen (Shure et al. 2006). These findings suggest that while our early results highlight the importance of spatial gradients and microsite variation, gap size will likely become a stronger determinant of productivity and community composition as succession

progresses, particularly as tree canopies close and resource competition intensifies (Shure et al. 2006).

PLANT LIFEFORM RESPONSES

In the years following canopy gap creation, our results parallel patterns observed in second-growth northern hardwood forests in north-central Wisconsin, where total ground-layer biomass in canopy gaps increased significantly relative to surrounding transition zones by the second-year post-disturbance, regardless of gap size (Dyer et al. 2010). After an initial period of lower biomass in gaps compared to undisturbed areas, ground-layer vegetation rapidly colonized and accumulated biomass, ultimately surpassing that of controls within two years—a dynamic also evident in our study (Dyer et al. 2010). Importantly, Dyer et al. (2010) found that gap size exerted only a minimal effect on total ground-layer biomass per unit area in the short term, reinforcing our conclusion that spatial position and resource gradients within and around gaps are more influential than gap size in structuring early biomass responses.

Graminoids exhibited a distinct spatial niche, peaking at mid-center positions in large gaps and on south-facing transects, suggesting a preference for moderate light regimes and residual canopy protection near edges. Their decline in north-facing matrix positions aligns with light limitations, while south-facing preferences may reflect warmer microclimates, enhancing growth. Increased graminoid biomass following canopy disturbance is a consistent pattern across temperate forest systems, with the most pronounced gains occurring in areas of elevated light availability near gap centers (Burton et al. 2014). In northern hardwood forests, graminoid productivity gains were greatest in the central zones of medium and large gaps, with only moderate increases observed at transition zones and in smaller gaps (Burton et al. 2014).

Similarly, our Southern Appalachian study revealed that graminoid biomass peaked at mid-center positions in large gaps but, conversely, was more productive in transition zones in small gaps, indicating a distinct spatial stratification not limited to the highest-light microsites.

Both studies identify localized light availability as the primary abiotic filter structuring graminoid dynamics, with biomass patterns closely tracking gradients in light from gap centers to the matrix. This convergence suggests that light gradients are a universal mechanism governing graminoid productivity after canopy disturbance, regardless of regional context. Temporal patterns also show broad agreement: graminoid biomass increases were sustained through years two and three in our system, complementing observations of peak productivity in year two, followed by a decline in large gaps in northern hardwood forests (Burton et al. 2014). Together, these findings underscore the generality of disturbance-mediated increases in graminoid productivity while highlighting system-specific differences in the spatial and temporal response patterns.

Despite clear biomass gains post-disturbance, the lack of significant spatial or gap-size effects for forbs in this study is consistent with findings from Burton et al. (2014) in northern hardwood forests. Burton et al. (2014) found that forb productivity was related to year and gap size but not to spatial zone within gaps and that productivity only differed significantly from pre-treatment levels in untreated controls and small gaps during the third-year post-treatment. Their results revealed that forb responses were highly individualistic, with some species (particularly spring ephemerals and mesic forest indicators) declining in larger gaps due to competitive exclusion, while colonizing forbs increased, leading to high variability and weak aggregate patterns at the lifeform level. This individualistic response pattern, combined with the temporal variability in forb dynamics observed by Burton et al. (2014)—including initial colonization

followed by subsequent declines as competitive exclusion intensified—helps explain why forbs in our study showed overall biomass gains but lacked significant treatment or spatial effects. Both studies demonstrate that forb responses to canopy disturbance are driven more by temporal dynamics, pre-existing conditions, and species-specific traits than by consistent spatial gradients or gap-size thresholds.

Rubus spp. exhibited strong spatial structuring in response to canopy gap creation, with substantially higher biomass gains near gap centers, with a clear decline in biomass observed toward more interior forest positions. This pattern aligns with a ruderal life history strategy and a reliance on high-light microsites, as previously described by Donoso and Nyland (2006).

The early dominance of *Rubus* in disturbed sites is well-documented: after heavy overstory removal, *Rubus* spp. often become the dominant ground-layer vegetation within two to three years, forming dense thickets that exploit increased resource availability (Donoso and Nyland 2006). This dominance is reinforced by their ability to persist in the seed bank and respond quickly to disturbance events and by the potential extended phenological activity that allows growth into autumn and winter (Faillace et al. 2018). Experimental studies show native (*Rubus* allegheniensis Porter) and exotic (*Rubus phoenicolasius* Maxim.) *Rubus* species can reduce the biomass of neighboring plants by at least 50% through rapid growth and large size rather than by exclusive preemption of soil nitrogen (Faillace et al. 2018).

Despite this initial surge, *Rubus* cover is typically transient. As tree regeneration accelerates, hardwood seedlings usually overtop the *Rubus* layer within five to seven years, leading to canopy closure and a subsequent decline in *Rubus* cover by years ten to fifteen (Donoso and Nyland 2006). The persistence and eventual decline of *Rubus*, though, depends on the presence of sufficient advance regeneration; sites lacking well-developed regeneration may

experience prolonged *Rubus* dominance and delayed tree establishment (Donoso and Nyland 2006; Williams et al. 2006).

A dense *Rubus* cover can delay or suppress hardwood regeneration by intercepting light and occupying space, yet it also provides ecosystem services such as moderating microclimate, reducing soil temperature extremes, and contributing to nutrient cycling. In some cases, *Rubus* thickets may transiently facilitate tree recruitment by protecting seedlings from browsing, but this effect is often short-lived and may be followed by reduced recruitment due to increased seed predation (Williams et al. 2006).

These findings highlight the importance of monitoring *Rubus* dynamics and ensuring adequate advance regeneration to guide stand development and achieve long-term regeneration goals. While *Rubus* plays a prominent role in early post-disturbance succession, its influence is context dependent. It must be balanced with the needs of other lifeforms and long-term forest structures.

STUDY LIMITATIONS & FUTURE RESEARCH

One limitation of this study is the absence of pre-treatment data for control plots, which precluded direct comparison of pre-and post-disturbance dynamics in undisturbed areas. This limits our ability to attribute observed changes in control plots solely to temporal variation rather than unmeasured pre-existing differences. Additionally, shrubs and ferns were excluded from statistical modeling due to their low post-disturbance occurrence, and the relatively short observation window may not capture delayed gap-size effects or long-term shifts in slower-growing species. The tested gap sizes may not have crossed critical thresholds for eliciting divergent responses in some groups.

Given the SAFE experiment's design as a long-term Femelschlag system with decadal gap expansions, future research should prioritize tracking how spatial productivity patterns evolve as gaps enlarge, and succession progresses. This will clarify whether gap size becomes a stronger driver of understory dynamics over time, particularly as resource competition intensifies. Long-term monitoring should also assess how repeated gap expansion influences *Rubus* spp. dominance and its potential consequences for tree regeneration and nutrient cycling.

To strengthen mechanistic inference in future studies, incorporating soil nutrient analyses—such as measurements of nitrogen mineralization and phosphorus availability—would be highly beneficial. Gap-based research in other systems has shown that integrating soil nutrient data with vegetation surveys can clarify how gap size and soil resource availability interact to shape understory diversity and community composition. For example, Lyu et al. (2021) demonstrated that soil organic matter, hydrolysable nitrogen, and available potassium varied significantly with gap size and were closely linked to plant diversity patterns in *Pinus massoniana* Lamb. plantations, highlighting the value of such integrative approaches for understanding successional dynamics.

These findings directly relate to experimental and natural disturbance regimes in the Southern Appalachians. The large-gap treatments, designed to simulate canopy openings from hurricanes like Hurricane Helene, revealed that localized light gradients and microtopographic variation override gap-size effects in structuring early responses. Rapid *Rubus* colonization in gap centers highlights a dual role: while fostering biodiversity and nutrient retention, persistent thickets may suppress tree regeneration if unmanaged. The mechanistic insights offer a framework for anticipating understory responses to silvicultural interventions and natural disturbances. As recovery is monitored following events like Helene's, these findings provide an

ecological reference for understanding successional trajectories and informing adaptive management in forests impacted by human activity and natural disturbances.

Conclusions

Our study demonstrates that early successional dynamics in Southern Appalachian mixed-oak forests are primarily driven by fine-scale spatial heterogeneity and resource gradients created by canopy gaps, rather than gap size itself. Proximity to gap centers, with associated increases in light availability, strongly structures ground-layer biomass accumulation and composition across lifeforms, with microhabitat effects most pronounced for rapid colonizers like *Rubus* spp. and varying patterns in graminoids, vines, and tree seedlings along light gradients. The ground-layer acts as both a driver and indicator of ecosystem function and resilience, underscoring the need to maintain environmental heterogeneity for biodiversity, carbon cycling, and forest health. Dominant taxa such as *Rubus* spp. play a dual role, enhancing early biodiversity and nutrient retention while potentially hindering tree regeneration, necessitating adaptive management that prioritizes fine-scale variation over larger disturbances.

These findings have implications beyond the Southern Appalachians, providing a framework for predicting responses to variable disturbances under climate change, including legacy effects and site-specific soil buffering. The SAFE's long-term design—tracking vegetation, microclimate, and soils across defined positions relative to gaps—allows researchers to understand how disturbances shape forest structure and function over time. As gaps expand and positions become less distinct, it will be especially important for future research to monitor changes in productivity, soil nutrients, and community composition across these gradients to

better support forest resilience. Ultimately, effective management hinges on appreciating spatial complexity to support biodiversity conservation, climate mitigation, and ecosystem stability.

REFERENCES

Allison, J.B. and Hale, L.B. (1997) Soil survey of Haywood County area, North Carolina. USDA Natural Resources Conservation Service, Washington, DC.

Bakker, M.R., Augusto, L. & Achat, D.L. Fine root distribution of trees and understory in mature stands of maritime pine (Pinus pinaster) on dry and humid sites. Plant Soil 286, 37–51 (2006). https://doi.org/10.1007/s11104-006-9024-4.

Bates, D., Mächler, M., Bolker, B., & Walker, S. (2015). Fitting Linear Mixed-Effects Models Using lme4. Journal of Statistical Software, 67(1), 1–48. https://doi.org/10.18637/jss.v067.i01.

Benz, B.L. (2020) ground-layer vegetation response to silvicultural treatments for oak (Quercus) regeneration in Southern Appalachian forests. MSc thesis, North Carolina State University, Raleigh, NC. Available at: https://www.lib.ncsu.edu/resolver/1840.20/38231. (accessed 31 June 2024).

Boring, L.R., Monk, C.D. and Swank, W.T. (1981) Early regeneration of a clear-cut southern Appalachian Forest. Ecology, 62: 1244–1253. https://doi.org/10.2307/1937289.

Burton, J.I., Mladenoff, D.J., Forrester, J.A. and Clayton, M.K. (2014), Experimentally linking disturbance, resources and productivity to diversity in forest ground-layer plant communities. J Ecol, 102: 1634-1648. https://doi.org/10.1111/1365-2745.12319.

Campbell, J.W., Hanula, J.L., and Waldrop, T.A. (2007). Effects of prescribed fire and fire surrogates on floral visiting insects of the Blue Ridge Province in North Carolina. Biological Conservation, 134(3), 393–404. https://doi.org/10.1016/j.biocon.2006.08.029.

Castelli, J.P., Casper, B.B., Sullivan, J.J. & Latham, R.E. (1999) Early understory succession following catastrophic wind damage in a deciduous forest. Canadian Journal of Forest Research, 29(12), 1997–2002. https://doi.org/10.1139/x99-171.

De La Cretaz, A.L. and Kelty, M.J. (2002), Development of Tree Regeneration in Fern-dominated Forest Understories After Reduction of Deer Browsing. Restoration Ecology, 10: 416-426. https://doi-org.prox.lib.ncsu.edu/10.1046/j.1526-100X.2002.02037.x.

Denslow, J.S., Ellison, A.M. and Sanford, R.E. (1998), Treefall gap size effects on above- and below-ground processes in a tropical wet forest. Journal of Ecology, 86: 597-609. https://doi.org/10.1046/j.1365-2745.1998.00295.x.

Donoso, P.J. and Nyland, R.D. (2006) Interference to hardwood regeneration in northeastern North America: The effects of raspberries (*Rubus* spp.) following clearcutting and shelterwood methods. Northern Journal of Applied Forestry, 23: 288–296. https://doi.org/10.1093/njaf/23.4.288.

Faillace, C.A., Caplan, J.S., Grabosky, J.C. and Morin, P.J. (2018) Beneath it all: Size, not origin, predicts belowground competitive ability in exotic and native shrubs. Journal of the Torrey Botanical Society, 145, 30–40. https://doi.org/10.3159/TORREY-D-16-00053.1.

Gilliam, F.S. (2007) The ecological significance of the herbaceous layer in temperate forest ecosystems. BioScience, 57: 845–858. https://doi.org/10.1641/B571007.

Grover, Z. (2020) Climate growth responses and carbon consequences of compositional change in mature Southern Appalachian oak-hickory forests. MSc thesis, North Carolina State University, Raleigh, NC. Available at: https://www.lib.ncsu.edu/resolver/1840.20/38062. (accessed 31 July 2024).

Grover, Z.S., Forrester, J.A., Keyser, T.L., King, J.S. and Altman, J. (2023) Growth response, climate sensitivity and carbon storage vary with wood porosity in a southern Appalachian mixed hardwood forest. Agricultural and Forest Meteorology, 332: 109358. https://doi.org/10.1016/j.agrformet.2023.109358.

Hadley, J.B. and Nelson, A.E. (1971) Geologic map of the Knoxville quadrangle, North Carolina, Tennessee, and South Carolina. U.S. Geological Survey Miscellaneous Geologic Investigations Map I-654, scale 1:250,000.

Jobbágy, E.G., Jackson, R.B. The distribution of soil nutrients with depth: Global patterns and the imprint of plants. Biogeochemistry 53, 51–77 (2001). https://doi.org/10.1023/A:1010760720215.

Kuznetsova, A., Brockhoff, P. B., & Christensen, R. H. B. (2017). lmerTest Package: Tests in Linear Mixed Effects Models. Journal of Statistical Software, 82(13), 1–26. https://doi.org/10.18637/jss.v082.i13.

Landuyt D, De Lombaerde E, Perring MP, et al. (2019) The functional role of temperate forest understory vegetation in a changing world. Glob Change Biol. 2019; 25: 3625–3641. https://doi-org.prox.lib.ncsu.edu/10.1111/gcb.14756.

Lenth R (2025). emmeans: Estimated Marginal Means, aka Least-Squares Means. R package version 1.11.1-00001, https://rvlenth.github.io/emmeans/.

Levin, D. A., & Wilson, A. C. (1976). Rates of evolution in seed plants: Net increase in diversity of chromosome numbers and species numbers through time. Proceedings of the National Academy of Sciences, 73(6), 2086-2090. https://doi.org/10.1073/pnas.73.6.2086.

Lieffers, V. J., Macdonald S. E., and Hogg E. H. 1993. Ecology of and control strategies for *Calamagrostis canadensis* in boreal forest sites. Canadian Journal of Forest Research. 23(10): 2070-2077. https://doi-org.prox.lib.ncsu.edu/10.1139/x93-258.

Lutz, H.J. (1930), The Vegetation of Heart's content, A Virgin Forest in Northwestern Pennsylvania. Ecology, 11: 1-29. https://doi.org/10.2307/1930778.

Lyu Q, Liu J, Liu J, Luo Y, Chen L, Chen G, Zhao K, Chen Y, Fan C, Li X. 2021. Response of plant diversity and soil physicochemical properties to different gap sizes in a *Pinus massoniana* plantation. PeerJ 9:e12222 https://doi.org/10.7717/peerj.12222.

McNab, W., Greenberg, C. H., & Berg, E. C. (2004). Landscape distribution and characteristics of large hurricane-related canopy gaps in a southern Appalachian watershed. Forest Ecology and Management, 196(2-3), 435-447. https://doi.org/10.1016/j.foreco.2004.04.004.

Mou, P., & Warrillow, M. P. (2000). Ice Storm Damage to a Mixed Hardwood Forest and Its Impacts on Forest Regeneration in the Ridge and Valley Region of Southwestern Virginia. The Journal of the Torrey Botanical Society, 127(1), 66–82. https://doi.org/10.2307/3088748.

Muller, R.N. (2003) Nutrient relations of the herbaceous layer in deciduous forest ecosystems. In: Gilliam, F.S. and Roberts, M.R. (eds) The herbaceous layer in forests of eastern North America, pp. 15–37. Oxford University Press, New York.

Natural Resources Conservation Service. PLANTS Database. United States Department of Agriculture. Accessed June 18, 2025, from https://plants.usda.gov.

North Carolina State Climate Office, NC State University. Cardinal [data retrieval interface]. Available at: https://products.climate.ncsu.edu/cardinal/request (accessed 6 August 2024).

North Carolina Wildlife Resources Commission. (2020) 2020 North Carolina white-tailed deer density. Available at: https://www.ncwildlife.gov/media/1663/open (accessed 13 March 2025).

Nowacki, G. J., & Abrams, M. D. (2008). The Demise of Fire and "Mesophication" of Forests in the Eastern United States. BioScience, 58(2), 123-138. https://doi.org/10.1641/B580207.

Phillips, D. L., & Shure, D. J. (1990). Patch-Size Effects on Early Succession in Southern Appalachian Forests. Ecology, 71(1), 204-212. https://doi.org/10.2307/1940260.

R Core Team (2023). *R: A Language and Environment for Statistical Computing.* R Foundation for Statistical Computing, Vienna, Austria. https://www.R-project.org/.

Retrieved from the Integrated Taxonomic Information System (ITIS), www.itis.gov, CC0. https://doi.org/10.5066/F7KH0KBK (accessed 22 July 2024).

Romey, W. L., Ascher, J. S., Powell, D. A., & Yanek, M. (2007). Impacts of Logging on Midsummer Diversity of Native Bees (Apoidea) in a Northern Hardwood Forest. Journal

of the Kansas Entomological Society, 80(4), 327–338. http://www.jstor.org/stable/25086399.

Royo, A. A. and Carson, W. P. 2006. On the formation of dense understory layers in forests worldwide: consequences and implications for forest dynamics, biodiversity, and succession. Canadian Journal of Forest Research. 36(6): 1345-1362. https://doi.org/10.1139/x06-025.

Runkle, J.R. (1982), Patterns of Disturbance in Some Old-Growth Mesic Forests of Eastern North America. Ecology, 63: 1533-1546. https://doi.org/10.2307/1938878.

Shure, D., Phillips, D. & Edward Bostick, P. Gap size and succession in cutover southern Appalachian forests: an 18 year study of vegetation dynamics. Plant Ecol 185, 299–318 (2006). https://doi.org/10.1007/s11258-006-9105-8.

Spicer, Michelle & Mellor, Hannah & Carson, Walter. (2020). Seeing beyond the trees: a comparison of tropical and temperate plant growth forms and their vertical distribution. Ecology. 101. https://doi.org/10.1002/ecy.2974.

Tappeiner, J., Zasada, J., Ryan, P. and Newton, M. (1991), Salmonberry Clonal and Population Structure: The Basis for a Persistent Cover. Ecology, 72: 609-618. https://doi.org/10.2307/2937201.

Wang, H. (2017) Estimating Forest Attributes From Spherical Images. MS thesis, Nanjing Forestry University, Nanjing, Jiangsu. Available at: http://ifmlab.for.unb.ca/LabPubs/theses/WangHZ2020a.pdf. (accessed 24 June 2025).

Williams, K., Westrick, L.J. and Williams, B.J. (2006) Effects of blackberry (*Rubus discolor*) invasion on oak population dynamics in a California savanna. Forest Ecology and Management, 228, 187–196. https://doi.org/10.1016/j.foreco.2006.03.002.

Woodbridge, M., Keyser, T., & Oswalt, C. (2022). Stand and environmental conditions drive functional shifts associated with mesophication in eastern US forests. Frontiers in Forests and Global Change, 5, 991934. https://doi.org/10.3389/ffgc.2022.991934.

CHAPTER 3 : EFFECTS OF CANOPY GAP CREATION ON GROUND-LAYER DIVERSITY AND COMMUNITY STRUCTURE IN MIXED-OAK FORESTS OF THE SOUTHERN APPALACHIANS

Abstract

Southern Appalachian mixed-oak forests are undergoing mesophication, a shift from open, oak-dominated stands to closed-canopy, shade-tolerant forests, threatening understory plant diversity and ecosystem function. We evaluated the effects of the initial entry of an expanding-gap silviculture experiment on ground-layer diversity and community structure. Canopy gaps of two sizes (0.1–0.4 ha and 0.7–1.3 ha) were created, and ground-layer plant communities were sampled before (2014) and after (2021, 2022) treatment across gap centers, edges, and adjacent forest matrix, with uncut controls for comparison. Gap creation rapidly increased species richness, with mean species counts rising from 32.8 pre-treatment to over 40 post-treatment, and the highest richness observed in gap centers and forest matrix zones. Shannon and Simpson's diversity indices also increased significantly and remained elevated through three years post-harvest. Multivariate analyses revealed strong compositional differentiation among zones, particularly in large gap centers, and a marked rise in habitat specialization, as indicated by the number of significant ($p \leq 0.05$) indicator species. Non-native species establishment was limited and largely ephemeral. These findings demonstrate that expanding-gap silviculture can quickly enhance ground-layer diversity and promote specialized assemblages, with effects extending into the surrounding forest matrix. This approach offers a promising strategy for restoring biodiversity and counteracting mesophication in temperate forests.

Introduction

Temperate forests are globally significant reservoirs of biodiversity and providers of essential ecosystem services, including carbon storage, atmospheric regulation, and wildlife habitat. Their complex, multi-layered structure—shaped by both natural processes and centuries of human influence—supports key ecological functions such as nutrient cycling, soil formation, and productivity (Gilliam 2016). As these forests face increasing pressures from climate change and land use, understanding the dynamics that sustain their structure, and function is more critical than ever.

Within this context, Southern Appalachian forests stand out as some of the most species-rich temperate ecosystems in eastern North America, supporting exceptionally high understory vascular plant diversity that underpins vital ecosystem processes (Whittaker 1956; Ulrey 2002). For example, native species richness of 55.2 species per 100 m² has been reported in riparian plots compared to 31.3 species per 100 m² in adjacent uplands, highlighting the region's remarkable capacity to sustain diverse plant communities across geomorphic gradients (Brown and Peet 2003). Recent work in Southern Appalachian rich cove forests demonstrates that both old growth (>125 years) and mature second growth (70 ± 10 years) stands support exceptionally high vascular plant richness, with an average of 79 species per 0.1 ha plot, and no significant differences in richness between age classes at any spatial scale from 0.01 m² (1.5 species) to 1000 m² (78.5–78.6 species) (Jackson et al. 2009). This native richness supports nutrient cycling, soil stabilization, and hydrological regulation, while riparian corridors further enhance propagule exchange and connectivity among plant populations (Brown and Peet 2003). Additionally, the high diversity of Southern Appalachian forests mediates community invasibility, as frequent flood-driven disturbances in riparian zones increase both native and exotic species influxes,

demonstrating the intricate balance of immigration and extinction processes that shape understory composition in this biodiversity hotspot (Brown and Peet 2003).

Despite their relatively small contribution to aboveground biomass, ground-layer plant communities are the principal reservoirs of vascular plant diversity in temperate forests, accounting for more than 80% of total species richness (Gilliam 2007; Spicer et al. 2020). Herbs alone comprise approximately 80% of all vascular plant species in these ecosystems, while trees represent only about 7% (Spicer et al. 2020). This striking pattern reflects a "downshifted" vertical distribution of biodiversity, with the vast majority of species reaching maturity within the first two meters above ground (Spicer et al. 2020). The ground-layer's ecological significance extends well beyond its diversity: it contributes disproportionately to nutrient cycling, carbon flux, and habitat provision (Muller 2003; Landuyt et al. 2019; Campbell et al. 2007). Although it constitutes less than 1% of aboveground biomass, ground-layer vegetation can account for 1–22% of annual carbon flux to soil through litter production and typically contains nutrient concentrations 1.5 to 5 times higher than overstory foliage, reflecting its high nutrient assimilation efficiency and strategic rooting in nutrient-rich surface soils (Landuyt et al. 2019; Bakker et al. 2006; Jobbágy and Jackson 2001). Ground-layer plants thus serve as critical mediators of nutrient cycling, intercepting and processing essential elements before they are lost from the system (Muller and Bormann 1976).

This ecological significance is rooted in the ground layer's remarkable diversity of lifeforms—including spring ephemerals, summer-flowering herbs, graminoids, ferns, vines, and low shrubs—which collectively display a wide array of phenologies, dispersal strategies, and growth forms These varied strategies allow the ground-layer to occupy a wide range of microhabitats and to maintain ecosystem functions across temporal (e.g., spring vs. summer) and

spatial gradients. The ground-layer also plays a vital role in forest hydrology and regeneration dynamics. It contributes 10–40% of total forest evapotranspiration, especially in more open forests where canopy density is reduced (Landuyt et al. 2019). As an ecological filter, the ground-layer influences the establishment, growth, and survival of future canopy trees through complex competitive and facilitative interactions. While dense ground-layer cover often reduces tree seedling performance, these interactions fundamentally shape forest composition and successional trajectories (Tappeiner et al. 1991; De La Cretaz and Kelty 2002; Lieffers et al. 1993). These multifaceted contributions underscore the need to broaden ecological research and management beyond a tree-centric perspective to encompass the full spectrum of plant growth forms that sustain temperate forest biodiversity and function.

Across the eastern deciduous forest range, forest composition and structure have shifted from open, oak-dominated woodlands to closed-canopy, mesophytic stands, with associated declines in biodiversity and ecosystem function (Nowacki and Abrams 2008; Alexander et al. 2021). Historically, frequent low- to moderate-intensity fires—often set by Native Americans—maintained open, oak-dominated forests by suppressing shade-tolerant competitors and promoting the regeneration of fire-adapted oaks (Nowacki and Abrams 2008). The widespread exclusion of fire in the twentieth century, however, has allowed shade-tolerant, fire-sensitive species (mesophytes) such as maples, beech, and cherries to proliferate in the understory and midstory (Abrams and Nowacki 1992; Nowacki and Abrams 2008; Alexander et al. 2021). This shift initiated a positive feedback cycle known as mesophication: as mesophytes become more abundant, they create cooler, shadier, and moister understory conditions, and their less flammable, rapidly decomposing litter further suppresses fire. These changes reinforce mesophyte dominance and make it increasingly difficult for fire-adapted oaks to regenerate.

A key manifestation of this process is the "oak bottleneck." Although oak seedlings may persist in the understory, they rarely progress into sapling and midstory size classes due to intense competition from mesophytes and the absence of fire to reduce this competition (Nowacki and Abrams 1992; Alexander et al. 2021). Over time, this leads to a demographic imbalance: mature oaks remain in the overstory, but there is little recruitment of younger oaks to replace them, setting the stage for eventual replacement by shade-tolerant species. This successional trajectory is supported by dendroecological evidence from Abrams et al. (1995), who demonstrated that periodic fire and small-scale disturbances historically maintained oak and pine dominance by facilitating their recruitment and suppressing shade-tolerant competitors. The cessation of these disturbances in the 20th century has led to a marked decline in oak regeneration and a concomitant rise in mesophytic species such as maples and beech, underscoring the critical role of disturbance regimes in sustaining oak-dominated forest ecosystems. Recent trait-based analyses confirm that these functional shifts—toward more shade-tolerant, less drought- and fire-tolerant tree communities—are widespread in oak-hickory forests across the eastern U.S., including the Southern Appalachians. Notably, the severity and rate of mesophication are strongly influenced by local stand structure, site moisture, and soil conditions, underscoring the need for site-specific management to sustain oak dominance and ecosystem function (Woodbridge et al. 2022). Considering these findings, there is a pressing need to develop and test silvicultural strategies that can counteract mesophication and restore the functional diversity of oak-hickory forests.

The Southern Appalachian Femelschlag Experiment (SAFE) was developed to address two interrelated challenges in eastern temperate forests: mesophication and the oak regeneration bottleneck (Nowacki and Abrams 2008; Nowacki and Abrams 1992). The Southern Appalachian

Femelschlag Experiment (SAFE) employs a dynamic, century-long expanding-gap silvicultural system that begins with conventional group-selection harvests and proceeds through successive entries to progressively enlarge initial 0.1–1.3 ha canopy openings. This approach emulates natural gap expansion and disturbance patterns, creating a gradient of light conditions intended to release oak and hickory cohorts from competitive shading and promote their growth into mid- and overstory classes. SAFE's design provides a unique opportunity to investigate how incremental gap enlargement influences long-term regeneration trajectories and understory community assembly in mixed oak forests.

The experimental design features initial harvest entries that create two gap sizes reflecting different scales of natural disturbance: smaller gaps of approximately 0.1 hectares, representing the upper limit of gaps typically generated by minor natural disturbances in old-growth forests (Runkle 1982), and larger gaps of 0.4 hectares, replicating intermediate-scale disturbances such as those caused by hurricanes and ice storms (McNab et al. 2004; Mou and Warrillow 2000). This dual-treatment approach creates a gradient of canopy openness and light availability intended to enhance conditions for oak and hickory establishment and growth, while simultaneously affecting understory plant communities and broader forest ecosystem processes. By sampling across this light-availability gradient during the peak growing season, we can directly test how spatial variation in canopy structure translates into patterns of understory diversity and species associations.

We investigated how the initial implementation of expanding-gap silviculture influences the diversity, composition, and structure of ground-layer plant communities in Southern Appalachian mixed-oak forests. Specifically, we assessed temporal and spatial responses of species richness, evenness, and diversity to gap creation by comparing ground-layer

communities in gap centers, edges, and adjacent forest matrix zones before treatment (2014) and at two and three years following the first harvest entry (2021 and 2022). By directly contrasting forest matrix zones in large gaps, small gaps, and uncut controls, we also evaluate whether the effects of gap creation on diversity extend beyond the immediate disturbance and whether these effects vary with gap size.

We also examined how gap creation shapes community composition and the emergence of distinct assemblages across spatial zones. Using multivariate analyses, we test whether gap centers, edges, and forest matrices develop unique species pools and whether these compositional differences persist or shift as the community recovers from disturbance. Additionally, we identified species that serve as reliable indicators of specific microhabitats, shedding light on patterns of habitat specialization and niche differentiation in response to gap creation.

Collectively, these objectives provide a framework for understanding how the early stages of expanding-gap silviculture affect understory plant communities and offer insights into the potential of such treatments to counteract mesophication, promote biodiversity, and foster a mosaic of specialized assemblages. While we focused on the initial entry, the findings lay the groundwork for predicting how subsequent gap expansions may further influence forest dynamics and ecological restoration in southern Appalachian forests undergoing mesophication.

Materials and Methods

STUDY SITE

The 60-hectare study site, known as the Southern Appalachian Femelschlag Experiment (SAFE; 35°28′N, 82°40′W), is in the Blue Ridge Physiographic Province of the southern

Appalachian Mountains, North Carolina, USA (Fig. 2.1). It is part of the Pisgah Ranger District within Pisgah National Forest, characterized by mountainous terrain with steep slopes averaging approximately 75° (range 66–81°). The experimental gaps within the site have aspects averaging 266° for large gaps (just east of due west) and 247° for small gaps (southwest), resulting in most gaps facing west or southwest. Elevations range from 847 m to 1117 m (Grover 2020). Site productivity varies with topographic position, with lower, moister slopes supporting greater productivity than drier ridges. The site index (SI; base age 50) for mixed oaks ranges from 17 m to 29 m along the topographic gradient, and the subset of plots used in this study includes plots with SI ≥ 21.3 m. The underlying geology is primarily felsic to mafic high-grade metamorphic biotite and granitic gneisses (Hadley and Nelson 1971). Soils are predominantly Inceptisols and Ultisols, ranging from shallow to deep, well-drained, and moderately to extremely acidic, with textures from coarse-loamy to clayey (Allison and Hale 1997).

The study area has milder winters and longer, warmer summers. The average minimum and maximum air temperatures for 1993–2023 were 5.82°C and 19.13°C, respectively. The mean annual precipitation is 1,084.85 mm (1993–2023). Mean annual air temperature reported from a nearby weather station (Candler 1 W) was 13.3°C, 12.9°C, 12.6°C, and 14.1°C and yearly precipitation was 1574 mm, 1221 mm, 1226 mm, and 771 mm across the years 2020, 2021, 2022, and 2023, respectively (North Carolina State Climate Office, NC State University 2024; Fig. 2.2).

The stand is a mature, second-growth upland hardwood mixed-oak forest that naturally regenerated around the 1920s, following federal acquisition and prior Indigenous management. Historical land use practices included high-grading, land clearing, and domestic livestock grazing. The area has also experienced significant disturbances, including ice storms, droughts,

disease (e.g., chestnut blight), and hurricanes, affecting stand growth over short and long periods (Grover et al. 2023). The main overstory species include various oaks (*Quercus alba L.*, *Q. rubra* L., *Q. montana* Willd., *Q. coccinea* Münchh., and *Q. velutina* Lam.), and hickories (*Carya cordiformis* (Wangenh.) K. Koch, *C. glabra* (Mill.) Sweet, *C. ovalis* (Wangenh.) Sarg. and *C. tomentosa* (Lam.) Nutt.), and tulip poplar (*Liriodendron tulipifera* L.). The midstory comprises shade-tolerant species such as sourwood (*Oxydendrum arboreum* (L.) DC.), flowering dogwood (*Cornus florida* L.), black gum (*Nyssa sylvatica* Marshall), and red maple (*Acer rubrum* L.). The oldest trees, particularly *Q. alba*, have an average age of 151 years, ranging from 91 to 215 (Grover et al. 2023). The forest structure is typical of mixed hardwood stands in the region, with an average basal area of 37 m^2 ha^{-1} and a density of 1086 stems ha^{-1}. In Buncombe County, white-tailed deer density was estimated at 11-20 deer per square mile as of 2020 (North Carolina Wildlife Resources Commission 2020).

Pre-treatment vegetation inventories followed the methods described by Grover et al. (2023). Initial harvests were conducted in fall - winter of 2019 with the intention of regenerating oak and hickory. Merchantable trees were hand-felled and removed via skidders and forwarders while unmerchantable material was cut post-harvest and retained on site. A midstory removal treatment was conducted (summer 2019) throughout the entire stand with all stems <20 cm dbh of non-mast producing species were injected with herbicide. This treatment retained *Quercus*, *Carya*, *Ilex* L., and *Cornus* species, resulting in an average basal area removed of 1.45 m^2 ha^{-1}.

STUDY DESIGN

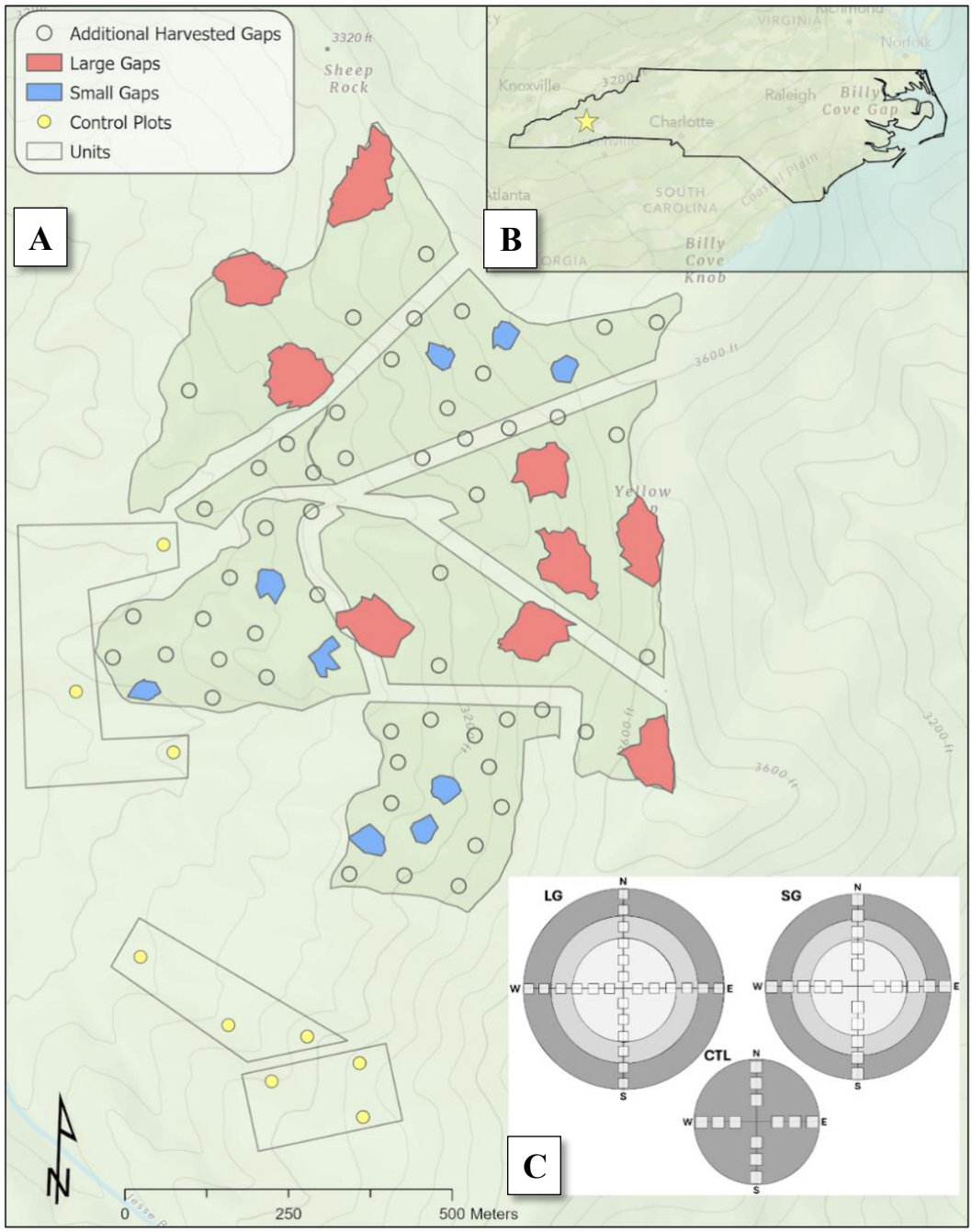

Figure 3.1. (A) Topographic map of the Southern Appalachian Femelschlag Experiment (SAFE) showing nine experimental units (grey outlines), with sampled large gaps (red), small gaps (blue), and control plots (yellow). Additional harvested (unsampled) gaps are shown as open circles. (B) Inset map showing SAFE site location in western North Carolina. (C) Schematic subplot layouts for large gap (LG), small gap (SG), and control (CTL) treatments, illustrating transects along cardinal directions and three ecological zones: gap centers (light), gap edge (medium), and forest matrix (dark). In controls, subplots span a single undisturbed forest zone. Neither schematic nor inset map is to scale.

The Southern Appalachian Femelschlag Experiment (SAFE) was implemented across nine forest units in Pisgah National Forest, North Carolina, with each experimental unit randomly assigned to one of three treatments: large canopy gaps (0.7–1.3 ha), small canopy gaps (0.1–0.4 ha), or unharvested controls, ensuring three units per treatment type (see Fig. 3.1). In this study, a plot refers to one discrete sampling location—either a large gap, small gap, or uncut control area—within a treatment unit. Plot centers were positioned using a grid system spaced 60–80 meters apart based on stand size and gap configuration.

Within each plot, subplots were systematically arranged along four cardinal-direction transects radiating from the plot center (north, south, east, and west), allowing comprehensive coverage of ecological gradients from gap center through the edge and into the surrounding forest matrix. Transects accommodated two main types of permanent subplots: regeneration subplots—circular plots of 0.002 ha for surveying seedlings and saplings less than 1.5 cm DBH—and ground-layer subplots, each 1 m^2 in size, spaced at regular 7.5-meter intervals from the plot center outward. To minimize trampling disturbance, ground-layer subplots were offset by 7 meters from regeneration subplots along each transect (Fig. 1.2).

The number and spacing of subplots varied by treatment to match the physical dimensions and spatial context of large gaps, small gaps, and controls. Large gap plots each consisted of 24 ground-layer subplots—six spaced at 7.5-meter intervals along each transect—extending from the center of the gap up to 22.5 meters into the matrix, offering the greatest sampled distance from the gap edge. Small gap plots contained 20 subplots per plot (five per transect), ranging from gap center to a maximum distance of 15 meters into the matrix from gap edge. Control plots included 12 subplots (three per transect), positioned at 0 meters (plot center), 7.5 meters, and 15 meters from the designated center along each cardinal direction. This spatial

arrangement provided consistent and ecologically meaningful sampling coverage, enabling fine-scale investigation of vegetation and microclimate responses across varying gap sizes and control conditions within the SAFE study area. In this study, all analyses and results focus exclusively on the ground-layer subplots (n = 504), hereby referred to simply as 'subplots.'

DATA COLLECTION

Summer Surveys

During the peak growing season, summer surveys were conducted from mid-July through early August in 2014 (pre-treatment), from early July to early September in 2021, and from mid-July to late August in 2022. In each year, all vascular herbaceous and woody plants less than 1 m tall rooted within each 1 m² subplot were identified to species using USDA PLANTS database codes (USDA, NRCS 2025). Percent cover was visually estimated for each species and lifeform (trees, shrubs, subshrubs [*Rubus* spp. L. only], graminoids, woody vines, and forbs (including herbaceous vines)) using seven ordinal cover classes: <1%, 1–<5%, 5–<25%, 25–<50%, 50–<75%, 75–<95%, and 95–100%. The midpoint of each class was used for quantitative analyses. Maximum height (to the nearest 0.01 m) was measured for each lifeform, and total percent cover of the subplot was recorded. In each 1 m² subplot, only vegetation with live stems or foliage less than 1 m in height was recorded. For all lifeforms except vines and *Rubus*, only individuals rooted within the subplot were included in cover and height measurements. For vines and *Rubus*, percent cover was estimated based on presence within the subplot, regardless of rooting location, because it was often difficult or impossible to determine where these individuals were rooted.

Spring Surveys

Spring surveys were conducted from late April to early May in both 2021 and 2022, targeting only herbaceous species that were reproductive (flowering or fruiting) or had reached peak vegetative development in spring. No other lifeforms (vines, subshrubs, shrubs, trees, ferns, graminoids) were recorded during spring surveys. Within each 1 m^2 subplot, the actual percent cover (to the nearest 0.5%) of each spring herbaceous species was visually estimated and recorded using USDA PLANTS codes. Total herbaceous cover, total spring species cover, and maximum height (cm) of the herbaceous layer were also recorded. Subplot locations for spring sampling matched those of summer: six subplots per transect in large gaps, five in small gaps, and three in controls.

DATA PROCESSING

Species to Genus-level Changes

To maintain taxonomic consistency across the study period (2014–2022), we used the original USDA PLANTS Database codes and scientific epithets recorded during the 2014 baseline surveys. This ensured that any subsequent taxonomic revisions did not affect our analyses, allowing direct comparison across years. All species-level identifications retained their original nomenclature regardless of later taxonomic updates.

Before analysis, we addressed taxonomic inconsistencies that arose from varying levels of species identification across sampling periods. Due to factors including surveyor expertise, plant phenological stage, and field conditions, some individuals could only be reliably identified to genus level (e.g., *Viola* spp. L., *Carex* spp. L.), while the same taxa were identified to species

level in other instances. To ensure taxonomic consistency and analytical accuracy, we systematically reviewed all genera containing both genus-level and species-level identifications.

For each genus with mixed identification levels, we examined the frequency of occurrence across all subplot-year combinations and assessed temporal consistency in species-level identifications between pre-treatment, 2021, and 2022 sampling periods. Taxa were lumped to genus level when: (1) species-level identifications were inconsistent across sampling periods for the same individuals (e.g., *Oxalis* spp. L. vs. *O. grandis* Small vs. *O. stricta* L.), (2) species-level entries comprised <5% of total occurrences for that taxonomic group (indicating predominantly genus-level identification). Species with consistent identification across all sampling periods and low rates of genus-level entries were retained at the species level.

This conservative approach prioritized taxonomic accuracy over potential species richness, resulting in 146–188 distinct taxonomic units for analysis, depending on the sampling timeframe. As a result, species richness metrics presented in this study likely represent more conservative estimates, as lumping reduces apparent diversity compared to species-level analyses.

Growing Season Dataset Construction

To evaluate understory plant diversity and composition across the full growing season, we combined spring and summer ground-layer vegetation datasets for each subplot. The spring surveys targeted only herbaceous species known to be reproductive or at peak vegetative development in spring, using a predetermined species list. In contrast, the summer surveys included all vascular herbaceous and woody species <1 m tall present in each subplot, resulting in a more comprehensive species inventory.

Because of this methodological difference, there was a substantial overlap in herbaceous species recorded in both seasons. To ensure that each species was only represented once per subplot in the final "growing season" dataset (May-August), we systematically reviewed all taxa present in both datasets. For each overlapping species, we compared its median and average percent cover, as well as its frequency of occurrence (*n*), between spring and summer. Species were assigned to the season in which they were more robustly represented, defined as having higher median or average cover and/or greater subplot frequency. For example, many spring ephemerals (e.g., *Anemone quinquefolia* L., *Aplectrum hyemale* (Muhl. ex Willd.) Torr.) showed higher cover in spring, while other herbaceous species were more abundant or widespread in summer.

After determining the season of greatest representation for each overlapping species, we removed duplicate entries from the less robust season. The remaining unique spring and summer records were then combined to create a single, non-redundant dataset representing the total ground-layer community for the growing season. This approach ensured that species' phenological dynamics were accurately reflected while avoiding inflation of diversity metrics due to double-counting.

Despite the initial intent to capture only spring-active species in the spring survey, many species exhibited greater abundance or cover in summer. Our approach to resolving overlap provides a realistic and ecologically meaningful snapshot of growing season diversity and composition across all treatment zones.

DATA ANALYSIS

Univariate analyses

Subplot positions were grouped into three spatial zones—center, edge, and forest matrix—based on their location relative to canopy gaps (Figure 3.1C). The center zone includes subplots within gap interiors, representing the most disturbed, high-light microhabitats; the edge zone comprises subplots at the gap boundary, where open-canopy and forest influences overlap; and the forest matrix zone consists of subplots beneath closed canopy conditions adjacent to gaps, within harvest units that received midstory removal but no direct canopy opening. Thus, these matrix subplots are not undisturbed backgrounds; only the uncut controls represent conditions without any harvest or midstory removal. This three-zone framework captures a gradient of disturbance intensity and microhabitat conditions while ensuring adequate replication for robust linear mixed-effects modeling of diversity metrics.

To evaluate temporal and spatial changes in understory plant diversity following gap creation, a series of linear mixed-effects models (LMMs) were fitted to combined pre-treatment (2014) and post-treatment (2021, 2022) gap treatment data. Uncut controls were excluded from these models due to the absence of pre-treatment data. Diversity metrics—including species richness, evenness, Shannon diversity, and Simpson's diversity—were calculated annually for each plot zone using PC-ORD v. 7.07 (McCune & Mefford 2016), yielding 54–63 zones per year and spanning 146–188 species per year.

For species richness (S), initial models included the main effects of treatment (large gap, small gap), spatial zone (center, edge, forest matrix), year (2014, 2021, 2022), all two- and three-way interactions, and random intercepts for forest unit (serving as experimental block) and plot nested within unit, reflecting the study's hierarchical design. Model selection was conducted by

sequentially removing non-significant interaction terms ($p > 0.05$) via backward elimination using maximum likelihood estimation. The final model for richness retained a two-way interaction between treatment and zone, with year included only as a main effect, and both random intercepts.

For evenness (E), Shannon (H′), and Simpson's (D) diversity indices, the final models included only the main effects of treatment, zone, and year, along with random intercepts for unit and plot within unit. Interactions among fixed effects were excluded after comparison indicated they did not significantly improve model fit. Where a random effect variance was estimated to be consistently zero, the term was omitted to maintain parsimony.

Throughout, model selection and fixed effect testing were performed under maximum likelihood estimation; final models were refitted using restricted maximum likelihood (REML) for unbiased inference and reporting. All Analysis of Variance tables were estimated using Satterthwaite's method for denominator degrees of freedom (as implemented in lmerTest), and Kenward-Roger degrees of freedom adjustment was applied for post hoc pairwise comparisons (as returned by emmeans). P-values for post hoc comparisons were adjusted using Tukey's method to control Type I error. All analyses were conducted in R (v4.3.2; R Core Team 2023) with the lme4 (Bates et al. 2015), lmerTest (Kuznetsova et al. 2017), and emmeans (Lenth 2025) packages. Where random effects had zero variance, they were excluded to avoid model singularity, and all main effects were retained given their ecological importance.

Multivariate analyses

For our multivariate analyses, subplots were aggregated into seven treatment zones—Large Gap Center (LGC: –22.5 m, –15 m, –7.5 m), Small Gap Center (SGC: –15 m, –7.5 m), Large Gap Edge (LGE: 0 m), Small Gap Edge (SGE: 0 m), Large Gap Forest (LGF: +7.5 m, +15

m), Small Gap Forest (SGF: +7.5 m, +15 m), and Control (CTA: 0 m, –7.5 m, –15 m)—to create ecologically meaningful categories (center, edge, forest matrix) without discarding any observations. This aggregation simplifies spatial comparisons across treatments while preserving all subplot data.

Because zones still differed in total sample size and dispersion—conditions known to bias PERMANOVA under heteroscedasticity and unequal group sizes—we employed Multi-Response Permutation Procedures (MRPP). MRPP is a non-parametric, permutation-based test that compares within- and between-group distances and remains robust to unequal replication. Analyses were conducted using PC-ORD version 7.0 with Euclidean distance as the distance measure to test for differences in understory plant community composition among treatment zones and between years using species abundance data (percent cover). Pairwise comparisons were conducted between all treatment zones for each year. Statistical significance was assessed at $\alpha = 0.05$.

Indicator Species Analysis (ISA) was performed using PC-ORD version 7.07 with a Monte Carlo randomization test (4999 permutations) to identify species significantly associated with specific treatment zones or years using the growing season species abundance dataset. Indicator values were calculated following the method of Dufrêne and Legendre (1997). Species were considered significant indicators when $p \leq 0.05$ and had indicator values ≥ 25. The analysis was performed separately for treatment zones and years, and only species occurring in at least 5% of sampling units were included.

Non-metric multidimensional scaling (NMS) ordinations were carried out using the Sørensen (Bray–Curtis) distance measure on growing season species cover data from 162 plots spanning 217 understory species. Up to six axes were initially evaluated, with a three-

dimensional solution selected based on minimum final stress, stability, and significant Monte Carlo permutation tests (R_n^2), demonstrating robust separation of real data from randomized runs. The final three-dimensional NMS solution produced a stress value of 21.79, nonmetric fit (R_n^2) of 0.953, and linear fit (R_l^2) of 0.645, indicating excellent preservation of ecological dissimilarities among plots and strong ordination integrity. Ordinations used random starting coordinates with thorough autopilot settings and a maximum of 500 iterations per run.

NMS ordinations were done using data only for gap treatments, with 18 gap-by-zone and year combinations (6 different zones x three different years (2014, 2021, 2022). For each gap-by-zone and year combination, principal axes rotations were applied to maximize interpretability of community trajectories over time. Axis scores were exported for subsequent plotting and analysis. Community trajectories and centroid shifts for each gap-zone × year combination were visualized to examine temporal and spatial changes in species composition.

Results

TEMPORAL & SPATIAL PATTERNS OF DIVERSITY

Linear mixed-effects models revealed strong and consistent effects of both spatial position (zone) and year on all measures of understory plant diversity, with no significant interactions between these factors (Table 3.1). Species richness, evenness, Shannon diversity, and Simpson's diversity all increased significantly from pre-treatment (2014) to two (2021) and three (2022) years post-treatment, indicating a robust and persistent positive response to gap creation.

Species richness (S) increased markedly following harvests, from a mean of 32.8 species per subplot in 2014 to 41.1 in 2021 and 40.8 in 2022 (both $p < 0.0001$ vs. 2014; Table 3.1a,

Figure 3.3). This temporal increase was paralleled by significant spatial differentiation: richness was highest in gap centers (42.7) and forest matrix zones (41.9), and lowest at gap edges (30.1). Pairwise comparisons confirmed that both centers and forest matrix zones supported significantly higher richness than edges (C–E: $p < 0.0001$; F–E: $p < 0.0001$), while centers and forest matrix zones did not differ (C–F: $p = 0.689$). When analyzed by gap size, large gap centers had the highest richness (46.9), significantly exceeding both large gap edges (31.0) and large gap forest subplots (41.0), while small gap centers (38.6) were also higher than small gap edges (29.3) but not forest (42.8). The center–edge contrast was more pronounced in large gaps (C–E: 15.9, $p < 0.0001$) than in small gaps (C–E: 9.3, $p < 0.0001$). The contrast between large gap centers and small gap centers was marginal (LGC–SGC: 8.26, $p = 0.0513$) with greater richness in large versus small gaps.

Evenness (E) also increased over time (2014: 0.77; 2021: 0.79, $p = 0.039$; 2022: 0.78, $p = 0.285$), with the highest values in forest matrix zones (0.80) and the lowest at edges (0.75; Figure 3.3). Centers were intermediate (0.79). Edges were significantly less even than both centers (C–E: 0.035, $p = 0.001$) and forest matrix zones (E–F: –0.050, $p < 0.0001$).

Shannon diversity (H′) and Simpson's diversity (D, logit-transformed) followed similar patterns: both increased significantly post-treatment (H′: 2.65 in 2014 to 2.93 in 2021 and 2.89 in 2022, both $p < 0.0001$; D: 2.11 in 2014 to 2.39 in 2021 and 2.37 in 2022, both $p < 0.001$). Both metrics were lowest at gap edges and highest in forest matrix zones, with centers intermediate. For example, Shannon diversity was 2.94 in centers, 2.54 at edges, and 2.98 in forest matrix zones (C–E: 0.39, $p < 0.0001$; E–F: –0.44, $p < 0.0001$). Simpson's diversity showed a similar pattern (C–E: 0.46, $p < 0.0001$; E–F: –0.54, $p < 0.0001$).

No significant zone × year or treatment × year interactions were detected for any metric, indicating that the spatial hierarchy of diversity among zones was stable through time and that diversity gains persisted between two- and three-years post-harvest.

TEMPORAL SHIFTS IN COMMUNITY COMPOSITION

The three-dimensional NMS ordination revealed distinct compositional gradients structured by specific plant taxa (Fig. 3.2). Axis 1 was strongly and negatively associated with *Rubus allegheniensis* Porter ($r^2 = 0.45$, $\tau = -0.58$), *Sanguinaria canadensis* L. ($r^2 = 0.24$, $\tau = -0.34$), *Ageratina altissima* (L.) R.M. King & H. Rob. var. *altissima* ($r^2 = 0.085$, $\tau = -0.44$), and *Pycnanthemum* spp. Michx. ($r^2 = 0.179$, $\tau = -0.37$). In contrast, positive associations on Axis 1 were led by *Quercus prinus* L. ($r^2 = 0.053$, $\tau = 0.31$), *Vaccinium* spp. L. ($r^2 = 0.072$, $\tau = 0.24$), and *Kalmia latifolia* L. ($r^2 = 0.063$, $\tau = 0.23$).

Axis 2 captured compositional variation driven by negative associations with *Desmodium nudiflorum* (L.) DC. ($r^2 = 0.368$, $\tau = -0.45$), *Amphicarpaea bracteata* (L.) Fernald ($r^2 = 0.253$, $\tau = -0.35$), *Botrychium virginianum* (L.) Sw. ($r^2 = 0.150$, $\tau = -0.32$), *Collinsonia canadensis* L. ($r^2 = 0.106$, $\tau = -0.22$), and *Thalictrum dioicum* L. ($r^2 = 0.029$, $\tau = -0.23$). Communities at higher scores on Axis 2 were characterized by *Phytolacca americana* L. ($r^2 = 0.100$, $\tau = 0.29$), *Vitis aestivalis* Michx. ($r^2 = 0.094$, $\tau = 0.20$), *Hieracium paniculatum* L. ($r^2 = 0.032$, $\tau = 0.24$), and *Nyssa sylvatica* Marshall ($r^2 = 0.032$, $\tau = 0.22$).

Axis 3 was dominated by strong negative association with *Toxicodendron radicans* (L.) Kuntze ssp. radicans ($r^2 = 0.369$, $\tau = -0.49$) and weaker negative correlations with *Fraxinus*

americana L. ($r^2 = 0.108$, $\tau = -0.28$) and *Uvularia puberula* Michx. ($r^2 = 0.095$, $\tau = -0.29$). Positive loadings on Axis 3 were characterized by *Acer rubrum* L. ($r^2 = 0.137$, $\tau = 0.251$).

Multi-Response Permutation Procedures (MRPP) found highly significant differences in community composition among treatment zones in both 2021 and 2022 (2021: T = -7.14, A = 0.058, $p < 0.0001$; 2022: T = -5.85, A = 0.048, $p < 0.0001$). The chance-corrected within-group agreement (A) values, while modest, are typical for ecological community data and indicate that treatment zones were more internally homogeneous than expected by chance, but with considerable overlap.

Pairwise MRPP comparisons revealed pronounced compositional differentiation among ground-layer plant communities across treatment zones two (2021) and three (2022) years after canopy gap harvest. The Large Gap Center (LGC) consistently differed from nearly all other zones—including Large Gap Forest (LGF), Small Gap Edge (SGE), Small Gap Forest (SGF), and the controls (CTA)—with most pairwise comparisons highly significant ($p < 0.01$). Differences between LGC and Small Gap Center (SGC) were not statistically significant, indicating similar species composition within gap centers, while all gap and forested zones showed clear differentiation from control plots, confirming lasting effects of gap creation on vegetation structure.

The strongest compositional contrasts emerged during the second-year post-disturbance, as evidenced by large *T* statistics and low *p* values (e.g., LGC vs. LGF, SGE, SGF, and CTA, all $p < 0.01$ in 2021). Although the strength of these differences diminished slightly by the third year, most key pairwise comparisons remained significant—particularly those involving LGC and controls or gap forests ($p < 0.01$). SGC also had significant differences in species assemblages as compared to CTA for both years (both $p < 0.001$). Notably, both the gap forest

zones (LGF and SGF) were significantly different from control zones by year two, strengthening by year three (Table 3.3).

HABITAT SPECIALIZATION & COMMUNITY DIFFERENTATION

Over the nine-year period from 2014 to 2022, the number of statistically significant indicator species rose, particularly in year two. Only three indicator species were detected in 2014, increasing to fifteen in gap plots for year two, but then decreasing to seven in gap plots by year three. Concurrently, the pool of taxonomic groups surveyed expanded from 146 in the pre-treatment growing season (2014) to 188 in 2021 and 184 in 2022, underscoring both enhanced sampling comprehensiveness and community enrichment following silvicultural treatments.

In 2014, three species exhibited significant indicator values ($p < 0.05$), with Large Gap Centers (LGC) treatments accounting for two of these associations (*Agrimonia* spp. L. IV = 35, $p = 0.033$, and *Hieracium paniculatum* L. = 33, $p = 0.0052$), with Small Gap Forest (SGF) yielding one (*Carex* spp. L. = 45, $p = 0.0094$; Table 3.3).

For year two, fifteen species attained statistical significance ($p < 0.05$) in the gap plots, marking a fivefold increase in indicator species richness. The greatest number of indicator species ($n = 9$, 60%) were found in LGC treatments—*Phytolacca americana* L. (IV = 62, $p = 0.0002$), *Poa* spp. L. (IV = 51, $p = 0.001$), *Robinia pseudoacacia* L. (IV = 39, $p = 0.003$), *Liriodendron tulipifera* (IV = 36, $p = 0.006$), *Carex* spp. L (IV = 34, $p = 0.014$) and *Vitis aestivalis* Michx. (IV = 32, $p = 0.019$)—representing the six highest indicator values recorded for that treatment zone. Small Gap Centers (SGC) emerged as a significant contributor with four species (*Ageratina altissima* (L.) R.M. King & H. Rob. var. *altissima* IV = 50, $p = 0.006$; *Phlox*

amplifolia Britton IV = 44; p = 0.003; *Ilex opaca* Aiton IV = 33, p = 0.028; and *Viola sororia* Willd. IV = 26, p = 0.27), compared to SGF contributing only one (grass family IV = 34, p = 0.007). While Control Treatment Area (CTA), contributed two species (*Magnolia fraseri* Walter IV = 39, p = 0.013; and *Goodyera pubescens* (Willd.) R. Br. IV = 26, p = 0.024; Table 3.3).

By year three, only nine species remained significant ($p < 0.05$), indicating decreased habitat differentiation, in comparison to year two. Dominant indicator values included *Magnolia fraseri* in CTA (IV = 52, p = 0.001), and in LGC treatments *Phytolacca americana* (IV = 37, p = 0.002), *Vitis aestivalis* (IV = 37, p = 0.002), and *Hieracium paniculatum* (IV = 36, p = 0.004), with *Polystichum acrostichoides* (Michx.) Schott (IV = 34, p = 0.006; Table 3.3) in LGF. LGC treatments continued to host the greatest number of indicators by treatment zone, with four indicators.

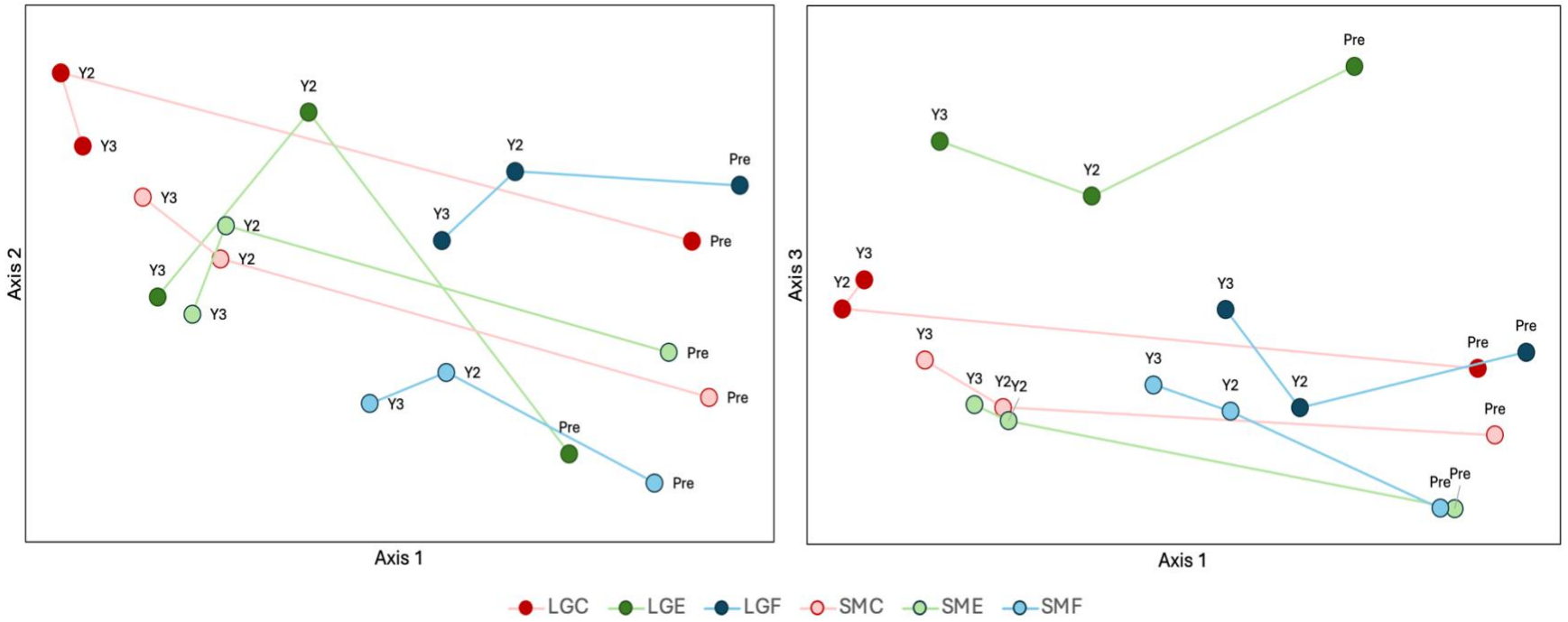

Figure 3.2. Trajectories of gap zone community centroids in non-metric multidimensional scaling (NMS) ordination space across three years (pre-treatment, Year 2, and Year 3 post-harvest) for large gap (LGC, LGE, LGF) and small gap (SMC, SME, SMF) treatments in the Southern Appalachian Mountains. Points represent mean axis scores by zone and year; lines connect temporal shifts within each zone. Left panel: Axes 1 vs. 2. Right panel: Axes 1 vs. 3.

Table 3.1a. Results of linear mixed-effects models testing effects of gap size (TRT), spatial zone (ZONE), and year (YR) on ground-layer diversity metrics (S, E, H′, D) for pre- and post-treatment periods. F- and p-values are from Type III tests: significant effects ($p < 0.05$) in bold.

	Metric											
	Species Richness (S)			Evenness (E)			Shannon diversity (H′)			Simpson's diversity (D)*		
Effect	df	F	p	df	F	p	df	F	p	df	F	p
TRT × ZONE × YR	4, 128	0.92	0.453	4, 128	2.34	0.059	4, 128	1.05	0.385	4, 128	1.11	0.353
ZONE × YR	4, 132	0.44	0.780	4, 136	0.63	0.642	4, 134	0.74	0.565	4, 134	0.33	0.855
TRT × ZONE	2, 138	**12.87**	**<.001**	2, 134	0.13	0.879	2, 138	1.17	0.314	2, 138	0.22	0.802
TRT × YR	2, 136	0.81	0.449	2, 132	0.093	0.911	2, 132	0.09	0.919	2, 132	0.07	0.934
TRT	1, 4	0.77	0.430	1, 4	5.88	0.072	1, 4	3.52	0.134	1, 4	5.16	0.086
ZONE	2, 138	**96.89**	**<.001**	2, 140	**13.52**	**<.001**	2, 140	**53.43**	**<.001**	2, 140	**35.68**	**<.001**
YR	2, 138	**43.58**	**<.001**	2, 140	**3.10**	**0.048**	2, 140	**20.42**	**<.001**	2, 140	**10.51**	**<.001**

* Logit-transformed

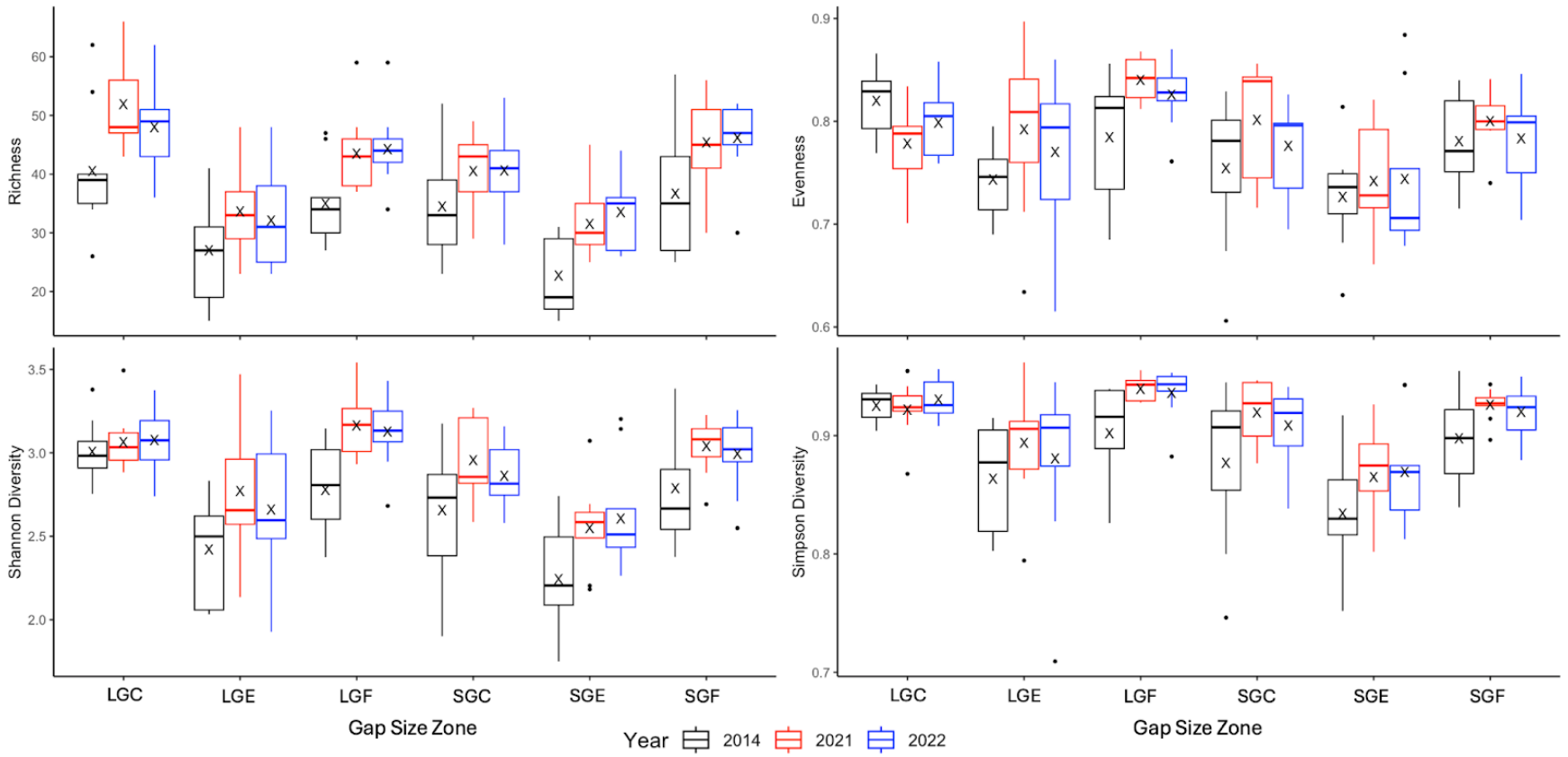

Figure 3.3. Boxplots showing four diversity metrics—(a) Richness (S), (b) Evenness (E), (c) Shannon diversity (H′), and (d) Simpson's diversity (D)—for seven treatment zones: Large Gap Center (LGC), Large Gap Edge (LGE), Large Gap Forest matrix (LGF), Small Gap Center (SGC), Small Gap Edge (SGE), and Small Gap Forest matrix (SGF). Data are presented for pre-treatment (2014; black), second post-treatment (2021; red), and third post-treatment (2022; blue) years. Means for each year–zone combination are indicated by "X"; outliers are shown as points.

Table 3.2. Multi-Response Permutation Procedure (MRPP) pairwise comparisons among treatment zones for the 2021 and 2022 growing seasons. T = MRPP test statistic; A = chance-corrected within-group agreement; p-values < 0.05 are bolded.

	Year 2			Year 3		
Comparison	**T**	**A**	**p**	**T**	**A**	**p**
LGC vs. LGE	-1.90	0.023	0.051	-1.09	0.014	0.133
LGC vs. LGF	-6.18	0.080	**<0.001**	-4.93	0.058	**0.001**
LGC vs. SGC	-1.19	0.013	0.121	0.21	-0.002	0.500
LGC vs. SGE	-3.39	0.039	**0.003**	-1.69	0.019	0.061
LGC vs. SGF	-5.39	0.065	**<0.001**	-3.70	0.044	**0.004**
LGC vs. CTA	-8.53	0.155	**<0.001**	-7.73	0.134	**<0.001**
LGE vs. LGF	-1.33	0.011	0.100	-2.28	0.024	**0.025**
LGE vs. SGC	-0.39	0.004	0.307	-0.41	0.004	0.291
LGE vs. SGE	-1.46	0.015	0.080	0.63	-0.007	0.724
LGE vs. SGF	-0.84	0.008	0.186	-1.29	0.014	0.106
LGE vs. CTA	-5.38	0.066	**<0.001**	-6.54	0.092	**<0.001**
LGF vs. SGC	-2.94	0.029	**0.008**	-3.73	0.034	**0.003**
LGF vs. SGE	-3.67	0.041	**0.002**	-2.60	0.026	**0.009**
LGF vs. SGF	-0.07	0.001	0.431	-0.76	0.007	0.216
LGF vs. CTA	-3.11	0.039	**0.013**	-3.79	0.049	**0.005**
SGC vs. SGE	0.50	-0.007	0.633	0.56	-0.008	0.685
SGC vs. SGF	-0.25	0.004	0.321	-0.29	0.004	0.325
SGC vs. CTA	-6.13	0.086	**<0.001**	-6.33	0.087	**<0.001**
SGE vs. SGF	-0.19	0.003	0.333	0.90	-0.013	0.828
SGE vs. CTA	-6.04	0.087	**<0.001**	-4.91	0.066	**0.001**
SGF vs. CTA	-3.02	0.043	**0.011**	-3.09	0.043	**0.009**

Table 3.3. Results from Indicator Species Analysis (ISA) of understory plant community composition, based on species abundance (% cover) data from pre-treatment (2014) and post-treatment (2021–2022) years. Analyses were conducted at the plot × zone level. Numbers in the table are indicator values (IV), representing the percent affinity of each species to its associated treatment zone and year. Species were considered significant indicators at $p \leq 0.05$ and IV ≥ 25. Only significant indicator species are shown for each group and year.

		Treatment	Controls		Small Gaps									Large Gaps								
		Year	Year 2	Year 3	Pre			Year 2			Year 3			Pre			Year 2			Year 3		
UDSA Code	Lifeform	Specific Epithet and Authority Zone	All	All	SGC	SGE	SGF	SGC	SGE	SGF	SGC	SGE	SGF	LGC	LGE	LGF	LGC	LGE	LGF	LGC	LGE	LGF
AGALA	Forb	*Ageratina altissima* (L.) R.M. King & H. Rob. var. *altissima*						50														
AGRIM	Forb	*Agrimonia* spp. L.												35								
CAREX	Graminoid	*Carex* spp. L.					45										34					
CARYA	Tree	*Carya* spp. Nutt.																				
COCA5	Forb	*Conyza canadensis* (L.) Cronquist															31					
DAGL	Graminoid	*Dactylis glomerata* L.															28					
GOPU	Forb	*Goodyera pubescens* (Willd.) R. Br.	26	32																		
HIPA2	Forb	*Hieracium paniculatum* L.												33						36		
ILOP	Tree	*Ilex opaca* Aiton						33			32											
LITU	Tree	*Liriodendron tulipifera* L.															36			32		
MAFR	Tree	*Magnolia fraseri* Walter	39	52																		
MONAR	Forb	*Monarda* spp. L.																			27	
PHAM4	Forb	*Phytolacca americana* L.															62			37		
PHAM7	Forb	*Phlox amplifolia* Britton						44														
POA	Graminoid	*Poa* spp. L.															51					
POAC4	Fern	*Polystichum acrostichoides* (Michx.) Schott																	29			34
POACEAE	Graminoid	Grass Family								34												
ROPS	Tree	*Robinia pseudoacacia* L.															39					
RUAL	Subshrub	*Rubus allegheniensis* Porter															32					
VIAE	Vine	*Vitis aestivalis* Michx.															32			37		
VISO	Forb	*Viola sororia* Willd.						26														
		Total Indicator Species:	2	2	0	0	1	4	0	1	1	0	0	2	0	0	9	0	1	4	1	1

Table 3.4. Non-native and invasive plant species detected in the species composition dataset across all sampling years. USDA codes and scientific epithets follow the USDA PLANTS database. Bolded species are classified as invasive in North Carolina according to the 2023 NC Invasive Plants List. For each species, the table reports the number of plot × zone combinations in which the species was observed (n), the indicator value (IV), and the treatment zone of maximum group association (Max Grp) for each year.

USDA Code	Specific Epithet and Authority	2014 (n)	2014 (IV)	2014 Max Grp	2021 (n)	2021 (IV)	2021 Max Grp	2022 (n)	2022 (IV)	2022 Max Grp
CEOR7	***Celastrus orbiculatus* Thunb.**	23	12	LGC	28	16	LGF	30	18	LGC
CLTE4	***Clematis terniflora* DC.**	0	–	–	1	11	LGE	0	–	–
DAGL	*Dactylis glomerata* L.	0	–	–	13	35	LGC	11	26	LGC
MIVI	***Microstegium vimineum* (Trin.) A. Camus**	0	–	–	5	10	SGC	2	6	SGC
POLYG4	*Polygonum* spp. L.**	1	11	LGE	5	3	LGC	3	5	LGF
ROMU	***Rosa multiflora* Thunb.**	1	11	LGF	2	9	LGF	2	11	LGF
TRIFO	*Trifolium* spp. L.***	0	–	–	9	12	LGC	0	–	–
TUFA	***Tussilago farfara* L.**	0	–	–	1	11	LGC	1	LGC	11

****Polygonum convolvulus* L. var. *convolvulus***
*****Trifolium repens* L.

Discussion

OVERVIEW

Expanding-gap silviculture produced a rapid and durable increase in ground-layer diversity while preserving a consistent spatial hierarchy among zones. Across two post-treatment censuses, richness, evenness, Shannon, and Simpson indices were all higher than pre-treatment, with gains expressed similarly in both years and across gap sizes. Spatially, gap centers and the surrounding forest matrix consistently supported richer and more even assemblages than gap edges, and the absence of zone × year interactions indicates these patterns were stable over the early post-harvest interval.

Community structure also reorganized in predictable ways. Ordination and MRPP showed clear, persistent compositional separation among zones, with large-gap centers forming the most distinctive assemblages relative to edges and gap-forest subplots. Species gradients along the NMS axes reflected shifts from forb- and bramble-dominated understories toward woody and ericaceous taxa, aligning with the observed diversity responses. Indicator species analysis further corroborated this restructuring: indicators surged in year two and then moderated in year three, with large-gap centers hosting the most and strongest indicators. Together, these results show that gap creation simultaneously elevates understory diversity and promotes spatially structured community differentiation, with large-gap centers acting as focal points for early post-harvest assembly.

NON-NATIVE SPECIES DYNAMICS

The introduction and spread of non-native species following forest disturbance is a central concern in the restoration and management of temperate forests. In this study,

comprehensive ground-layer vegetation surveys conducted before (2014) and after (2021, 2022) canopy gap creation revealed that, despite a substantial increase in overall species richness post-treatment, the entry and establishment of non-native species remained limited. Of the 63 species detected exclusively in the post-treatment period, only five (~8%) were non-native, and just three—*Microstegium vimineum* (Japanese stiltgrass), *Clematis terniflora* (sweet autumn clematis), and *Tussilago farfara* (coltsfoot)—are classified as invasive in North Carolina according to the NC Invasive Plants List (North Carolina Native Plant Society & North Carolina Invasive Plant Council 2023).

According to the list, *Microstegium vimineum* is a level 1 (Severe Threat). It was observed in five plot zones in 2021 but declined to two zones in 2022, with indicator values dropping from 10 to 6. This pattern suggests a transient response to canopy opening rather than sustained expansion. *Clematis terniflora* (level 2, Significant Threat) appeared in only one plot zone in 2021 and was absent in 2022. *Tussilago farfara* (level 2) was present in one plot zone in both years, with stable indicator values. Meanwhile, established invaders such as *Celastrus orbiculatus* (Chinese bittersweet) and *Rosa multiflora* (multiflora rose) persisted before and after treatment, with *C. orbiculatus* showing a modest post-disturbance increase that prompted targeted management intervention in 2022.

These findings indicate that, despite increased resource availability and disturbance associated with gap creation, the influx of non-native and invasive species was modest and largely ephemeral. The most aggressive invader, *M. vimineum*, did not exhibit persistent expansion, and other non-natives either remained rare or stable in occurrence. The overall proportion of new non-natives was low, and the most problematic species did not establish widespread dominance.

This pattern is consistent with the diversity–invasibility relationships described by Brown and Peet (2003). Their work in southern Appalachian forests demonstrated that, while riparian zones with high native richness and frequent disturbance supported greater exotic richness, upland forests—particularly at fine spatial scales—showed little relationship between native diversity and exotic invasion. Instead, high native diversity and limited propagule pressure in upland settings appeared to confer resistance to invasion. In the present study, the substantial increase in native species richness following gap creation did not translate into a corresponding surge in non-native establishment, supporting the hypothesis that diverse, upland forest communities can buffer against invasion, even after disturbance (Brown and Pete 2003).

Collectively, these results suggest that canopy-gap creation in species-rich upland forests may not dramatically elevate the risk of non-native plant invasion in the short term. However, the entry of a small number of invasive species underscores the need for continued monitoring and rapid management response to new incursions. These findings reinforce the importance of maintaining high native diversity as a strategy for limiting the ecological impact of non-native species in managed forest landscapes.

CONTEXTUALIZING SPECIES RICHNESS GAINS

When compared to the broader literature, the species richness gains observed in this study are notable for both their scale and rapidity and are directly comparable to those reported in other restoration-focused research. For example, following a decade of oak restoration treatments in southern Appalachian hardwood forests, results showed that the most intensive treatment—shelterwood harvest combined with prescribed fire—resulted in an average gain of approximately 8 species per unit over nine years, while repeated fire and oak shelterwood with

midstory herbicide treatments yielded gains of 12 and 6 species, respectively, with no increase in controls (Benz et al. 2025). The absolute differences between treatments and controls were generally in the range of 6–12 species per unit, and post-treatment richness values typically ranged from 50 to 65 species per unit, depending on treatment and year. These gains are directly comparable to the zone-level increases observed in the present study, where gains of up to 13 species were recorded between treated and control zones within just two to three years, and the highest post-treatment richness values in gap centers and forest matrix zones approached or exceeded the upper range reported by Benz et al. (2025). This alignment underscores that the magnitude of diversity enhancement achieved through harvested gaps is on par with, or even exceeds, the gains observed in other leading restoration approaches, reinforcing the ecological significance and broader relevance of these results.

Similarly, in a 17-year study of herbaceous plant communities following shelterwood-with-reserves regeneration harvests in southern Appalachian cove and upland hardwood forests, researchers found that herbaceous species richness was consistently higher in cove hardwood forests (36–41 species per plot) than in upland hardwood forests (16–17 species per plot), with shelterwood harvests having a neutral or slightly positive effect on richness, especially in upland sites (Greenberg et al. 2025). However, the differences in richness between harvested and mature stands were generally modest, often amounting to only a few species per plot, and the largest observed increases rarely exceeded 5 species per plot over 17 years (Greenberg et al. 2025).

The apparent magnitude of diversity responses to forest management depends critically on spatial scale, as diversity patterns can vary dramatically between fine-scale and broad-scale observations. For example, the mean species richness per 4 m^2 quadrat was documented to be relatively stable across management types in northern hardwood forests, typically differing by

less than 3–7 species, with values ranging from 4.3 in old-growth to 10.6 in uneven-aged stands (Scheller and Mladenoff 2002). But, when examining estimated total stand-level richness, differences became much more pronounced, with values spanning from 34.8 species in old-growth to 57.2 species in uneven-aged stands—a difference of over 20 species between some stand types. These stand-level richness estimates are comparable to the zone-level richness observed in the present study, where post-treatment values frequently exceeded 40 species per zone and differences between treated and control zones often surpassed 10 species. Thus, while fine-scale quadrat comparisons may suggest only modest changes, both studies demonstrate that at broader spatial scales, management interventions can yield substantial and ecologically meaningful gains in species richness. The magnitude and pattern of richness gains observed following canopy gap creation are consistent with those documented by Scheller and Mladenoff (2002) at the stand level.

A more pronounced response to large-scale natural disturbance—hurricane followed by salvage logging—in a high-elevation Southern Appalachian Forest was previously documented (Elliott et al. 2002). Three years after the disturbance, the salvage-logged site supported 93 species at the stand scale, compared with 59 species in the adjacent undisturbed forest, a difference of 34 species. At the subplot scale (1 m^2 quadrats aggregated), mean richness rose from 23.3 species in the undisturbed forest to 33.3 species in the disturbed forest, an increase of 10 species per subplot. The authors attributed both the magnitude and persistence of these diversity gains to enhanced environmental heterogeneity and the simultaneous presence of early- and late-successional species in the disturbed area (Elliott et al. 2002).

Taken together, these comparisons demonstrate that the species richness gains achieved through silviculture methods in this study are not only rapid and robust, but also well within or

above the upper range of outcomes reported from both experimental and natural disturbance regimes in temperate forests. While many long-term studies of silvicultural interventions document only modest increases in richness—often just a few species per sampling unit, and sometimes less—here, the observed gains routinely exceeded 10 species per zone within a short post-treatment window. This magnitude of response is matched only by the most intensive restoration treatments or large-scale natural disturbances, such as those documented by Benz et al. (2025) and Elliott et al. (2002), and far surpasses the incremental changes typically seen in more moderate or fine-scale management scenarios. Importantly, these results underscore the capacity of expanding-gap approaches to generate ecologically meaningful enhancements in ground-layer diversity, reinforcing their value as a tool for biodiversity conservation and ecosystem restoration in mixed-oak forests.

Conclusions

This study demonstrates that the initial entry of an expanding-gap silvicultural system in Southern Appalachian mixed-oak forests can rapidly and substantially enhance ground-layer plant diversity, restructure community composition, and promote habitat specialization. By situating these findings within the broader context of the literature, it becomes clear that the diversity gains observed here are not only statistically significant, but also biologically consequential providing a compelling benchmark for future research and management aimed at sustaining the rich understory communities characteristic of the southern Appalachians. The observed increases in species richness, evenness, and overall diversity—especially within gap centers and forest matrix zones—were not only statistically robust but also ecologically meaningful, with gains frequently exceeding 10 species per zone within just two to three years

post-harvest. These effects extended beyond the immediate footprint of canopy gaps, as midstory removal in the surrounding matrix also resulted in persistent diversity gains and increased light availability, underscoring the broader ecological impact of integrated silvicultural interventions.

Importantly, the influx of non-native species following disturbance was modest and largely ephemeral, suggesting that high native diversity and limited propagule pressure in upland forests can buffer against invasion even after significant canopy and midstory manipulation. When contextualized within the broader literature, the magnitude and rapidity of richness gains observed here are on par with, or exceed, those reported for other leading restoration treatments and large-scale natural disturbances, reinforcing the biological relevance of these results.

As the first step in a planned, long-term system, this study provides a critical benchmark for evaluating the ecological potential of expanding-gap silviculture to counteract mesophication and restore biodiversity in temperate forests. While the current findings are promising, they represent only the initial phase of a dynamic process. Future research should continue to monitor these communities as gap expansions proceed, with particular attention to the persistence of diversity gains, the trajectories of indicator species and specialized assemblages, and the ongoing risk of non-native species establishment. By integrating continued empirical monitoring with adaptive management, expanding-gap approaches may offer a powerful tool for sustaining a diverse understory community that characterize the southern Appalachians, informing both regional conservation strategies and broader efforts to restore resilience in temperate forest ecosystems.

REFERENCES

Abrams MD, Nowacki GJ. 1992. Historical Variation in Fire, Oak Recruitment, and Post-Logging Accelerated Succession in Central Pennsylvania. Bulletin of the Torrey Botanical Club. 119(1):19-28. https://doi.org/10.2307/2996916.

Abrams, M. D., Orwig, D. A., & Demeo, T. E. (1995). Dendroecological Analysis of Successional Dynamics for a Presettlement- Origin White-Pine-Mixed-Oak Forest in the Southern Appalachians, USA. Journal of Ecology, 83(1), 123–133. https://doi.org/10.2307/2261156.

Alexander HD, Siegert C, Brewer JS, Kreye J, Lashley MA, McDaniel JK, Paulson AK, Renninger HJ, Varner JM. (2021). Mesophication of Oak Landscapes: Evidence, Knowledge Gaps, and Future Research. BioScience. 71(5):531-542. https://doi.org/10.1093/biosci/biaa169.

Allison, J.B. and Hale, L.B. (1997) Soil survey of Haywood County area, North Carolina. USDA Natural Resources Conservation Service, Washington, DC.

Anderson, M.J. (2001), A new method for non-parametric multivariate analysis of variance. Austral Ecology, 26: 32-46. https://doi-org.prox.lib.ncsu.edu/10.1111/j.1442-9993.2001.01070.pp.x.

Bates, D., Mächler, M., Bolker, B., & Walker, S. (2015). Fitting Linear Mixed-Effects Models Using lme4. Journal of Statistical Software, 67(1), 1–48. https://doi.org/10.18637/jss.v067.i01.

Benz, B.L. (2020). Ground-layer vegetation response to silvicultural treatments for oak (*Quercus*) regeneration in Southern Appalachian forests. MSc thesis, North Carolina State University, Raleigh, NC. Available at: https://www.lib.ncsu.edu/resolver/1840.20/38231. (accessed 31 June 2024).

Brown, R.L. and Peet, R.K. (2003), Diversity and invasibility of southern Appalachian plant communities. Ecology, 84: 32-39. https://doi-org.prox.lib.ncsu.edu/10.1890/0012-9658(2003)084[0032:DAIOSA]2.0.CO;2.

Campbell, J.W., Hanula, J.L., and Waldrop, T.A. (2007). Effects of prescribed fire and fire surrogates on floral visiting insects of the Blue Ridge Province in North Carolina. Biological Conservation, 134(3), 393–404. https://doi.org/10.1016/j.biocon.2006.08.029.

Donoso, P.J. and Nyland, R.D. (2006) Interference to hardwood regeneration in northeastern North America: The effects of raspberries (*Rubus* spp.) following clearcutting and shelterwood methods. Northern Journal of Applied Forestry, 23: 288–296. https://doi.org/10.1093/njaf/23.4.288.

Dufrêne, M. and Legendre, P. (1997), Species assemblages and indicator species: the need for a flexible asymmetrical approach. Ecological Monographs, 67: 345-366. https://doi-org.prox.lib.ncsu.edu/10.1890/0012-9615(1997)067[0345:SAAIST]2.0.CO;2.

Gilliam, F.S. (2007) The ecological significance of the herbaceous layer in temperate forest ecosystems. BioScience, 57: 845–858. https://doi.org/10.1641/B571007.

Gilliam, F.S. (2016), Forest ecosystems of temperate climatic regions: from ancient use to climate change. New Phytol, 212: 871-887. https://doi.org/10.1111/nph.14255.

Grover, Z. (2020) Climate growth responses and carbon consequences of compositional change in mature Southern Appalachian oak-hickory forests. MSc thesis, North Carolina State University, Raleigh, NC. Available at: https://www.lib.ncsu.edu/resolver/1840.20/38062. (accessed 31 July 2024).

Grover, Z.S., Forrester, J.A., Keyser, T.L., King, J.S., and Altman, J. (2023). Growth response, climate sensitivity, and carbon storage vary with wood porosity in a southern Appalachian mixed hardwood forest. Agricultural and Forest Meteorology, 332: 109358. https://doi.org/10.1016/j.agrformet.2023.109358.

Hadley, J.B. and Nelson, A.E. (1971) Geologic map of the Knoxville quadrangle, North Carolina, Tennessee, and South Carolina. U.S. Geological Survey Miscellaneous Geologic Investigations Map I-654, scale 1:250,000.

Jackson, B. C., Pittillo, J. D., Allen, H. L., Wentworth,h T. R., Bullock, B. P., Loftis D. L. (2009). Species Diversity and Composition in Old-Growth and Second-Growth Rich Coves of The Southern Appalachian Mountains. Castanea, 74(1), 27-38. https://doi.org/10.2179/07-017.1.

Kern CC, Palik BJ, Strong TF. Ground-layer plant community responses to even-age and uneven-age silvicultural treatments in Wisconsin northern hardwood forests. Forest Ecology and Management. 2006;230(1–3):162–170. https://doi.org/10.1016/j.foreco.2006.03.034.

Kuznetsova, A., Brockhoff, P. B., & Christensen, R. H. B. (2017). lmerTest Package: Tests in Linear Mixed Effects Models. Journal of Statistical Software, 82(13), 1–26. https://doi.org/10.18637/jss.v082.i13.

Landuyt D, De Lombaerde E, Perring MP, et al. (2019) The functional role of temperate forest understory vegetation in a changing world. Glob Change Biol. 2019; 25: 3625–3641. https://doi-org.prox.lib.ncsu.edu/10.1111/gcb.14756.

LeGrand, H., B. Sorrie, and T. Howard. 2025. Vascular Plants of North Carolina [Internet]. Raleigh (NC): North Carolina Biodiversity Project and North Carolina State Parks. Available from https://auth1.dpr.ncparks.gov/flora/index.php.

Lenth R (2025). emmeans: Estimated Marginal Means, aka Least-Squares Means. R package version 1.11.1-00001, https://rvlenth.github.io/emmeans/.

McNab, W., Greenberg, C. H., & Berg, E. C. (2004). Landscape distribution and characteristics of large hurricane-related canopy gaps in a southern Appalachian watershed. Forest Ecology and Management, 196(2-3), 435-447. https://doi.org/10.1016/j.foreco.2004.04.004.

Mou, P., & Warrillow, M. P. (2000). Ice Storm Damage to a Mixed Hardwood Forest and Its Impacts on Forest Regeneration in the Ridge and Valley Region of Southwestern Virginia. The Journal of the Torrey Botanical Society, 127(1), 66–82. https://doi.org/10.2307/3088748.

Muller, R. N., & Bormann, F. H. (1976). Role of *Erythronium americanum* Ker. in Energy Flow and Nutrient Dynamics of a Northern Hardwood Forest Ecosystem. Science, 193(4258), 1126–1128. http://www.jstor.org/stable/1742725.

Muller, R.N. (2003) Nutrient relations of the herbaceous layer in deciduous forest ecosystems. In: Gilliam, F.S. and Roberts, M.R. (eds) The herbaceous layer in forests of eastern North America, pp. 15–37. Oxford University Press, New York.

Natural Resources Conservation Service. PLANTS Database. United States Department of Agriculture. Accessed June 30, 2025, from https://plants.usda.gov.

North Carolina State Climate Office, NC State University. Cardinal [data retrieval interface]. Available at: https://products.climate.ncsu.edu/cardinal/request. (accessed 6 August 2024).

North Carolina Wildlife Resources Commission. (2020) 2020 North Carolina white-tailed deer density. Available at: https://www.ncwildlife.gov/media/1663/open. (accessed 13 March 2025).

Nowacki, G. J., & Abrams, M. D. (1992). Community, edaphic, and historical analysis of mixed oak forests of the Ridge and Valley Province in central Pennsylvania. Canadian Journal of Forest Research. 22(6): 790-800. https://doi-org.prox.lib.ncsu.edu/10.1139/x92-108.

Nowacki, G. J., & Abrams, M. D. (2008). The Demise of Fire and "Mesophication" of Forests in the Eastern United States. BioScience, 58(2), 123-138. https://doi.org/10.1641/B580207.

R Core Team (2023). *R: A Language and Environment for Statistical Computing.* R Foundation for Statistical Computing, Vienna, Austria. https://www.R-project.org/.

Retrieved from the Integrated Taxonomic Information System (ITIS), www.itis.gov, CC0. https://doi.org/10.5066/F7KH0KBK. (accessed 22 July 2024).

Runkle, J.R. (1982), Patterns of Disturbance in Some Old-Growth Mesic Forests of Eastern North America. Ecology, 63: 1533-1546. https://doi.org/10.2307/1938878.

Scheller, R.M. and Mladenoff, D.J. (2002), Understory species patterns and diversity in old-growth and managed northern hardwood forests. Ecological Applications, 12: 1329-1343. https://doi-org.prox.lib.ncsu.edu/10.1890/1051-0761(2002)012[1329:USPADI]2.0.CO;2.

Spicer, Michelle & Mellor, Hannah & Carson, Walter. (2020). Seeing beyond the trees: a comparison of tropical and temperate plant growth forms and their vertical distribution. Ecology. 101. https://doi.org/10.1002/ecy.2974.

Ulrey, C.J. 2002. The relationship between soil fertility and the forests of the southern Appalachian region. Ph.D. dissertation, North Carolina State University, Raleigh, North Carolina. Available at: http://www.lib.ncsu.edu/resolver/1840.16/5804. (accessed 5 July 2025).

Whittaker, R.H. (1956), Vegetation of the Great Smoky Mountains. Ecological Monographs, 26: 1-80. https://doi-org.prox.lib.ncsu.edu/10.2307/1943577.

Woodbridge, M., Keyser, T., & Oswalt, C. (2022). Stand and environmental conditions drive functional shifts associated with mesophication in eastern US forests. Frontiers in Forests and Global Change, 5, 991934. https://doi.org/10.3389/ffgc.2022.991934.

CHAPTER 4 : SYNTHEIS AND FUTURE RECOMMENDATIONS

Synthesis

This thesis addresses the pressing challenge of sustaining biodiversity and productivity in Southern Appalachian mixed-oak forests, ecosystems increasingly threatened by mesophication, altered disturbance regimes, and the oak regeneration bottleneck. As established in Chapter 1, the Southern Appalachian Femelschlag Experiment (SAFE) was conceived to rigorously test whether expanding-gap silviculture could restore ecological complexity, promote oak and hickory regeneration, and maintain the rich ground-layer diversity that characterizes these forests.

The findings from Chapters 2 and 3 demonstrate that expanding-gap silviculture induces rapid and substantial changes in both ground-layer productivity and diversity. Biomass accumulation patterns revealed significant productivity responses to canopy gap treatments, with large gaps accumulating 73% more biomass from pre-treatment (2014) to 2022 (24,512 g to 42,526 g) and small gaps showing a 78% increase over the same period (20,104 g to 35,720 g). Throughout the study, large gaps consistently maintained approximately 19% higher biomass than small gaps, quantitatively supporting the enhanced productivity potential of gap-based silvicultural approaches and underscoring the importance of disturbance intensity in driving understory productivity responses.

Despite these robust productivity gains, the spatial patterns of productivity and diversity responses were not always aligned. Both biomass and diversity peaked in gap centers, but the pronounced difference in diversity between matrix and control plots was not mirrored by a similar pattern in ground-layer biomass. Forest matrix zones adjacent to gaps exhibited significantly higher species richness and diversity than uncut controls, yet total ground-layer

biomass did not show a corresponding increase in these matrix zones relative to controls. This divergence suggests that diversity and productivity may respond differently to canopy and midstory manipulations, with diversity gains potentially extending into the surrounding matrix due to increased light and microhabitat heterogeneity, even when productivity remains relatively unchanged.

The SAFE experiment further revealed that spatial proximity to gap centers, rather than gap size per se, was the primary determinant of ground-layer biomass dynamics during the early successional period. Total biomass and key plant lifeforms—including trees, *Rubus* spp., and graminoids—showed pronounced increases near gap centers, with a generally linear decline toward the forest matrix. Light availability and canopy openness emerged as the dominant abiotic filters structuring these patterns, as localized increases in light facilitated the rapid colonization and growth of ruderal and light-demanding taxa.

Analyses of lifeform responses highlighted the complexity of early successional dynamics. *Rubus* spp. exhibited strong spatial structuring, dominating gap centers and declining sharply toward the forest interior. Graminoids and tree seedlings also displayed distinct spatial niches, with aspect and microhabitat conditions further modulating their responses. Pre-treatment biomass was a significant predictor of post-disturbance recovery for most groups, emphasizing the legacy effects of advanced regeneration.

The results from Chapter 3 show that expanding-gap silviculture not only enhances ground-layer diversity but also accelerates the development of specialized assemblages and compositional differentiation among zones. Species richness increased markedly from pre-treatment levels to post-treatment, with the highest values in gap centers and forest matrix zones. Shannon and Simpson's diversity indices also increased and remained elevated through three

years post-harvest. Multivariate analyses revealed strong compositional differentiation, particularly in large gap centers, and a fourfold increase in the number of significant indicator species, signaling emerging habitat specialization. These findings underscore the capacity of gap-based management to foster fine-scale environmental heterogeneity and support a dynamic mosaic of specialized understory assemblages.

Despite increased resource availability following canopy disturbance, the establishment of non-native species was limited and largely ephemeral. The influx of non-native taxa did not keep pace with the substantial gains in native diversity, suggesting that high native richness may have helped to buffer against invasion, even after significant disturbance. This result provides reassurance that expanding-gap silviculture can enhance biodiversity without dramatically increasing the risk of biological invasion in the short term.

Collectively, these findings reinforce the ecological importance of fine-scale spatial heterogeneity in driving ecosystem response to disturbance. The ground-layer emerges as both a driver and a barometer of ecosystem function and resilience, responding rapidly and spatially to disturbance in ways that can be harnessed to meet both conservation and regeneration goals. The divergence between productivity and diversity responses further highlights the need for integrated management approaches that consider multiple dimensions of ecosystem function.

Management Implications

Looking ahead to the planned gap expansions in 2029, several key questions arise regarding the persistence and trajectory of the observed patterns. As gaps are enlarged, it is likely that the spatial gradients in light, microclimate, and resource availability will intensify, potentially amplifying both productivity and diversity responses. Long-term monitoring will be

essential to determine whether gap size becomes a stronger determinant of understory dynamics as succession progresses and resource competition increases. Future research should address the temporal stability of diversity gains by investigating whether the elevated species richness and habitat specialization observed in the early post-treatment years persist, diminish, or further increase as gaps expand and close over time. The trajectories of different lifeforms, particularly the dominance of *Rubus* spp. and other ruderal taxa, require careful observation to understand their implications for tree regeneration and long-term carbon sequestration. It will also be important to assess whether the current divergence between diversity and biomass responses persists or converges as the system matures and competitive hierarchy's shift.

Based on the findings of this thesis, several recommendations are offered for the management of Southern Appalachian mixed-oak forests and similar temperate systems. Management interventions should prioritize the creation and maintenance of spatially heterogeneous environments, as these support both high productivity and biodiversity. As the SAFE experiment proceeds with gap enlargement, adaptive management should be employed to track ecological responses and adjust treatments as needed to balance regeneration, diversity, and ecosystem function. Ensuring the presence of robust, advanced regeneration before disturbance will facilitate rapid and resilient post-disturbance recovery, particularly for target canopy species. Continued monitoring for non-native and invasive species remains essential, especially as disturbance regimes are intensified and competitive pressure increases.

In conclusion, the initial implementation of expanding-gap silviculture in the SAFE experiment demonstrates a promising pathway for restoring biodiversity, enhancing productivity, and counteracting mesophication in Southern Appalachian mixed-oak forests. By leveraging fine-scale spatial heterogeneity and lifeform dynamics, this approach offers a flexible and

adaptive framework for sustaining resilient, multifunctional forest ecosystems. As future gap expansions proceed, ongoing research and adaptive management will be critical to realizing the full potential of this strategy and informing broader efforts to restore and conserve temperate forest biodiversity in a changing world.

APPENDICES

Appendix A

DESTRUCTIVE SAMPLING

General Protocol Overview

Destructive 1 m² subplots were used to sample ground layer biomass in spring and summer, following a standardized protocol for visual cover estimation, biomass harvest, and sample processing. In each subplot, total vegetation cover and cover by lifeform were visually estimated to the nearest 10% (summer) or 0.1% (spring). All live aboveground plant material rooted within the subplot and <1 m tall was clipped to the mineral soil, oven-dried at 50°C to constant weight and weighed to the nearest 0.01 g. Subplots were not permanently marked for future relocation.

Summer (Peak-Growing Season) Collections (2021)

In summer 2021, 68 destructive subplots were established across all treatments (large gap, small gap, control), distributed among all experimental units. Within each selected plot, three subplots were placed along the northeast transect at ~5 m, 10 m, and at the gap edge relative to the gap center (or at 5, 10, and 15 m from the center in controls). All ground-layer lifeforms (herbs, trees, shrubs, graminoids, vines, ferns/fern allies, subshrubs) were included in cover estimation and biomass harvest. Additional targeted subplots (n = 5) were established to ensure representation across all cover classes and lifeforms for allometric regression development.

Additional High-Cover Rubus Biomass Sampling (2025)

To improve the accuracy of *Rubus* spp. biomass estimation at high percent cover, we conducted an additional round of destructive sampling in September 2025. The initial 2021

summer sampling did not capture *Rubus* plots exceeding 55% cover, and allometric equations calibrated to those data required extrapolation for many annual survey plots. To address this, 10 supplemental clip-quad samples (0.5 m² each) targeting roadside *Rubus*-dominated patches with 50–95% cover were collected, processed, and used to extend the empirical range of our allometric relationships. This supplemental effort supports more reliable biomass estimation in subplots with dense *Rubus* growth.

Spring (Ephemeral Community) Collections (2024)

In spring 2024, 35 1m² destructive subplots were established with a specific focus on the spring herbaceous community, defined as species that are reproductive, flowering, or reach peak vegetative development before canopy closure. Subplots were distributed to ensure at least two per experimental unit and to fill pre-defined cover class bins (e.g., 0.1–10%, 10–20%, up to 40+% cover). Only spring herbaceous species were included in cover estimates and biomass harvest; other lifeforms (summer herbs, woody species, graminoids, ferns, etc.) were excluded. Quadrat placement was selective to ensure adequate representation of the full range of spring herbaceous cover, and sampling was stratified across both "Gap" and "Matrix" microhabitats.

Exclusion of Spring from Main Analyses

Although destructive biomass sampling was conducted in both spring and summer, only summer (peak growing season) biomass data were included in the primary analyses of ground layer productivity. This decision was based on the consistently low contribution of spring forbs to total ground layer biomass across all treatments and years. For example, average spring forb biomass in all treatments ranged from 1.3–8.9 g/m²(2021–2023), with maximum values rarely exceeding 75 g/m², and standard deviations indicating low variability within and among treatments (see Table 1.x). In contrast, summer ground layer biomass was an order of magnitude

higher and more responsive to treatment effects (see Chapter 2). Therefore, spring biomass data were excluded from further statistical analyses of treatment effects on total ground layer productivity.

Table A1. Regression equations for estimating biomass (g/m²) from percent cover (x) by lifeform. Models are either power ($y = ax^b$) or linear ($y = ax + b$) regressions, as indicated. Sample size (n), coefficient of determination (R^2), and standard error of estimate (SE) are shown for each model.

Lifeform	n	Regression Equation	R^2	SE
Ferns	23	$y = 0.188x^{1.466}$	0.761	1.35
Forbs	59	$y = 1.872x + 2.833$	0.699	27.04
Graminoids	36	$y = 2.200x + 0.592$	0.895	16.24
Rubus spp.	37	$y = 3.090x^{0.740}$	0.462	1.21
Shrubs	15	$y = 1.360x^{1.152}$	0.880	0.62
Trees	65	$y = 0.628x^{1.451}$	0.623	1.32
Vines	51	$y = 0.820x^{1.433}$	0.611	1.27
Spring	35	$y = 0.655x^{1.082}$	0.879	0.55

CONTROL TESTING

To ensure that observed treatment effects were not confounded by pre-existing spatial or temporal variation in control plots, we conducted a dedicated analysis of biomass change in controls by lifeform at the subplot level. This approach aligns with best practices for validating experimental baselines in forest ecology, thereby enhancing the interpretability of treatment contrasts. Biomass data for control subplots were extracted for the years 2021 and 2022. For each subplot and lifeform, we calculated the change in aboveground biomass as:

$$\Delta Biomass = Biomass_{2022} - Biomass_{2021}$$

For each lifeform (graminoids, herbs, *Rubus* spp., vines, and trees), we fit linear mixed-effects models to test for inherent spatial structuring in biomass change among control subplots.

The response variable was the calculated biomass change (2022–2021). The fixed effects included cardinal direction (N, S, E, W) and distance from the plot center (GC, MC, E), while random effects accounted for the nested experimental design (Unit, Plot nested within Unit, and Direction nested within Plot nested within Unit). Models were fitted using the `lmerTest` package in R, and model assumptions were checked via residual and Q-Q plots.

All analyses were performed using R Statistical Software (v4.3.2; R Core Team 2023) with the lme4 (Bates et al. 2015), lmerTest (Kuznetsova et al. 2017), and emmeans (Lenth 2025) packages. Significance tests for pairwise comparisons were adjusted using Tukey's HSD method. *Rubus* spp. had insufficient nonzero biomass change; therefore, statistical modeling was not pursued due to a lack of data.

Analysis of aboveground biomass change (2022–2021) in control subplots revealed no significant effects of cardinal direction or distance from plot center for graminoids, trees, or vines, indicating spatial homogeneity in these groups over the study period. Forbs were the exception, exhibiting a significant aspect effect: north-facing subplots showed lower mean biomass change compared to west-facing subplots (mean difference: -13.67 g/m^2; $p = 0.0309$), suggesting some background environmental heterogeneity in undisturbed plots. *Rubus* spp. displayed negligible biomass change in controls, precluding meaningful statistical analysis.

Overall, these results support using control plots as a valid baseline for treatment comparisons in most lifeforms, highlighting the need to acknowledge aspect-driven variability for forbs in undisturbed forest conditions. All models were checked for normality and homoscedasticity, and the limited sample sizes for some lifeforms warrant cautious interpretation of non-significant results.

2014 vs 2020 Biomass Comparison

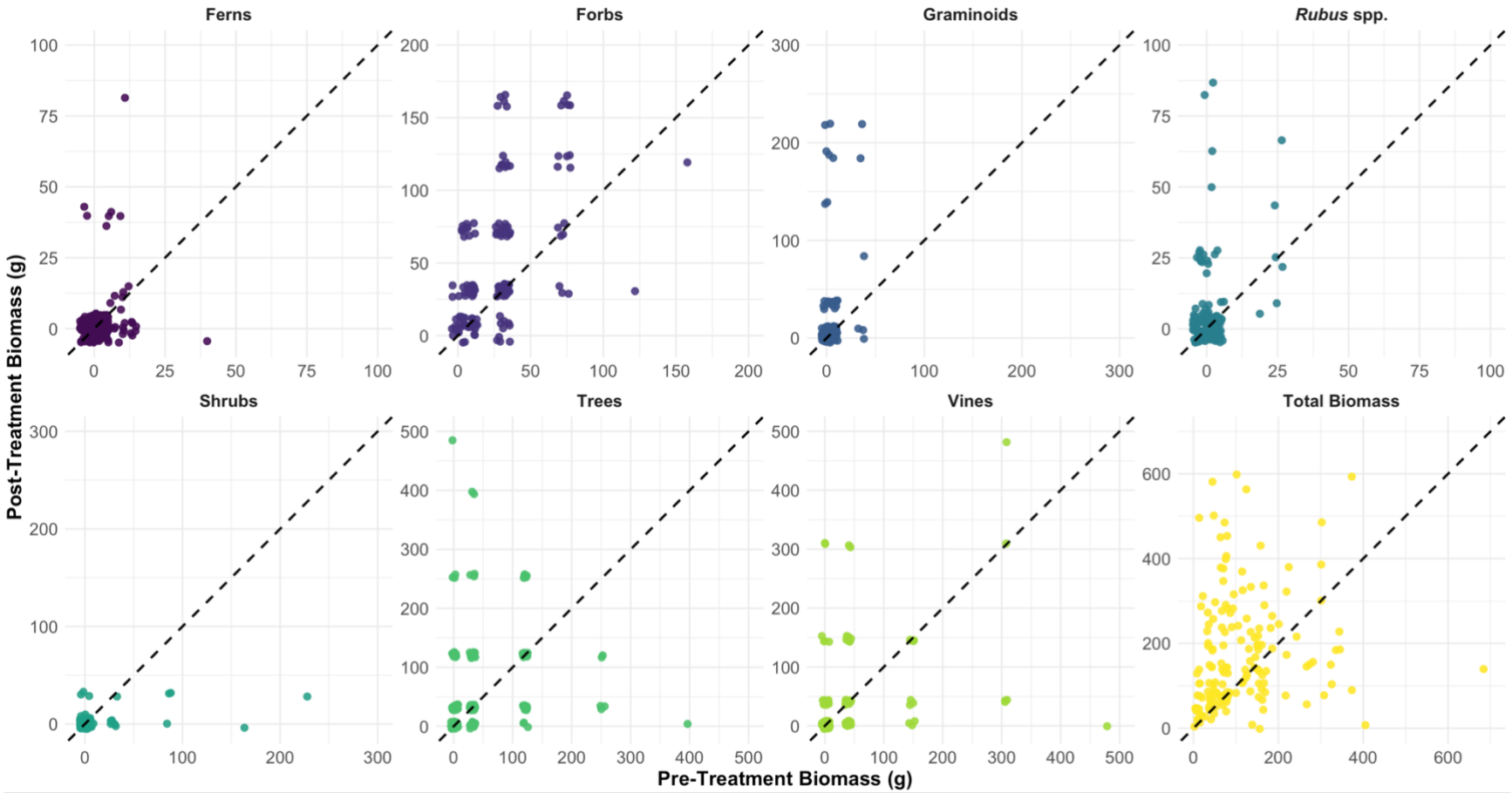

Figure A1a. Pre- and post-treatment biomass for each lifeform and total biomass in 2020. Each point represents a subplot. The dashed 1:1 line indicates no net change; points above the line increased in biomass post-treatment, points below decreased, and points along the y-axis at x = 0 represent newly established individuals.

2014 vs 2021 Biomass Comparison

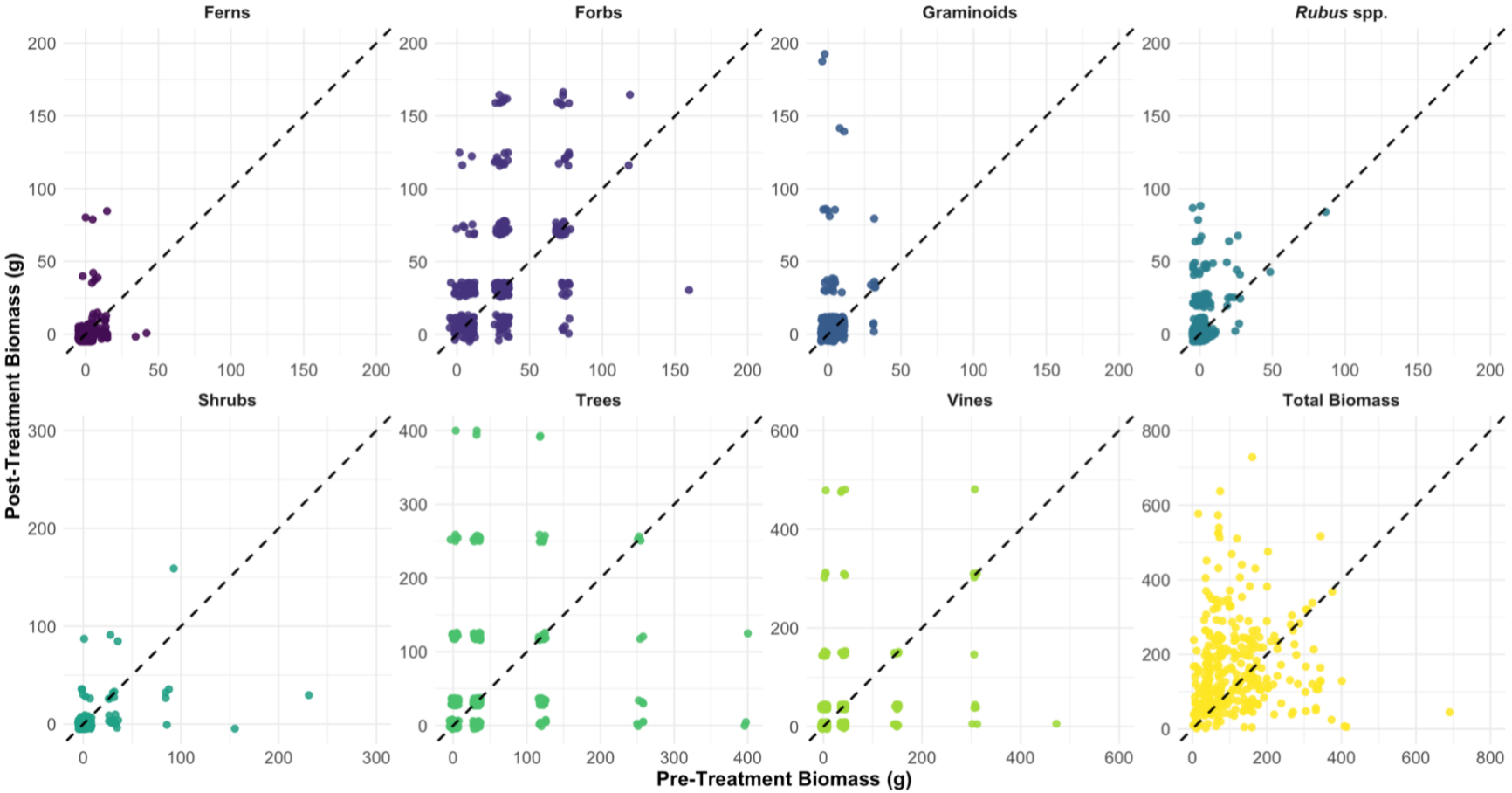

Figure A1b. Pre- and post-treatment biomass for each lifeform and total biomass in 2021. Each point represents a subplot. The dashed 1:1 line indicates no net change; points above the line increased in biomass post-treatment, points below decreased, and points along the y-axis at x = 0 represent newly established individuals.

Table A2. Mixed-effects model results for treatment, direction, and distance effects on photosynthetic photon flux density (PPFD), canopy openness, and soil moisture in gap and control plots. Degrees of freedom (df), F-statistics, and p-values are shown for each interaction and main effect term. Significant results are bolded.

Interaction Term	Model	PPFD			Openness			Soil Moisture		
		df	F	p	df	F	p	df	F	p
Treatment x Direction x Distance	Gaps	12, 280.9	1.30	0.217	12, 281.1	1.10	0.357	12, 283.2	0.64	0.807
Direction x Distance	Gaps	12, 280.9	0.84	0.608	12, 280.8	0.56	0.872	12, 283.2	1.19	0.289
	Controls	6, 63.8	1.22	0.309	6, 63.0	1.80	0.113	6, 72.0	0.88	0.513
Treatment x Direction	Gaps	3, 53.8	0.65	0.589	3, 53.5	0.88	0.456	3, 53.35	1.00	0.402
Treatment x Distance	Gaps	4, 272.7	**2.62**	**0.036**	4, 273.0	**5.57**	**< .001**	4, 283.2	0.69	0.601
Treatment	Gaps	1, 4.1	0.06	0.824	1, 15.3	**15.71**	**0.001**	1, 4.0	0.55	0.498
Direction	Gaps	3, 50.7	**4.59**	**0.006**	3, 50.2	2.25	0.094	3, 50.3	0.39	0.763
	Controls	3, 24.3	0.33	0.805	3, 21.1	0.28	0.842	3, 24.0	1.62	0.211
Distance	Gaps	4, 272.7	**11.41**	**< .001**	4, 273.0	**9.17**	**< .001**	4, 279.2	1.09	0.361
	Controls	2, 63.8	1.39	0.257	2, 61.2	2.60	0.082	2, 70.0	1.16	0.321

Appendix B

Table B1. Species detected exclusively in pre-treatment (2014) or post-treatment (2021–2022) ground-layer vegetation surveys, with USDA PLANTS codes, scientific names, and non-native status. The "Non-native" column indicates species that are non-native to North Carolina according to the Vascular Plants of North Carolina database (LeGrand, Sorrie & Howard 2025). For genus-level taxa, a "–" denotes genera with both native and non-native species present in Buncombe County; for these, non-native status could not be assigned at the genus level. In this dataset, only two genera—*Hypericum* spp. L. (non-native of concern: *Hypericum perforatum* L.) and *Lespedeza* spp. Michx. (non-native of concern: *Lespedeza cuneata* (Dum. Cours.) G. Don)—are flagged with a "–". However, only the native *Lespedeza repens* (L.) W. Bart. was detected in our samples.

USDA Code	Specific Epithet and Authority	Non-native
	Only found in Pre-treatment (2014) surveys	
ACPA	*Actaea pachypoda* Elliott	
ARNU2	*Aralia nudicaulis* L.	
FRVI	*Fragaria virginiana* Duchesne	
HEAM6	*Heuchera americana* L.	
PAQU	*Panax quinquefolius* L.	
	Only found in Post-treatment (2021 & 2022) surveys	
AGPE	*Agrostis perennans* (Walter) Tuck.	
ANSO	*Antennaria solitaria* Rydb.	
ANVI3	*Anemone virginiana* L.	
ARABI2	*Arabis* spp. L.	
ASQU	*Asclepias quadrifolia* Jacq.	
BOCY	*Boehmeria cylindrica* (L.) Sw.	
CACO26	*Cardamine concatenata* (Michx.) Sw.	
CADI10	*Cardamine diphylla* (Michx.) Wood	
CAFL22	*Calycanthus floridus* L.	
CIRA	*Cimicifuga racemosa* (L.) Nutt.	
CLTE4	*Clematis terniflora* DC.	*
COCA5	*Conyza canadensis* (L.) Cronquist	
CUSCU	*Cuscuta* spp. L.	
CYPA19	*Cypripedium parviflorum* Salisb.	
DAGL	*Dactylis glomerata* L.	*
DOUM2	*Doellingeria umbellata* (Mill.) Nees	
DRMA4	*Dryopteris marginalis* (L.) A. Gray	
ERHI2	*Erechtites hieraciifolia* (L.) Raf. ex DC.	

EUAM7	*Euonymus americana* L.	
FAGR	*Fagus grandifolia* Ehrh.	
GAUR	*Gaylussacia ursina* (M.A. Curtis) Torr. & Gray ex Gray	
GAUR2	*Galax urceolata* (Poir.) Brummitt	
GNOB	*Gnaphalium obtusifolium* L.	
HAVI4	*Hamamelis virginiana* L.	
HEMI3	*Helianthus microcephalus* Torr. & Gray	
HEST	*Helianthus strumosus* L.	
HYAR	*Hydrangea arborescens* L.	
HYPER	*Hypericum* spp. L.	–
JUTE	*Juncus tenuis* Willd.	
LACTU	*Lactuca* spp. L.	
LESPE	*Lespedeza* spp. Michx.	–
LICA16	*Ligusticum canadense* (L.) Britt.	
LYLA	*Lysimachia lanceolata* Walter	
MIRE	*Mitchella repens* L.	
MIVI	*Microstegium vimineum* (Trin.) A. Camus	*
MOHY3	*Monotropa hypopithys* L.	
MOUN3	*Monotropa uniflora* L.	
OBVI	*Obolaria virginica* L.	
OEBI	*Oenothera biennis* L.	
OSCL2	*Osmunda claytoniana* L.	
PAAU3	*Packera aurea* (L.) A. Love & D. Love	
PACA11	*Paronychia canadensis* (L.) Alph. Wood	
PALU2	*Passiflora lutea* L.	
PENST	*Penstemon* Schmidel	
PIST	*Pinus strobus* L.	
POPU4	*Polygonatum pubescens* (Willd.) Pursh	
PRAL3	*Prenanthes altissima* L.	
PRVU	*Prunella vulgaris* L.	
PTAQ	*Pteridium aquilinum* (L.) Kuhn	
PYPU	*Pyrularia pubera* Michx.	
QUMO4	*Quercus montana* Willd.	
RHGL	*Rhus glabra* L.	
RHMA4	*Rhododendron maximum* L.	
SANI	*Salix nigra* Marsh.	
SIST	*Silene stellata* (L.) W.T. Aiton	

SOCA3	*Solanum carolinense* L.	
TARAX	*Taraxacum* spp. F.H. Wigg.	
TIDI	*Tipularia discolor* (Pursh) Nutt.	
TRIFO	*Trifolium* spp. L.	*
TRILL	*Trillium* spp. L.	
TUFA	*Tussilago farfara* L.	*
VIHA2	*Viola hastata* Michx.	
VIHI2	*Viola hirsutula* Brainerd	

Table B2. USDA codes with associated taxonomic groups and authority. Taxonomic groups present pre-treatment, year 2, and year 3 are listed.

USDA Code	Specific Epithet and Authority	Lifeform
ACPE	*Acer pensylvanicum* L.	Tree
ACRU	*Acer rubrum* L.	Tree
ACPA	*Actaea pachypoda* Elliott	Forb
ACRA7	*Actaea racemosa* L.	Forb
ADPE	*Adiantum pedatum* L.	Fern
AGALA	*Ageratina altissima* (L.) R.M. King & H. Rob. var. *altissima*	Forb
AGRIM	*Agrimonia* spp. L.	Forb
AGPE	*Agrostis perennans* (Walter) Tuck.	Graminoid
AMAR3	*Amelanchier arborea* (Michx. f.) Fernald	Tree
AMGL2	*Amorpha glabra* Desf. ex Poir.	Shrub
AMBR2	*Amphicarpaea bracteata* (L.) Fernald	Forb
ANQU	*Anemone quinquefolia* L.	Forb
ANVI3	*Anemone virginiana* L.	Forb
ANPL	*Antennaria plantaginifolia* (L.) Richardson	Forb
ANSO	*Antennaria solitaria* Rydb.	Forb
ARABI2	*Arabis* spp. L.	Forb
ARNU2	*Aralia nudicaulis* L.	Forb
ARTR	*Arisaema triphyllum* (L.) Schott	Forb
ARMA7	*Aristolochia macrophylla* Lam.	Vine
ARSE3	*Aristolochia serpentaria* L.	Vine
ASEX	*Asclepias exaltata* L.	Forb
ASQU	*Asclepias quadrifolia* Jacq.	Forb
ASCO4	*Aster cordifolius* L.	Forb
ASDI	*Aster divaricatus* L.	Forb
ASTERACEAE	Aster Family	Forb
ASTER	*Aster* spp. L.	Forb
ASBI4	*Astilbe biternata* (Vent.) Britt.	Forb
ATFI	*Athyrium filix-femina* (L.) Roth	Fern
ATFIA2	*Athyrium filix-femina* (L.) Roth ssp. *asplenioides* (Michx.) Hultén	Fern
AULA	*Aureolaria laevigata* (Raf.) Raf.	Forb
BELE	*Betula lenta* L.	Tree
BOCY	*Boehmeria cylindrica* (L.) Sw.	Forb
BOVI	*Botrychium virginianum* (L.) Sw.	Fern
BRER2	*Brachyelytrum erectum* (Schreb. ex Spreng.) P. Beauv.	Graminoid

CAFL22	*Calycanthus floridus* L.	Shrub
CADI3	*Campanula divaricata* Michx.	Forb
CACO26	*Cardamine concatenata* (Michx.) Sw.	Forb
CADI10	*Cardamine diphylla* (Michx.) Alph. Wood	Forb
CADI5	*Carex digitalis* Willd.	Graminoid
CAPE6	*Carex pensylvanica* Lam.	Graminoid
CAREX	*Carex* spp. L.	Graminoid
CAVI4	*Carex virescens* Muhl. ex Willd.	Graminoid
CACA18	*Carpinus caroliniana* Walter	Tree
CARYA	*Carya* spp. Nutt.	Tree
CADE12	*Castanea dentata* (Marshall) Borkh.	Tree
CAPU9	*Castanea pumila* (L.) Mill.	Shrub
CATH2	*Caulophyllum thalictroides* (L.) Michx.	Forb
CEOR7	*Celastrus orbiculatus* Thunb.	Vine
CHLY2	*Chelone lyonii* Pursh	Forb
CHMA3	*Chimaphila maculata* (L.) Pursh	Forb
CIRA	*Cimicifuga racemosa* (L.) Nutt.	Forb
CILUC	*Circaea lutetiana* L. ssp. *canadensis* (L.) Asch. & Magnus	Forb
CLTE4	*Clematis terniflora* DC.	Vine
CLVI4	*Clematis viorna* L.	Vine
CLVI5	*Clematis virginiana* L.	Vine
COCA4	*Collinsonia canadensis* L.	Forb
COAM	*Conopholis americana* (L.) Wallr.	Forb
COCA5	*Conyza canadensis* (L.) Cronquist	Forb
COMA6	*Coreopsis major* Walter	Forb
COAL2	*Cornus alternifolia* L. f.	Shrub
COFL2	*Cornus florida* L.	Tree
CUSCU	*Cuscuta* spp. L.	Vine
CYAC3	*Cypripedium acaule* Aiton	Forb
CYPA19	*Cypripedium parviflorum* Salisb.	Forb
DAGL	*Dactylis glomerata* L.	Graminoid
DANTH	*Danthonia* spp. DC.	Graminoid
DEPU2	*Dennstaedtia punctilobula* (Michx.) T. Moore	Fern
DEGL5	*Desmodium glutinosum* (Muhl. ex Willd.) Alph. Wood	Forb
DENU4	*Desmodium nudiflorum* (L.) DC.	Forb
DICHA2	*Dichanthelium* spp. (Hitchc. & Chase) Gould	Graminoid
DIQU	*Dioscorea quaternata* J.F. Gmel.	Forb

DOUM2	*Doellingeria umbellata* (Mill.) Nees	Forb
DRMA4	*Dryopteris marginalis* (L.) A. Gray	Fern
ERHI2	*Erechtites hieraciifolia* (L.) Raf. ex DC.	Forb
ERPU	*Erigeron pulchellus* Michx.	Forb
EUAM7	*Euonymus americanus* L.	Forb
EUFI	*Eupatorium fistulosum* Barratt	Forb
EUPU10	*Eupatorium purpureum* L.	Forb
FAGR	*Fagus grandifolia* Ehrh.	Tree
FRVI	*Fragaria virginiana* Duchesne	Forb
FRAM2	*Fraxinus americana* L.	Tree
GAUR2	*Galax urceolata* (Poir.) Brummitt	Forb
GASP5	*Galearis spectabilis* (L.) Raf.	Forb
GACI2	*Galium circaezans* Michx.	Forb
GALA4	*Galium latifolium* Michx.	Forb
GALIU	*Galium* spp. L.	Forb
GAUR	*Gaylussacia ursina* (M.A. Curtis) Torr. & A. Gray ex A. Gray	Shrub
GENTI	*Gentiana* spp. L.	Forb
GEMA	*Geranium maculatum* L.	Forb
GNOB	*Gnaphalium obtusifolium* L.	Forb
GOPU	*Goodyera pubescens* (Willd.) R. Br.	Forb
POACEAE	Grass Family	Graminoid
HAVI4	*Hamamelis virginiana* L.	Tree
HEMI3	*Helianthus microcephalus* Torr. & A. Gray	Forb
HEST	*Helianthus strumosus* L.	Forb
HEAM6	*Heuchera americana* L.	Forb
HIPA2	*Hieracium paniculatum* L.	Forb
HOPUP3	*Houstonia purpurea* L. var. *purpurea*	Forb
HULU2	*Huperzia lucidula* (Michx.) Trevis.	Fern
HYAR	*Hydrangea arborescens* L.	Shrub
HYPER	*Hypericum* spp. L.	Shrub
ILMO	*Ilex montana* Torr. & A. Gray ex A. Gray	Shrub
ILOP	*Ilex opaca* Aiton	Tree
IRIS	*Iris* spp. L.	Forb
JUTE	*Juncus tenuis* Willd.	Graminoid
KALA	*Kalmia latifolia* L.	Shrub
LACTU	*Lactuca* spp. L.	Forb
LACA3	*Laportea canadensis* (L.) Weddell	Forb

LEERS	*Leersia* spp. Sw.	Graminoid
LESPE	*Lespedeza* spp. Michx.	Forb
LICA16	*Ligusticum canadense* (L.) Britton	Forb
LILIU	*Lilium* spp. L.	Forb
LIBE3	*Lindera benzoin* (L.) Blume	Shrub
LITU	*Liriodendron tulipifera* L.	Tree
LOBEL	*Lobelia* spp. L.	Forb
LUZUL	*Luzula* spp. DC.	Graminoid
LYLI	*Lyonia ligustrina* (L.) DC.	Shrub
LYLA	*Lysimachia lanceolata* Walter	Forb
LYQU2	*Lysimachia quadrifolia* L.	Forb
MAAC	*Magnolia acuminata* (L.) L.	Tree
MAFR	*Magnolia fraseri* Walter	Tree
MARA7	*Maianthemum racemosum* (L.) Link	Forb
MEVI	*Medeola virginiana* L.	Forb
MIVI	*Microstegium vimineum* (Trin.) A. Camus	Graminoid
MIRE	*Mitchella repens* L.	Forb
MONAR	*Monarda* spp. L.	Forb
MOHY3	*Monotropa hypopithys* L.	Forb
MOUN3	*Monotropa uniflora* L.	Forb
MUHLE	*Muhlenbergia* spp. Schreb.	Graminoid
NYSY	*Nyssa sylvatica* Marshall	Tree
OBVI	*Obolaria virginica* L.	Forb
OEBI	*Oenothera biennis* L.	Forb
OSCL	*Osmorhiza claytonii* (Michx.) C.B. Clarke	Fern
OSCI	*Osmunda cinnamomea* L.	Fern
OSCL2	*Osmunda claytoniana* L.	Fern
OSRE	*Osmunda regalis* L.	Fern
OXALI	*Oxalis* spp. L.	Forb
OXAR	*Oxydendrum arboreum* (L.) DC.	Tree
OXRI	*Oxypolis rigidior* (L.) Raf.	Forb
PAAU3	*Packera aurea* (L.) Á. Löve & D. Löve	Forb
PAQU	*Panax quinquefolius* L.	Forb
PACA11	*Paronychia canadensis* (L.) Alph. Wood	Forb
PAQU2	*Parthenocissus quinquefolia* (L.) Planch.	Vine
PALU2	*Passiflora lutea* L.	Forb
PENST	*Penstemon* spp. Schmidel	Forb

PHHE11	*Phegopteris hexagonoptera* (Michx.) Fée	Fern
PHMA7	*Philadelphus maculatus* (C.L. Hitchc.) Hu	Shrub
PHAM7	*Phlox amplifolia* Britton	Forb
PHLE5	*Phryma leptostachya* L.	Forb
PHAM4	*Phytolacca americana* L.	Forb
PIST	*Pinus strobus* L.	Tree
POA	*Poa* spp. L.	Graminoid
POPE	*Podophyllum peltatum* L.	Forb
POBI2	*Polygonatum biflorum* (Walter) Elliott	Forb
POPU4	*Polygonatum pubescens* (Willd.) Pursh	Forb
POLYG4	*Polygonum* spp. L.	Forb
POAC4	*Polystichum acrostichoides* (Michx.) Schott	Fern
POTEN	*Potentilla* spp. L.	Forb
PRAL3	*Prenanthes altissima* L.	Forb
PRENA	*Prenanthes* spp. L.	Forb
PROSA	*Prosartes* spp. D. Don	Forb
PRVU	*Prunella vulgaris* L.	Forb
PRSE2	*Prunus serotina* Ehrh.	Tree
PTAQ	*Pteridium aquilinum* (L.) Kuhn	Fern
PYCNA	*Pycnanthemum* spp. Michx.	Forb
PYPU	*Pyrularia pubera* Michx.	Shrub
QUAL	*Quercus alba* L.	Tree
QUCO2	*Quercus coccinea* Münchh.	Tree
QUMO4	*Quercus montana* Willd.	Tree
QUPR2	*Quercus prinus* L.	Tree
QURU	*Quercus rubra* L.	Tree
QUVE	*Quercus velutina* Lam.	Tree
RANUN	*Ranunculus* spp. L.	Forb
RHCA4	*Rhododendron calendulaceum* (Michx.) Torr.	Shrub
RHMA4	*Rhododendron maximum* L.	Shrub
RHGL	*Rhus glabra* L.	Shrub
ROPS	*Robinia pseudoacacia* L.	Tree
ROMU	*Rosa multiflora* Thunb.	Vine
RUAL	*Rubus allegheniensis* Porter	Subshrub
RUOC	*Rubus occidentalis* L.	Subshrub
RUBUS	*Rubus* spp. L.	Subshrub
SANI	*Salix nigra* Marshall	Tree

SACA13	*Sanguinaria canadensis* L.	Forb
SANIC	*Sanicula* spp. L.	Forb
SAAL5	*Sassafras albidum* (Nutt.) Nees	Tree
SCEL	*Scutellaria elliptica* Muhl. ex Spreng.	Forb
SCUTE	*Scutellaria* spp. L.	Forb
SETE3	*Sedum ternatum* Michx.	Forb
SIST	*Silene stellata* (L.) W.T. Aiton	Forb
SMGL	*Smilax glauca* Walter	Vine
SMRO	*Smilax rotundifolia* L.	Vine
SMILA2	*Smilax* spp. L.	Vine
SOCA3	*Solanum carolinense* L.	Forb
SOCU	*Solidago curtisii* Torr. & A. Gray	Forb
SOLID	*Solidago* spp. L.	Forb
STLA5	*Stachys latidens* Small ex Britton	Forb
STPU	*Stellaria pubera* Michx.	Forb
TARAX	*Taraxacum* spp. F.H. Wigg.	Forb
THDI	*Thalictrum dioicum* L.	Forb
THNO	*Thelypteris noveboracensis* (L.) Nieuwl.	Fern
TIDI	*Tipularia discolor* (Pursh) Nutt.	Forb
TORAR	*Toxicodendron radicans* (L.) Kuntze ssp. *radicans*	Vine
TRADE	*Tradescantia* spp. L.	Forb
TRIFO	*Trifolium* spp. L.	Forb
TRILL	*Trillium* spp. L.	Forb
TUFA	*Tussilago farfara* L.	Forb
UVPE	*Uvularia perfoliata* L.	Forb
UVPU2	*Uvularia puberula* Michx.	Forb
VACCI	*Vaccinium* spp. L.	Shrub
VEPA3	*Veratrum parviflorum* Michx.	Forb
VIAC	*Viburnum acerifolium* L.	Shrub
VIHA2	*Viola hastata* Michx.	Forb
VIHI2	*Viola hirsutula* Brainerd	Forb
VISO	*Viola sororia* Willd.	Forb
VIOLA	*Viola* spp. L.	Forb
VIAE	*Vitis aestivalis* Michx.	Vine
ZITR	*Zizia trifoliata* (Michx.) Fernald	Forb